Kuwait in flow: A goal programming demand release schedule for the afternoon commuter

by

Salem Sulaiman Al-Mansour

B.S., Wichita State University, 2022

A THESIS

submitted in partial fulfillment of the
requirements for the degree

MASTER OF SCIENCE

Department of Industrial and Manufacturing Systems Engineering
Carl R. Ice College of Engineering

KANSAS STATE UNIVERSITY
Manhattan, Kansas

2025

Approved by:

Major Professor
Dr. Jessica L. Heier Stamm

Copyright

Abstract

Traffic congestion remains one of the most persistent challenges in urban environments, particularly in regions experiencing rapid population growth and limited availability of transportation data. In Kuwait, high automobile dependency, coupled with the absence of advanced traffic data and management systems, has intensified congestion and reduced network efficiency. Traditional Dynamic Traffic Assignment (DTA) models, while effective in capturing time-dependent traffic behavior, require detailed Origin–Destination data, making them impractical in contexts such as Kuwait. This research introduces a novel modeling framework that integrates the Cell Transmission Model (CTM) with Goal Programming (GP) to develop an optimization-based approach to traffic demand management. The GP–CTM model prescribes a demand release schedule that prevents road capacity from being exceeded, thereby mitigating congestion preemptively. The model was applied to a case study in the Sabah Al-Salem area of Kuwait, using school-related demand as the primary source of recurrent congestion. Results showed that the optimized demand release schedule achieved full demand clearance within the one-hour time horizon, while reducing average network occupancy by 64% compared to a baseline 'all-at-once' release policy. The findings demonstrate that the GP–CTM framework can deliver Dynamic Traffic Assignment–like insights without O-D data, providing aggregate-level understanding of system-wide congestion dynamics. This work offers policymakers a practical, computationally tractable tool for formulating demand management strategies and highlights a shift toward prescriptive and preemptive, system-level approaches in traffic management research.

Contents

List of Figures

List of Tables

بِسْمِ ٱللَّٰهِ ٱلرَّحْمَٰنِ ٱلرَّحِيمِ

Acknowledgments

First and foremost, all praise to the Most High, Allah (SWT). I extend my deepest gratitude to my professor and committee members, friends, family, and my wife. It is often difficult to capture complex feelings concisely; therefore, my acknowledgment will be lengthy.

To my advisor, *Dr. Jessica Heier Stamm*: thank you for your guidance throughout this process. Navigating this journey was challenging, but your support gave me the agency to reach the finish line.

To my home country *Kuwait*, I extend my deepest gratitude. I would like to express my sincere thanks to the *State of Kuwait* and the *Ministry of Higher Education* for their financial support through the graduate scholarship program. This support not only made this research possible, but also provided me and many others with the opportunity to pursue our academic and professional aspirations abroad.

To my friends, *Abdullah "Johar"*, *Dhari*, *Tariq*, and *Omar* who always believe in my ability to persevere and achieve my goals, thank you. Especially my dear friend *Rinki*—today, I have completed the task...

To my siblings, *Yousef, Sarah* and *Jasem,* I don't even know where to start. Without your love and support, I would lack the inspiration that drives me. *Annie*, I know you are watching—I love you immensely. To my Father, *Sulaiman*, and Mother *Linda*, you are the foundation of the man you see today, I will forever be indebted to you.

To my son, *Ibrahem*: My North Star. All my work is for you to show that the greatest rewards in life lie on the other side of our toughest challenges.

Finally, to my beautiful wife, *Sarah*: your unwavering support came at times when I had nothing left to give. You lit my path and guided me gracefully. I admire you and your work; by observing you, I have learned what it truly means to be a professional and I have attempted to apply it to my own work. Your originality overflows in all that you do, and it is an honor to acknowledge you in my thesis. Thank you for being my *muse*.

Dedication

This work is dedicated to a collection of pivotal people in my life — to my mother and father, who taught me hard work and dedication to excellence; to my Aunt “Annie,” who showed me unconditional love; to my son, Ibrahem, as a reminder that through hard work and perseverance, anything can be achieved; and last, but certainly not least, to my one true love, my beloved wife, Sarah. Without you, I would not have made it this far. You lit my path when I had nothing left in me. You all built the man you see in me today.

This work is as much yours as it is mine.

”Whatever you can do, or dream you can do, begin it. Boldness has genius, power, and magic in it. Begin it now.”

–Goethe

Chapter 1

Introduction

The modern automobile was originally a solution to a mobility constraint, transforming travel from a lengthy and time-consuming endeavor into an everyday activity. Today, in urban societies, personal automobiles have become the dominant mode of transportation, often to the exclusion of alternative options. This transformation was made possible by pioneers such as Karl Benz and Henry Ford, whose innovations—particularly Ford's introduction of the assembly line—made vehicles affordable for the masses. Yet, this newfound accessibility produced an unintended consequence: traffic congestion. Congestion arises when the capacity of a road network is exceeded by the number of vehicles within it, a condition that disrupts the smooth flow of movement. Although often viewed as a modern problem, evidence of congestion dates back to ancient Rome [1]. As Maxwell argues, "congestion may well be an unavoidable but manageable consequence of a transport system," [2], reflecting not failure but the limits of capacity within an active and dynamic network.

1.1 Traffic In Context

Building on this perspective, congestion can be understood as the physical manifestation of an imbalance between supply and demand within the transportation network. When demand for road space surpasses available capacity, flow efficiency deteriorates. Thoker describes congestion as a condition arising ”when traffic demand is great enough that the interaction between vehicles slows the speed of the traffic stream,” marking the point at which capacity is effectively exceeded [3]. This frames congestion as an operational issue confined within the network rather than as a systemic imbalance driven by latent demand. Thus, the focus of modern traffic management is in developing strategies that manage demand and optimize the existing network's performance under its current capacity.

As populations grow and reliance on personal vehicles increases, travel demand rises correspondingly, intensifying congestion across urban networks. What was once a solution to limited mobility has now become a constraint on movement itself. The widespread preference for individual travel, combined with increasingly connected infrastructure, has amplified this effect and made congestion a persistent feature of modern cities. However, prevailing definitions of demand and congestion often fail to account for these evolving dynamics. Traditional approaches tend to treat congestion as a reactive issue within the network, rather than as a systemic imbalance between demand and capacity, thereby limiting the effectiveness of management strategies.

To address this limitation, definitions of congestion can be expanded to incorporate the spatial dimension of demand — particularly the influence of urban population density and the concentration of travel demand at specific sources. Considering where demand originates, rather than only how much exists, offers an additional management perspective that accounts for the uneven distribution of traffic demand volumes relative to roadway capacity. This argument aligns with Maxwell's interpretation of congestion as a manageable outcome rather than a system failure, but the lens can be expanded further to reflect the evolving structure of modern urban environments. The emergence of large metropolitan areas has created zones of concentrated travel demand that function like reservoirs of potential energy — stored mobility that can be released into the network, a *potential travel demand*. This concept emphasizes that congestion is not only the result of current traffic volumes but also of a lack of consideration of how demand is concentrated within urban environments.

While the underlying causes of congestion stem from imbalances between demand and capacity, its manifestation on the roadway can be understood more precisely through a technical lens. Traffic congestion can arise in two primary ways: non-recurrent and recurrent. Non-recurrent congestion results from unexpected disruptions such as accidents, road maintenance, or adverse weather conditions that temporarily reduce roadway capacity [3]. In contrast, recurrent congestion occurs predictably due to recurring travel patterns—such as daily commuting, holiday travel, or evacuation scenarios—where demand consistently exceeds network capacity during specific time periods [3].

1.2 Congestion In Kuwait

Kuwait provides an instructive case study, as its urban structure is almost entirely automobile dependent. Walking and cycling infrastructure remain limited, and public transport options—such as buses—are underutilized due to cultural and social preferences. Also, Kuwait's population has risen from approximately 1.6 million in 1990 to nearly 5 million in 2023 [4] (see Figure 1.1). In this setting, congestion is prevalent with drivers spending on average 67 minutes in traffic per day [5]. According to the Central Statistics Bureau in Kuwait, there are 2.5 million vehicles registered in Kuwait with 2 million of those being private vehicles [6]. Combining this statistic with the population explosion, you can see that for every 2 people there is a car. This combination of rapid population growth, vehicle dependency, and limited modal diversity underscores the need for demand-side management strategies that address congestion at its source.

The challenge of managing congestion in Kuwait is compounded by limitations in transportation data and modeling capabilities. Traditional approaches, such as Dynamic Traffic Assignment (DTA) models, rely on detailed Origin–Destination (O–D) data to represent and forecast travel demand [1]. However, Kuwait's data collection practices are not yet equipped

[1] Origin–destination data describe the movement of travelers or vehicles between defined points in a network, capturing where trips begin and where they end.

to provide this level of detail, constraining the applicability of conventional models. To effectively manage congestion under such conditions, there is a need for a modeling framework that can operate with modest data requirements while still capturing the relationship between demand and network capacity. This gap motivates the development of a demand management model that defines and regulates potential travel demand preemptively, before it manifests as congestion within the network.

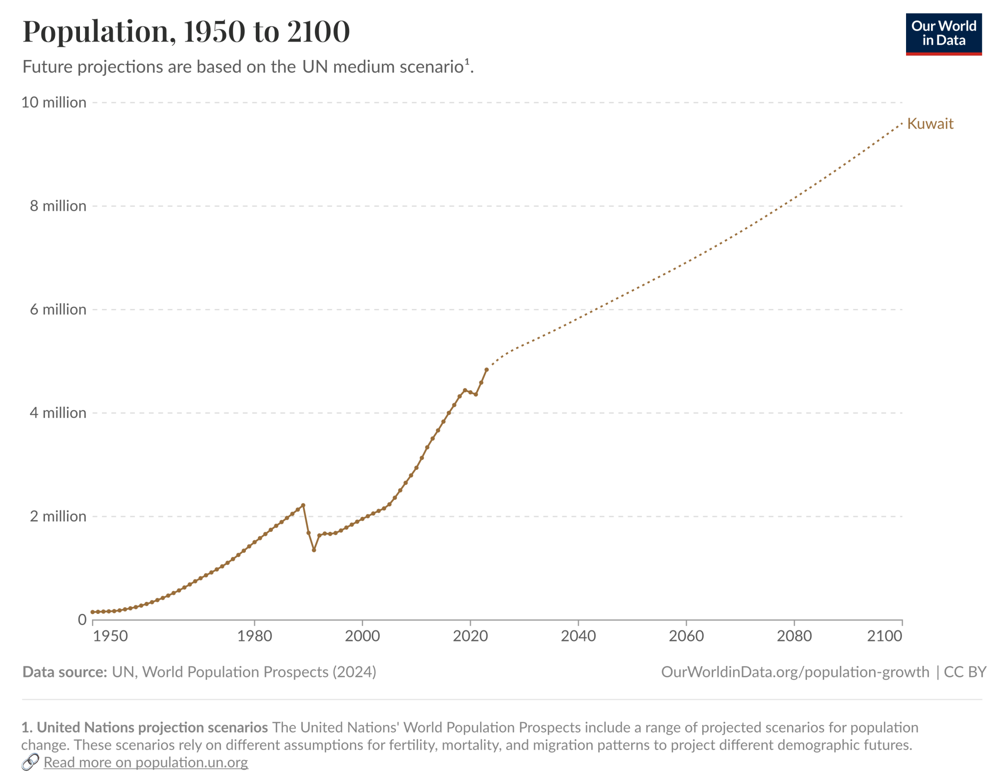

Figure 1.1: Population growth in Kuwait from 1950 to 2023.

Problem definition:

- Congestion is commonly defined as an imbalance between travel demand and capacity within the network boundaries; however, this definition overlooks how the concentration and spatial distribution of demand reduce effective network capacity, making the traditional understanding inherently limited.
- Congestion is handled reactively due to the mis-framing and its relation to congestion.

- Existing macroscopic models tend to describe system behavior rather than prescribe actionable control strategies.
- DTA models require O–D data that is not available in countries such as Kuwait and other data-lacking regions.

Research questions:

I. How can traffic demand be re-imagined through an industrial engineering lens and managed using a system-level modeling framework?

II. Can the cell transmission model be integrated with goal programming to balance multiple, conflicting traffic management objectives?

III. How can such a model be implemented using aggregate data to achieve results comparable to Dynamic Traffic Assignment approaches without requiring extensive O–D pair data?

1.3 Motivation & Contribution

The intended objective of this research is to develop a demand management policy using the cell transmission model as the representation of traffic network dynamics and the goal programming optimization modeling framework to prescribe demand values to the system in a way that ensures road demand does not exceed capacity which preemptively mitigates congestion before travel demand enters the traffic network.

The primary contribution of this work is twofold. First, it extends the definition of traffic demand from an industrial engineering perspective, reframing it as a controllable and schedulable variable rather than a static input. This reconceptualization shifts the focus of traffic management strategies toward proactive demand control rather than reactive congestion mitigation. Second, the research develops a computationally tractable model that mimics the behavior of Dynamic Traffic Assignment (DTA) models but eliminates the need for detailed Origin–Destination data. This makes the framework suitable for application in data-limited environments such as Kuwait and similar developing regions, while still providing scalable, network-wide insights into traffic dynamics.

1.4 Thesis Outline

The rest of the document is organized as follows: Chapter 2 discusses the state of the field, introducing traffic management strategies and the modeling techniques used to mathematically represent traffic networks at different levels of granularity. It also reviews goal programming, an optimization technique not commonly applied in transportation engineering, and identifies gaps in the field that influence the research questions developed for this study. Chapter 3 discusses the methods that serve as the basis for the proposed model, including the mathematical formulations and their differences, and identifies gaps in their application or formulation. A novel network transformation procedure is then proposed. Finally, the GP–CTM model is presented, its formulation discussed, and extensions are introduced to address the previously identified gaps. Chapter 4 introduces the case study area and discusses its suitability as the testbed for this model. The NTP proposed in Chapter 3 is applied to Sabah Al Salem, and testing and validation are performed on a validation network to ensure the model is computationally feasible and functions as designed. Finally, the model is applied to the Sabah Al Salem network, and the results and key findings are analyzed and assessed. Chapter 5 presents a discussion of the key findings from the model's application, the limitations of the model, directions for future work, and concluding remarks.

Chapter 2

Through the Lens - A Literature Review

2.1 Traffic from a High Level

The definition of traffic carries a great deal of nuance, as the term is used across multiple disciplines to describe the movement of entities through networks of interconnected nodes and arcs. In data network theory, traffic refers to the movement of messages through communication links, characterized by their rates, routes, and temporal patterns [7]. Similarly, in communication engineering, traffic is measured in terms of the rate and volume of information exchanged between systems. In transportation engineering, the same concept applies, though the entities in motion are vehicles moving through physical road networks rather than data packets [2].

Across these fields, the underlying principles remain consistent: traffic represents the flow of entities constrained by capacity and time. When that capacity is approached or exceeded, congestion emerges—a condition that has long been central to the study of transportation systems. According to Maxwell, the terms traffic and congestion became synonymous as early as the nineteenth century, reflecting that traffic was often used loosely as a stand-in for congestion. This interchangeability has shaped how both terms are understood in practice. However, he also argues that congestion is not a flaw in the system but an unavoidable—yet manageable—byproduct of movement, implying that it should be treated as a controllable variable rather than an external problem [2].

Maxwell critiques the prevailing definitions and understandings of congestion in transportation engineering. He argues that ineffective congestion management stems not from a lack of tools or models, but from the way congestion is being defined [2]. His research reviews how congestion has been addressed and identifies where existing approaches fall short. He argued that congestion-pricing models relied on limited predictive assumptions, which weakened their effectiveness as management strategies. While he does not redefine congestion, he suggests queuing models as the next step in effective management. Building on Maxwell's critique, this research addresses the lack of a clear and functional definition of congestion. This research posits that incorporating demand concentration at its sources within urban networks can enable more effective demand-management strategies through a holistic, systems-thinking approach.

2.2 Traffic Management

Traffic management plays a critical role in sustaining modern mobility systems. As infrastructure expansion becomes increasingly costly and spatially constrained, system-based management strategies offer a more efficient path toward reducing congestion, travel time, and economic loss. The field itself is highly interdisciplinary, with contributions from economists, computer scientists, civil and industrial engineers, and information systems experts—each providing distinct perspectives and methods for addressing the challenges of network efficiency and congestion mitigation. This section reviews the development and scope of traffic management research, identifying key questions, methodological trends, and areas of convergence across disciplines.

2.2.1 Types of Vehicle Traffic

Traffic can generally be classified into two categories: recurrent and non-recurrent [3]. While these terms are largely self explanatory, a clear distinction is essential to understand how each influences network performance and what management strategies are used in each case. Recurrent traffic refers to predictable congestion patterns that occur regularly, commonly known as commuter traffic or rush hour congestion. This form of traffic produces congestion at consistent times and for similar durations each day. In contrast, non-recurrent traffic results from irregular or unexpected events such as traffic accidents, weather disruptions or road construction.

Recurrent traffic is a well-documented phenomenon, supported by extensive empirical data and long-term observation. Consequently, the development of management strategies for recurrent congestion relies on clear and consistent evidence. In contrast, non-recurrent traffic is inherently stochastic, requiring predictive modeling to estimate its occurrence and impact. This study focuses on recurrent congestion, as it consistently affects network performance and provides a measurable basis for evaluating and estimating the impact of management interventions.

Recurrent traffic has historically been addressed through traffic management strategies that fall into two main categories: supply-side and demand-side approaches. Supply-side strategies aim to increase roadway capacity or improve operational efficiency through flow control, while demand-side strategies seek to manage or redistribute demand to reduce peak surges. This literature review examines both perspectives, though the primary focus of this research lies on demand-side management.

2.2.2 Traffic Flow Control: Supply-Side Management

Traffic flow control, the foundation of supply-side traffic management, operates within the boundaries of the transportation network. Focusing on link-level and intersection-level control, the strategies of this category of traffic management are higher in granularity. Unlike infrastructure expansion, which physically adds capacity, traffic flow control (TFC) seeks to optimize the network within its existing limits. The objective is to understand and regulate traffic dynamics by measuring current conditions, assessing network state, and adjusting system parameters such as signal timing, lane usage, highway inflow, and routing strategies. This approach, widely used in intelligent transportation systems (ITS), follows a monitor–analyze–control cycle [8, 9]. These control actions are informed by continuous data collection, including crowd-sourced inputs, roadway sensors (e.g., RFID gateways), and connected vehicle or floating car data. Together, these sources enable real-time, adaptive flow optimization [9] [10] [11].

At its core, traffic flow control aims to maintain vehicle movement, increase the effective capacity of network links, and prevent congestion by dynamically managing flow as demand nears capacity. This distinction is critical, as network expansion alone does not guarantee improved traffic conditions. Braess's paradox illustrates this, showing that adding capacity can, under certain network and behavioral conditions, worsen congestion due to redistributed flow [12]. In this sense, flow control acts as the operational "connective tissue" of the traffic network, working to keep movement stable and efficient even under high demand.

Signal Timing & Ramp Metering

Signal timing and ramp metering represent two fundamental tools for managing traffic flow at critical control points within a network. Both operate at the boundaries of movement—signal timing at intersections and ramp metering at freeway entry points—where local control decisions have system-wide implications. Intersections and on-ramps often serve as bottlenecks, constraining throughput even under moderate demand levels. Traditional control strategies rely on fixed-time parameters that cannot adapt to changing traffic conditions, leading to unnecessary delays or capacity breaches. Adaptive control methods, including dynamic signal timing and responsive ramp metering, address these inefficiencies reducing idle time and maintaining smooth network operation.

Recent research has focused on adaptive methods that adjust signal phases based on real-time flow conditions. For example, Chin [13] developed a signal timing plan using genetic algorithms to dynamically optimize phase durations under Malaysian traffic conditions. Al-Othman [14] proposed a fuzzy logic–based control framework that adjusts signal timings according to intersection saturation levels, demonstrating improved performance over static configurations in Kuwait City. Similarly, Kolte [15] employed a deep learning architecture combining convolutional and graph convolutional networks to predict optimal signal parameters and adapt to varying roadway conditions. Expanding beyond signalized control, Elhenawy [16] developed a theoretical model for un-signalized intersections using a game theory–based "Chicken Game" formulation to coordinate connected autonomous vehicles.

Expanding this concept of localized control beyond intersections, ramp metering applies similar adaptive principles to highway entry points. Ramp metering regulates the rate at which vehicles enter the freeway, maintaining flow stability by preventing sudden demand surges that exceed mainline capacity. Shaaban [17] provide a comprehensive review of adaptive ramp metering strategies, highlighting the shift from fixed-time control toward responsive, feedback-based and machine-learning-driven approaches. Both ramp metering and signal timing represent temporal control strategies, regulating the timing of vehicle releases to maintain network equilibrium.

Lane Assignment and Dynamic Routing

While signal timing focuses on the temporal control of flow, lane assignment and dynamic routing address the spatial organization of vehicles within the network. Both aim to optimize the distribution of traffic across available infrastructure to minimize congestion. Traditionally, lane assignment strategies have designated lanes according to vehicle type, destination, or operational priority—for instance, dedicated bus, freight, or express lanes. More recent studies, such as Guan et al. [18], extend this concept to mixed traffic environments, introducing dynamic lane management frameworks that adapt in real time to interactions between human-driven and autonomous vehicles. Similarly, Dao [19] explored platoon assignments and lane selection for flow optimization. In contrast, dynamic routing operates at both the network and link levels, using real-time traffic data to redirect vehicles toward less congested routes and balance network loads. Lioudakis [20] developed a middle-ware system that integrates road sensor data and optimization algorithms to provide real-time route updates, minimizing congestion and total travel time while also accounting for emissions impacts. Together, lane assignment and dynamic routing complement signal control by addressing the spatial dimension of flow optimization.

2.2.3 Demand-Side Management

Demand-side management operates at a higher, less granular level than supply-side strategies, which typically focus on link- and intersection-level control. Its primary goal is to distribute demand across the network, either temporally or spatially, to minimize congestion before it forms. Common strategies explored in this literature review include reservation systems, congestion pricing, evacuation planning, and management of the morning and afternoon commuter problem. Reservation systems aim to schedule access to congested areas by controlling the influx of demand relative to available capacity. Congestion pricing attempts to redistribute travel demand by incentivizing off-peak travel or alternative routes through dynamic tolling or fees. Evacuation planning, while often applied to emergency scenarios, focuses on utilizing the network efficiently to ensure timely clearance during stochastic or high-impact events. The commuter problem addresses how to manage peak-hour traffic caused by the simultaneous release of demand from institutions such as schools and workplaces. This is often done through temporal staggering or coordinated release strategies to reduce peak congestion. The modeling framework proposed in this study aligns with demand-side management principles by regulating the release of travel demand at its source, thereby preventing congestion from forming downstream.

Demand Reservation and Congestion Pricing

Reservation systems distribute demand temporally by spreading vehicle entries over time instead of allowing them to accumulate simultaneously. Zhao [21] introduces a citywide reservation strategy that approves or denies requests based on the current demand level, effectively making demand visible to the network. Edara and Teodorovic [22] apply this concept to highway systems by regulating the number of vehicles permitted to enter. This enables traffic operators to maintain stable traffic flow by controlling the rate of entry into the system. However, such systems face challenges with user buy-in and potential economic implications for businesses that depend on high levels of activity during peak periods. In contrast, congestion pricing redistributes demand spatially. This strategy incentivizes drivers to choose alternative routes or travel modes by adjusting the cost of using congested links [23, 24]. Because drivers typically aim to minimize travel costs, pricing mechanisms leverage this tendency to ease congestion on overloaded routes and improve overall network efficiency. However, determining appropriate pricing levels can be challenging, especially when multiple vehicle types share the same roadway. This often results in uneven or potentially inequitable pricing schemes.

Evacuation Planning and the Commuter Problem

Evacuation planning and commuter scheduling share similar principles. Both aim to flatten the peak of the demand curve to maintain flow efficiency [25, 26]. While evacuation modeling deals with stochastic events such as natural disasters, the underlying logic—sequencing departures, staging releases, and distributing flow—mirrors the objectives of everyday demand management. Addressing the commuter problem is concerned with how to schedule work times in a way that maintains existing commuting routines, minimizing disruption to daily life, while flattening the travel demand distribution [27].

Ultimately, the effectiveness of these strategies depends on how "demand" itself is defined and understood. In transportation systems, demand represents the desire to use a road segment within a specific time frame, as defined by highway capacity manuals [28]. However, when demand is characterized purely as a traffic volume or flow-rate issue, management efforts become reactive—addressing congestion after it forms rather than mitigating its underlying causes. For example, congestion pricing, a common demand management strategy, adjusts tolls or fees in response to traffic density but does so based on observed or anticipated congestion rather than the spatial and temporal concentration of travel demand. This framing confines demand within network boundaries, focusing on flow regulation instead of addressing how and where demand originates.

2.3 Macro, Micro & the In Between

A key consideration in traffic management is understanding traffic dynamics. To capture the nuances of these dynamics and design more effective solutions, several network models have been developed. In traffic engineering, these models provide mathematical representations of physical road networks and the flows that occur within them. Because infrastructure expansion is costly and field experiments are difficult to implement, researchers rely on mathematical models to test hypotheses and evaluate strategies without disrupting the real-world system. Their main contribution lies in providing a deeper understanding of how traffic systems behave, enabling more effective design and management strategies.

Traffic modeling supports both descriptive and predictive analysis—it helps explain traffic behavior and evaluate system performance. Because traffic networks involve both deterministic elements, such as control parameters and demand in recurrent traffic scenarios like rush hour or the morning commute, and stochastic elements, such as traffic accidents or fluctuations in weather, different modeling perspectives are used to capture these dynamics.

These models are generally classified into three categories based on levels of granularity: microscopic, mesoscopic, and macroscopic. Each level captures the traffic system at a different spatial and behavioral resolution. Microscopic models simulate individual driver behavior, vehicle–infrastructure interactions, and vehicle trajectories, often implemented in simulation platforms such as SUMO or VISSIM. Mesoscopic models occupy the middle ground, representing traffic as groups or “platoons” of vehicles rather than individuals. At the opposite end, macroscopic models adopt a system-level perspective, describing traffic flow in aggregate terms such as density, speed, and volume. Each modeling approach serves a distinct purpose, with microscopic models offering high behavioral realism and macroscopic models providing computational efficiency. The choice of model thus depends on the trade-off between detail and scalability.

Microscopic Models

The earliest microscopic traffic models were introduced in the 1950s by Reuschel and Pipes, marking the beginning of vehicle-level traffic flow analysis [29,30]. At the most detailed level of traffic modeling, microscopic models focus on the behavior and interactions of individual vehicles within the network [31]. These models aim to capture two primary forms of interaction within the traffic system: vehicle-to-vehicle (V2V) and vehicle-to-infrastructure (V2I) dynamics. The primary behavioral variables captured in microscopic models include vehicle spacing, desired speed, and interactions with neighboring vehicles, all of which reflect the driver–vehicle unit, often referred to as the vehicle–conductor pair. This concept treats the driver and vehicle as a single cognitive–mechanical entity whose combined decisions shape individual movement within the network. This focus on detailed, vehicle-level interactions represents the essence of microscopic modeling—capturing the fine-grained dynamics of traffic flow, vehicle behavior, and driver decision-making. However, this level of detail comes at the cost of scalability, since modeling each vehicle’s behavior and interaction requires significant computational resources, making large-scale network simulation challenging.

Mesoscopic Models

Mesoscopic models occupy the intermediate level between microscopic and macroscopic representations of traffic flow [31]. The term mesoscopic itself derives from the prefix meso-, meaning 'middle' or 'intermediate,' reflecting its hybrid nature. At this level, groups of vehicles—often referred to as platoons—are modeled collectively to capture their aggregate influence on the traffic network [19]. These vehicle groups retain microscopic characteristics in their internal interactions but are treated as macroscopic units when describing overall network dynamics. Mesoscopic models are particularly useful in studying the integration of autonomous vehicles (AVs) into traffic systems—a rapidly expanding area of research. Studies suggest that the coordinated movement of AVs can enhance network capacity and stability, even benefiting non-autonomous vehicles through smoother flow patterns. However, these benefits remain largely theoretical, as they depend on reaching a critical mass of fully autonomous vehicles—a condition not yet realized in practice. Mesoscopic simulation is commonly implemented using software such as SUMO, which provides flexible frameworks for both mesoscopic and microscopic modeling approaches.

According to Benalia [31], mesoscopic models can generally be categorized into four main types: (1) time-difference distribution models, which describe the probabilistic variation in inter-vehicle time gaps; (2) cluster models, which group vehicles based on shared characteristics such as speed, length, or vehicle type; (3) gas-kinetic models, which treat driver interactions as stochastic processes similar to particle behavior in gases—introducing the concept of phase-space density to describe vehicle concentration over time and space; and (4) hybrid models, which combine elements from multiple modeling approaches to balance realism with computational efficiency. Hybrid mesoscopic models have become increasingly popular due to their ability to capture key behavioral effects while maintaining manageable computational complexity.

Macroscopic Models

At the system level view, macroscopic models provide an aggregate perspective of traffic flow, focusing on high level relationships rather than individual vehicle behaviors [31]. Several foundational models exist within this category, including the Lighthill–Whitham–Richards (LWR) model [32], Payne–Whitham (PW) model [33], Aw–Rascle–Zhang (ARZ) model [34], the Macroscopic Fundamental Diagram (MFD) [35], and the Cell Transmission Model (CTM) [36, 37]. This paper primarily focuses on the CTM framework. The macroscopic perspective abstracts from the finer details of driver behavior or vehicle interactions, instead representing traffic as a continuous flow, similar to a fluid. Because of this aggregate treatment, macroscopic models are generally less computationally demanding and less sensitive to local disturbances. These models are valuable for estimating key system-level metrics such as average travel time, mean fuel consumption, and emissions, offering a scalable approach to analyzing overall network performance.

The framework of a macroscopic traffic model is typically defined by three key variables: flow, density, and speed. Traffic flow refers to the number of vehicles passing a given point per unit of time, usually expressed as vehicles per hour. Traffic density describes the concentration of vehicles per unit length of roadway, commonly expressed as vehicles per mile or kilometer. Speed represents the average velocity of vehicles over a section of road, expressed in distance per unit of time (e.g., kilometers per hour). These variables are interrelated through the fundamental traffic flow equation, which forms the basis for most macroscopic traffic models.

This research adopts the macroscopic modeling framework due to its balance between computational efficiency and representational realism. While microscopic and mesoscopic models provide finer granularity, they are often limited by scale and data requirements. Macroscopic models, by contrast, enable system-wide optimization and are particularly suitable for analytical and simulation-based studies of large networks. In practice, all modeling approaches involve trade-offs, but the macroscopic perspective offers a pragmatic balance between accuracy and computational feasibility for the objectives of this study. Among these, the CTM framework introduced by Daganzo [36, 37] provides a discretized and computationally tractable implementation of the kinematic wave theory, forming one layer of this study's modeling approach.

2.4 Daganzo's Cell Transmission Model

The Cell Transmission Model (CTM), introduced by Daganzo in 1994, is a first-order macroscopic model derived from the Lighthill–Whitham–Richards (LWR) kinematic wave theory [36]. It simulates traffic dynamics using nonlinear minimum operators that govern the flow of vehicles between adjacent cells based on traffic density and capacity constraints. It was later expanded by Daganzo to include different types of cell interactions, making it more descriptive of traffic networks [37]. It discretizes both space and time to describe traffic flow dynamics using conservation laws, enabling the modeling of congestion propagation and queue spillback. Rather than solving continuous partial differential equations directly, CTM approximates them through a discrete representation of the conservation of vehicles across space and time. The roadway is divided into cells, each representing a segment with inflow and outflow boundaries that model the accumulation and dissipation of vehicles over time. Unlike the Macroscopic Fundamental Diagram (MFD), which captures network-wide relationships, CTM explicitly models local link–node interactions, enabling it to represent spillback at intersections, backward shockwave propagation from braking, and flow control at merging and diverging points. Because it maintains an aggregate structure while preserving spatial resolution, the CTM scales effectively from corridor-level to citywide applications, balancing computational efficiency with network realism.

Several researchers have extended Daganzo's original formulation to accommodate more realistic traffic phenomena and network behaviors. For instance, Ukkusuri [38] introduced a path-based CTM for dynamic user equilibrium problems, while Zhu [39] developed a dynamic system optimum formulation that prevents non-physical holding-back flows. Wang [40] further applied the CTM to traffic signal timing under oversaturated conditions, demonstrating its adaptability for operational control and real-time network management. Collectively, these advancements highlight the CTM's versatility and its evolution from a purely descriptive model to one capable of supporting prescriptive and optimization-based traffic management strategies.

While the CTM effectively models traffic dynamics, its original formulation is descriptive rather than prescriptive. To extend its utility for optimization, Ziliaskopoulos [41] reformulated the CTM as a linear program to solve the system-optimal traffic assignment problem, in accordance with Wardrop's second principle. This formulation minimizes cumulative vehicle occupancy across time—effectively minimizing total system travel time—subject to constraints reflecting conservation of flow, link capacity, jam density, and merge/diverge behavior. This approach bridges the gap between descriptive traffic modeling and prescriptive network optimization. Building on this foundation, the present research extends the CTM framework from a descriptive to a prescriptive modeling tool. Ziliaskopoulos's proof that the CTM can be formulated as a linear program provides the theoretical foundation for this extension, enabling the model to incorporate multiple, potentially conflicting objectives within traffic network optimization.

However, a key limitation of this extension lies in the linearization of flow propagation constraints, which only approximate the actual flow dynamics simulated by the original CTM as noted in [39, 42]. Specifically, the nonlinear sending and receiving functions in CTM—typically expressed through minimum operators—are simplified in linear programming formulations to ensure tractability. While this enables faster computation and compatibility with optimization solvers, it may reduce the model's ability to capture fine-grained traffic phenomena such as shockwave propagation, stop-and-go behavior, and spillback effects.

2.5 Dynamic Traffic Assignment

In operations research, the assignment problem seeks to optimally allocate resources to tasks in order to minimize total cost or time. In transportation systems, the analogous problem—known as traffic assignment—seeks to determine how vehicles are distributed across a network in response to demand and route conditions. Wardrop's first principle introduces the concept of user equilibrium (UE), which assumes that each driver chooses the route that minimizes their own travel time [43]. In equilibrium, all used routes between any origin–destination pair have equal and minimal travel times; no driver can improve their travel time by unilaterally changing routes [44]. As previously stated, Braess's Paradox further illustrates this behavior, showing that adding a new link to a network can counterintuitively increase overall travel times, as drivers re-optimize selfishly in a way that worsens collective performance [12]. Wardrop's second principle defines the system optimum (SO) condition, in which traffic is distributed across the network to minimize total system travel time [43]. Unlike UE, SO represents a cooperative condition: some drivers may experience longer individual travel times if doing so reduces the overall congestion burden on the system.

Achieving SO conditions typically requires centralized control or incentive mechanisms—such as congestion pricing or access restrictions—to influence route choice. These principles also underpin evacuation planning, where the objective is to minimize total clearance time while ensuring network safety and efficiency. The distinction between UE and SO lies in the trade-off between stability and optimality. UE represents a Nash equilibrium—stable because no driver can improve their travel time individually—while SO achieves the globally optimal flow distribution at the expense of individual autonomy.

Recent developments in traffic modeling have extended these static principles into dynamic frameworks, giving rise to Dynamic Traffic Assignment (DTA). DTA explicitly incorporates the time dimension, modeling how traffic conditions and route choices evolve over time [45]. When combined with macroscopic models such as the cell transmission model (CTM), DTA provides a dynamic representation of network flow that can be formulated and solved using optimization techniques, including linear and goal programming. While Dynamic Traffic Assignment (DTA) provides a powerful framework for modeling time-dependent traffic behavior, its implementation relies heavily on detailed origin–destination pair data to define travel demand across the network [45, 46]. In practice, this data is often difficult to obtain—particularly in developing or data-sparse regions such as Kuwait—where comprehensive (O-D) matrices or high-resolution sensor data are unavailable. As a result, applying DTA in such contexts becomes computationally and practically infeasible.

2.6 Goal Programming

Goal Programming (GP) extends the linear programming framework to handle decision problems with multiple, and often conflicting, objectives. Introduced by Charnes and Cooper in 1961 [47] and later expanded by Romero [48], GP minimizes deviations from pre-specified goals rather than optimizing a single criterion. It is a widely used multi-criteria decision-making technique for balancing competing objectives in complex systems.

In transportation research, GP has been applied primarily to strategic-level problems such as transport planning, mode split, and resource allocation [49]. However, its application in traffic network modeling and control remains limited, there is little to no research directly applying GP to system-level traffic optimization or policy design. Existing studies have mainly focused on long-term planning objectives, while operational or network-level optimization problems have traditionally relied on linear, nonlinear, or simulation-based formulations. This gap presents an opportunity to explore GP as a framework for developing policy-oriented, system-level strategies that balance multiple objectives in traffic management.

This research employs goal programming as a prescriptive extension of the cell transmission model. By formulating multi-objective trade-offs—such as minimizing congestion while maintaining network efficiency—within a single framework, GP enables realistic and balanced decision-making in the presence of conflicting objectives. Its flexibility and interpretability make it well-suited for addressing the multi-dimensional nature of traffic management. Additionally, the structured development of goals within GP offers a potential pathway for addressing the "holding-back" phenomenon described by Aziz [42], who propose maximizing flow through cells as a mitigation strategy. Although this research does not directly address that shortcoming, it is identified as an area for future exploration.

2.7 Research Gap & Contribution

Despite decades of research in traffic management and modeling, several critical gaps remain. First, the concepts of demand and congestion are incomplete in the context of urban environments, as they often neglect the spatial concentration of demand and its systemic relationship to network capacity. Addressing this limitation through a more holistic framework can enable more effective demand management strategies. Many existing Dynamic Traffic Assignment (DTA) models, while analytically powerful, rely heavily on detailed origin–destination pair data to estimate and predict network behavior. This dependency makes them impractical in data-limited environments such as Kuwait. On the control side, most adaptive or optimization-based strategies operate locally—at the level of intersections— rather than addressing system-wide flow interactions. Consequently, while effective in isolation, these methods lack scalability and coordination across the broader network. Demand-side strategies, such as commuter scheduling and temporal demand redistribution, have shown potential to flatten congestion peaks, but remain largely decoupled from spatial control methods. Overall, existing approaches are fragmented, focusing on either temporal or spatial optimization but rarely integrating both dimensions within a unified framework.

This research addresses these limitations by developing a goal programming–based cell transmission model (CTM–GP) framework that combines temporal and spatial perspectives of traffic management. The proposed model reconceptualizes "demand" from an industrial engineering perspective—as the controllable inflow of users into a constrained system—rather than merely as observed traffic volume. By integrating this redefinition into the CTM framework, the model achieves scalability and adaptability across an entire network while maintaining computational efficiency. Unlike conventional DTA models, the CTM–GP approach offers aggregate-level decision support that mimics dynamic assignment behavior without requiring detailed O–D data. Additionally, the framework introduces a scheduled release mechanism that regulates inflow temporally, providing a realistic and implementable congestion mitigation strategy. Together, these contributions advance the field toward a more integrated, system-level approach to traffic management.

Building on the identified gaps and contributions, this study seeks to address the following research questions:

I. How can traffic demand be re-imagined through an industrial engineering lens and managed using a system-level modeling framework?

II. Can the cell transmission model be integrated with goal programming to balance multiple, conflicting traffic management objectives?

III. How can such a model be implemented using aggregate data to achieve results comparable to Dynamic Traffic Assignment approaches without requiring extensive O–D pair data?

Chapter 3

Methods & Model

3.1 The Foundation: Methodology

This section presents the methodological framework and modeling approach adopted in this research. The discussion proceeds in four parts. First, the cell transmission model, introduced in the literature review, is described in greater detail alongside its linear programming extension by Ziliaskopoulos. Second, goal programming is introduced as an extension of the works of Daganzo and Ziliaskopoulos, enabling the integration of the CTM with goal programming to address multiple objectives. Third, a network transformation technique is proposed and outlined to demonstrate how a geographical map can be transformed and represented as a cell network. Finally, the complete formulation of the GP-CTM model is presented and discussed.

The model developed in this study builds upon the foundational contributions of Daganzo and the subsequent extension by Ziliaskopoulos. Specifically, Ziliaskopoulos demonstrated that Daganzo's CTM could be reformulated as a linear program to determine the optimal conditions of a traffic network — proving its use as a prescriptive tool. The present research advances this line of inquiry by extending the CTM through a goal programming framework. Daganzo originally introduced the CTM to represent the dynamics of traffic flow within a cellular structure of a transportation network. This extension enables the CTM to identify optimal solutions in contexts where multiple, and often conflicting, objectives compete for the same resources.

3.1.1 Daganzo's Cell Transmission Model

The traffic dynamics in this research are modeled using the cell transmission model (CTM) proposed by Daganzo. This method allows the model to represent key traffic phenomena such as congestion propagation and queue spill-backs in a computationally efficient manner. The CTM is particularly well-suited for large-scale network applications, as it balances physical realism with tractability. The following section outlines the structure of the CTM and its role in modeling and simulating traffic flow dynamics.

In 1994–1995, Daganzo introduced the cell transmission model, a discrete approximation of the Lighthill–Whitham–Richards (LWR) hydrodynamic traffic flow model. The CTM is a macroscopic model, meaning it represents traffic conditions from an aggregate perspective. It assumes that the collective behavior of vehicles depends on the surrounding traffic environment, where flow and density mutually influence one another. The model represents traffic dynamics through a piecewise linear fundamental diagram that relates speed, flow, and density. Flow propagation is captured using nonlinear minimum operators that determine the sending capacity of an upstream cell and the receiving capacity of the downstream cell. These operators ensure that vehicle flow respects both the available supply in the upstream cell and the remaining capacity in the downstream cell. Within this framework, vehicle speed decreases as density increases—reflecting congestion effects—while lower densities correspond to higher speeds and free-flow conditions.

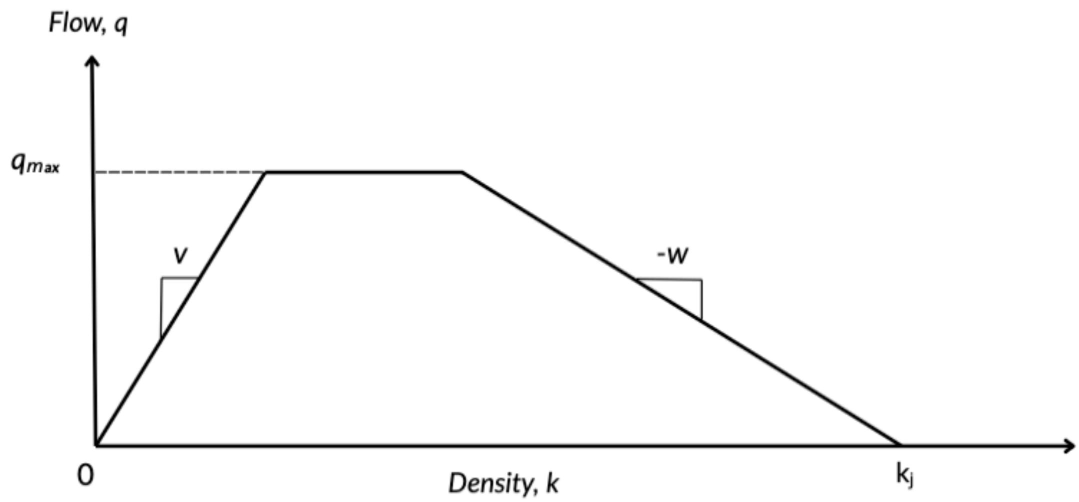

Figure 3.1: Flow–density relationship for the generalized cell transmission model (adapted from Daganzo, 1994).[1]

At the time, macroscopic traffic models were formulated using node–arc networks, where nodes correspond to intersections or decision points in the physical road system, and arcs represent the directional roadway segments that connect those intersections. Traditional macroscopic models, such as the Lighthill–Whitham–Richards (LWR) model and the Macroscopic Fundamental Diagram (MFD), primarily captured how congestion evolved over time but did not distinguish where within a segment it occurred. The cell transmission model extends this structure by discretizing each node-arc connection into smaller sections known as

[1]Figure 3.1 illustrates the relationship between flow and density in the Cell Transmission Model, where v represents the free-flow speed, $-w$ the backward wave speed, q_{max} the maximum flow (capacity), and k_j the jam density.

cells [2], each representing a homogeneous portion of roadway characterized by unidirectional traffic conditions such as density, flow, and speed. This cellular structure introduces a spatial component, allowing the model to pinpoint the location and propagation of congestion within the network. Although it is categorized as a macroscopic model, some researchers describe it as semi-mesoscopic, since it provides greater spatial detail about the network topology than traditional macroscopic approaches.

Cell Transmission Model Notation

Notation & Parameters

v Free–flow speed (ft/s).

w Backward–propagation speed (ft/s).

$n_i(t)$ Occupancy of cell i at time t.

$y_i(t)$ Inflow into cell i at time t.

$S_i(t)$ Sending capacity of cell i at time t.

$R_i(t)$ Receiving capacity of cell i at time t.

δ Backward–propagation factor, defined as the ratio of free–flow speed to backward wave speed $\left(\frac{v}{w}\right)$, used in computing receiving flow.

$N_i(t)$ The maximum number of vehicles that can occupy cell i.

$Q_i(t)$ The maximum number of vehicles that can flow out of cell i, constraint by the available occupancy in the downstream cell.

Each arc in the network is divided into a sequence of cells. A vehicle moving from one

[2]The cells in the CTM are connected via cell connector arcs but are virtual connections that do not carry traffic volume.

cell to the next requires exactly one discrete time step, a rule Daganzo referred to as the ”time-scan” strategy. Through this discretization, the CTM captures the propagation of traffic dynamics both spatially and temporally. The rule assumes that vehicles are traveling at free-flow speed — that is, driving at the speed limit and able to traverse a cell within a single time step. Formally, the cell length (L) in feet is defined as the product of the free-flow speed (v) in ft/s and the time step in seconds (Δt) as shown in equation 3.1.1. Once the cell length is established, the number of cells (n) along an arc is calculated by dividing the total arc length by the cell length L as shown in equation 3.1.2.

$$L = v \cdot \Delta t \tag{3.1.1}$$

$$n = \frac{\text{Arc Length (ft.)}}{\text{Cell Length (ft.)}} \tag{3.1.2}$$

The occupancy of cell i at time t, denoted by $n_i(t)$, represents the number of vehicles within that cell and captures the state of the traffic system at that time. Two additional capacity parameters are defined: $N_i(t)$ and $Q_i(t)$, These parameters represent the storage capacity of a cell and its discharge capacity per time step, respectively. These parameters are fixed for each cell as they depend on its physical characteristics, such as length, number of lanes, and jam density [3]. $N_i(t)$ is the product of a cell's length and its jam density. For example, at jam density, a single 500-foot cell on a one-lane road may hold approximately 10 vehicles, while a two-lane segment of the same length can hold 20. In contrast, $Q_i(t)$ is determined by the time discretization step and the cell's physical discharge capacity. For instance, if the free-flow speed is 50 km/h and the time step Δt is 10 seconds, then one

[3] Jam Density is denoted by k_j and represents the physical maximum capacity of the road segment when vehicles are bumper to bumper

vehicle could travel about 500 feet in one time step. If the discharge capacity of a lane is 2,000 vehicles per hour, this equates to roughly 5 vehicles per 10-second time step, meaning $Q_i(t) = 5$ vehicles can flow out of cell i to its downstream neighbor per time step.

The CTM for ordinary cell connectors is governed by a conservation (occupancy-update) equation (Eq. 3.1.3) and a flow rule (Eq. 3.1.4). The flow rule determines vehicle transfer between adjacent cells via a minimum operator applied to the upstream sending function and downstream receiving function (Eqs. 3.1.5 – 3.1.6). The conservation equation then updates each cell's occupancy by adding inflow and subtracting outflow, ensuring mass balance. Applied recursively, these relations make the state at time $t+1$ depend only on the state at time t.

$$n_i(t+1) \;=\; n_i(t) \;+\; y_i(t) \;-\; y_{i+1}(t) \tag{3.1.3}$$

$$y_i(t) \;=\; \min\Big\{S_i(t),\; R_i(t)\Big\} \tag{3.1.4}$$

$$S_i(t) \;=\; \min\Big\{n_i(t),\; Q_i(t)\Big\} \tag{3.1.5}$$

$$R_i(t) \;=\; \min\Big\{Q_i(t),\; \delta\big[N_i(t) - n_i(t)\big]\Big\} \tag{3.1.6}$$

Although equations (3.1.3 – 3.1.6) describe the dynamics of ordinary cell connectors—that is, single-direction cell connections—the framework also defines several other cell types to represent network boundaries and intersections. Source cells inject vehicles into the network according to time-dependent demand profiles derived from (O–D) data, subject to the receiving capacity of the first downstream cell. Sink cells remove vehicles exiting the network. Diverging junctions split flow from one upstream cell into multiple downstream cells according to fixed split ratios α_{ij}, while merging junctions combine flow from multiple upstream cells into one downstream cell using priority coefficients β_{kj} to allocate available capacity. These extensions preserve vehicle conservation and flow feasibility throughout the network [37]. The present study builds on this formulation through a linear programming representation of the CTM introduced by [41].

The cell transmission model distinguishes five types of cells within a road network (see figure 3.2): source cells, which have no upstream cells and only provide inflow; ordinary cells, which have one upstream and one downstream cell; merging cells, which have two upstream cells and one downstream cell; diverging cells, which have one upstream cell and two downstream cells; and sink cells, which have one upstream cell and no downstream cells, marking the end of the network. Source and sink cells are assumed to have infinite capacity, while all other cell types are constrained by the variables N_i^t and Q_i^t. Each cell type captures specific traffic flow dynamics that the CTM is designed to simulate, with source cells marking the beginning, diverging and merging cells modeling intersections, and sink cells being the end of the network.

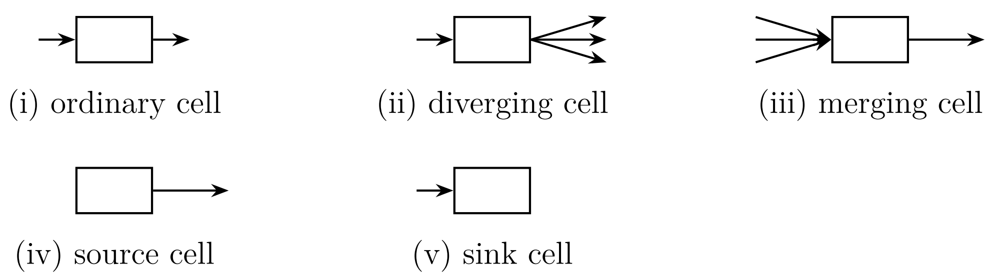

Figure 3.2: Classification of cell types (adapted from Ziliaskopoulos LP-CTM)

3.1.2 Ziliaskopoulos's Linear Program of the Cell Transmission Model

The cell transmission model (CTM) is well-suited as a macroscopic traffic model — as discussed in section 2.3 — providing valuable spatial and temporal insights of traffic flows. However, it does not inherently identify optimal roadway conditions for traffic management.

This shortcoming was addressed by Ziliaskopoulos [41], who reformulated the CTM as a linear program (LP) designed to determine optimal cell occupancies and flow values, thereby determining the systems optimal operating conditions. His work demonstrated that the CTM can be expressed as an LP to achieve a system-optimum solution, initially for a single-source, single-destination network. This reformulation laid the foundation for later extensions of the CTM into broader optimization and control frameworks, which will be explored in the following section.

Ziliaskopoulos's work highlights two key gaps in the field of dynamic traffic assignment. Analytical formulations are often extensions of static models, which rely on simplifying assumptions and therefore fail to capture the physical dynamics of traffic flow within a network. Simulation-based models, on the other hand, address these simplifications but do not provide optimality conditions. The solution proposed by Ziliaskopoulos was to combine the dynamics of the cell transmission model with a linear programming framework, producing optimal conditions for the dynamic traffic assignment problem. This approach allows for both system-level insights into congestion and network efficiency as well as the identification of optimality conditions.

Using the linear programming framework, he showed that combining the CTM with LP can determine the optimal conditions of each cell i at each time step t. However, the study was limited in scope, as it was applied only to a small example network consisting of 10 cells and 11 arcs. Additionally, while the LP formulation enables efficient optimization, it represents a linearized approximation of the nonlinear dynamics in the original CTM, and therefore may not fully capture phenomena such as traffic shockwaves or flow spillback [39, 42]. More broadly, the challenge lies not only in scaling this formulation to real-world networks but also in developing a deeper understanding of the trade-offs between competing objectives and how they interact in practice.

Formulation Differences: CTM vs. LP

Several key differences distinguish Ziliaskopoulos's Linear Programming formulation of the cell transmission model from the original CTM. In the LP-CTM, cell occupancy is denoted by x_i^t, whereas the original CTM uses $n_i(t)$. Similarly, flow between cells is represented as y_{ij}^t where flow leaves cell i at time t and arrives to cell j at $t+1$ which maintains the "*time-scan*" strategy. In contrast to the CTM, which expresses only the downstream end flow $y_i(t)$. Despite these notational differences, the underlying cell types remain the same. As shown in Figure 3.2, there are five types: C_S, C_R, C_O, C_M, and C_D representing the set of cells C[4]. Connector types describe the connections between adjacent cells, denoted by the (i, j) indices that specify the beginning and ending cells. The connector type is determined by the cells it links [5]; for example, a connector joining one upstream and one downstream cell is classified as ordinary. The cell connector types are denoted by $\mathcal{E}_S$, $\mathcal{E}_R$, $\mathcal{E}_O$, $\mathcal{E}_M$, and $\mathcal{E}_D$ representing the set of cell connectors $\mathcal{E}$[6]. As specified by Daganzo [37], diverging cells cannot directly connect to merging cells. This constraint reflects the model's assumption that a cell can either distribute flow to multiple downstream cells (diverge) or receive flow from multiple upstream cells (merge), but not both. Such a configuration would be structurally inconsistent and does not correspond to any realistic road geometry.

Having defined the structural composition of the network, the LP-CTM next formalizes cell relationships and time discretization through a series of sets and parameters. While the CTM model does not distinguish downstream and upstream neighbors, the LP-CTM defines them in sets denoted by $\Gamma(i)$ and $\Gamma^{-1}(i)$. To maintain the time scan functionality of the CTM, the LP-CTM defines a set of discrete time intervals $\mathcal{T}$ with τ representing the

[4] C_S: Sink cells, C_R: Source cells, C_O: Ordinary cells, C_M: Merging cells, C_D: Diverging cells

[5] Cells are connected by cell connectors; in the LP-CTM, the term 'link' is not used to describe connections between cells, to avoid confusion with the actual network links

[6] $\mathcal{E}_S$: Sink cell connector, $\mathcal{E}_R$: Source cell connector, $\mathcal{E}_O$: Ordinary cell connector, $\mathcal{E}_M$: Merging cell connector, $\mathcal{E}_D$: Diverging cell connector.

discretization time step[7]. Both models define time-invariant parameters that describe the physical properties of the network, denoted by N_i^t, Q_i^t, and δ_i^t. The LP-CTM introduces one time-dependent parameter, the demand inflow d_i^t, which is specified exogenously by the modeler to represent origin demand. Destination information is not required due to the single-destination structure of the model.

The constraints of the linear programming formulation of the cell transmission model include flow conservation (cell mass balance), sending and receiving constraints, connector capacity restrictions for merges and diverges, source and sink constraints, and initial conditions. Ziliaskopoulos reformulated the CTM by expressing its dynamic update rules as a system of linear equalities (for flow conservation) and linear inequalities (for sending/receiving and capacity limits), thus replacing the nonlinear "min" operators of the original CTM with tractable linear approximations that can be solved using standard optimization methods. These constraints operate at two levels: the cell level and the cell-connector level, with further distinctions based on the type of cell involved. The next section examines these constraints in detail, with commentary on their mathematical formulation.

With these variables and parameters defined, Ziliaskopoulos formulated the LP-CTM to minimize the total accumulation of vehicles within the network by optimizing the spatiotemporal distribution of cell occupancies. The key distinction lies in the prescriptive nature of the LP-CTM formulation. While the CTM describes the system's functionality at an aggregate level, it does not prescribe optimal state conditions for the network. This distinction is captured by the objective function of the LP-CTM, which minimizes aggregate vehicle occupancy over the time horizon to ensure the most efficient utilization of available capacity and a reduction in overall congestion shown in equation 3.1.7.

[7] i.e. $\mathcal{T} = \{\tau, 2\tau, 3\tau, ..., |\mathcal{T}|\ \tau\ \}$

Objective Function:

$$\text{Minimize} \quad Z = \sum_i \sum_t x_i^t \tag{3.1.7}$$

Model Constraints

Cell Mass Conservation:

$$x_i^t - x_i^{t-1} - \sum_k y_{ki}^{t-1} + \sum_j y_{ij}^{t-1} = 0, \quad \begin{array}{c} \forall i \in \mathcal{C} \setminus \mathcal{C}_R, \mathcal{C}_S, \\ \forall t \in \mathcal{T}, \end{array} \tag{3.1.8}$$

Equation (3.1.8) expresses the flow balance principle as applied to all cells except source and sink cells. The constraint balances inflows and outflows to cells ensuring that vehicle movements through the network evolve consistently with the system's traffic dynamics. Enforcing a zero residual in this balance ensures that vehicles cannot accumulate artificially within a cell, except when restricted by the receiving capacity of the downstream cell. In Daganzo's original CTM [36, 37], this conservation rule was applied recursively to update cell occupancies at each time step. In the LP formulation, the same relationship is retained but expressed as a linear equality constraint, making it suitable for optimization. Figure 3.3 illustrates this relationship by decomposing Equation (3.1.8) into its constituent parts, highlighting how changes in cell occupancy (Term A) are coupled with the combined inflow and outflow dynamics (Term B).

$$\underbrace{x_i^t - x_i^{t-1}}_{A} - \underbrace{\sum_k y_{ki}^{t-1} + \sum_j y_{ij}^{t-1}}_{B} = 0,$$

Figure 3.3: Decomposition of the LP-CTM cell mass conservation constraint.

Term $\boldsymbol{A}$ represents the change in cell occupancy between time intervals $t-1$ and t, while term $\boldsymbol{B}$ groups the total inflow and outflow terms that together determine the net vehicle exchange between adjacent cells (see Figure 3.3). The incoming inflow indexed by (k,i) represents the total inflow entering cell i from all upstream neighbors k in the previous time step. The outgoing flow indexed by (i,j) represents the outflow leaving cell i to a downstream neighbor j in the previous time step. The equality ensures that any change in cell occupancy is exactly balanced by the combination of these flow components, preserving vehicle conservation across the network.

Source Cell Mass Conservation:

$$x_i^t - x_i^{t-1} + y_{ij}^t = d_i^{t-1}, \quad \begin{array}{l} \forall i \in \mathcal{C}_R, \\ \forall j \in \Gamma(i), \\ \forall t \in \mathcal{T} \end{array} \tag{3.1.9}$$

In the LP formulation, source cells are governed by a specialized mass conservation constraint, shown in equation 3.1.9, that connects external demand with the internal cell network. Unlike ordinary cells, which balance inflows and outflows from neighboring cells, source cells admit demand directly from outside the network. Thus, the change in occupancy of a source cell at time t equals the admitted demand from the previous time step minus the outflow, ensuring consistency between external inflows and the network's internal dynamics.

Diverging Cell Constraints:

$$\sum_j y_{ij}^t - x_i^t \leq 0, \quad \begin{array}{l} \forall i \in \mathcal{C}_D, \\ \forall t \in \mathcal{T}, \end{array} \tag{3.1.10}$$

$$\sum_j y_{ij}^t \leq Q_i^t, \quad \begin{array}{l} \forall i \in \mathcal{C}_D, \\ \forall t \in \mathcal{T} \end{array} \tag{3.1.11}$$

Inequalities (3.1.10) and (3.1.11) represent the physical conservation constraints that govern diverging cells within the network. These inequalities preserve model feasibility by enforcing the physical boundaries within which traffic flow must operate. For interpretation refer to Figure 3.2: (ii) Diverging cell, which illustrates a diverging cell characterized by a single inflow and multiple outflows. Inequality (3.1.10) constrains the total outflow from cell i to its downstream neighbors j at time t, ensuring it does not exceed the occupancy of cell i in the same time interval. Inequality (3.1.11) limits the total outflow from cell i by its sending capacity Q_i^t, which represents the maximum flow that can be discharged during time t. Together, these constraints preserve the physical feasibility of the network by enforcing flow conservation and capacity consistency for diverging cells.

Merging Cell Constraints:

$$\sum_i y_{ij}^t \leq Q_j^t, \quad \begin{array}{l} \forall j \in \mathcal{C}_M, \\ \forall t \in \mathcal{T} \end{array} \tag{3.1.12}$$

$$\sum_{i} y_{ij}^{t} + \delta_j^t X_j^t \leq \delta_j^t N_j^t, \quad \begin{array}{l} \forall j \in \mathcal{C}_M, \\ \forall t \in \mathcal{T} \end{array} \tag{3.1.13}$$

Merging cells are characterized by multiple incoming flows and a single outgoing flow, as illustrated in Figure 3.2(iii) Merging cell. Before introducing the constraints associated with these cell types, it is necessary to clarify the notation and sets involved. Q_j^t denotes the receiving capacity of the downstream cell j; $\Gamma^{-1}(j)$ denotes the set of upstream cells to j, with the superscript -1 indicating upstream direction; and δ_j^t represents the backward propagation factor, which scales the receiving capacity based on how rapidly congestion propagates upstream. This parameter effectively limits the inflow from upstream cells when the downstream cell approaches its jam density. In Daganzo [37], the propagation factor was defined as a binary condition. Specifically, $\delta = 1$ when the occupancy x_i^{t-1} in the previous time step is less than the receiving capacity Q_i^t of cell i in the current time step, and $\delta = w/v$ otherwise [8]. In the linear programming formulation of the CTM, however, δ_i^t is typically treated as a constant parameter, with its value chosen by the modeler rather than derived dynamically from cell states.

The constraints for merging cells account for all flows entering the downstream merging cell j from its upstream cells i. Inequality 3.1.12 limits the total inflow from the upstream cells to the receiving capacity of the downstream cell j. Inequality 3.1.13 introduces the propagation factor δ_j^t on the downstream cell, ensuring that congestion effects are accurately represented within the network. The sum of the inflow from all upstream cells i and the downstream j cell's occupancy, both scaled by the propagation factor, are constrained by the downstream cell's maximum occupancy, also scaled by the same factor.

[8]When w = v, the ratio w/v = 1, indicating a balance between forward and backward wave speeds, often associated with transitional traffic states. When w < v, w/v < 1, reflecting congestion, where backward-moving shockwaves travel slower than vehicles under free-flow conditions.

Cell Connector Constraints

Connector level constraints regulate flows along individual cell connectors between cells, replacing the CTM's min-operators with linear inequalities. The cell connector type is named according to the types of cells it connects, as illustrated in Figure 3.2.

Ordinary & Source Cell Connector Constraints:

$$y_{ij}^t - x_i^t \leq 0, \quad \begin{array}{c} \forall (i,j) \in \mathcal{E}_O \cup \mathcal{E}_R, \\ \forall t \in \mathcal{T} \end{array} \tag{3.1.14}$$

$$y_{ij}^t \leq Q_i^t, \quad \begin{array}{c} \forall (i,j) \in \mathcal{E}_O \cup \mathcal{E}_R, \\ \forall t \in \mathcal{T} \end{array} \tag{3.1.15}$$

$$y_{ij}^t \leq Q_j^t, \quad \begin{array}{c} \forall (i,j) \in \mathcal{E}_O \cup \mathcal{E}_R, \\ \forall t \in \mathcal{T} \end{array} \tag{3.1.16}$$

$$y_{ij}^t + \delta_j^t X_j^t \leq \delta_j^t N_j^t, \quad \begin{array}{c} \forall (i,j) \in \mathcal{E}_O \cup \mathcal{E}_R, \\ \forall t \in \mathcal{T} \end{array} \tag{3.1.17}$$

The inequalities (3.1.14)–(3.1.17) define the flow constraints for ordinary and source cell connectors. Their collective role is to ensure that vehicle movements remain physically feasible within the network. The first inequality (3.1.14) restricts outflow from each upstream cell to the number of vehicles currently occupying it, ensuring that discharge cannot exceed available occupancy. The second and third inequalities (3.1.15) and (3.1.16) limit the sending and receiving flows, respectively, so that neither surpasses the physical flow capacities of the upstream and downstream cells. Finally, inequality (3.1.17) incorporates the backward propagation factor δ_j^t, which adjusts the allowable inflow based on downstream congestion, ensuring that flow remains consistent with capacity limitations when cells approach their jam density.

Sink Connector Constraints:

$$y_{ij}^t - x_i^t \le 0, \quad \begin{array}{c} \forall (i,j) \in \mathcal{E}_S, \\ \forall t \in \mathcal{T} \end{array} \tag{3.1.18}$$

$$y_{ij}^t \le Q_i^t, \quad \begin{array}{c} \forall (i,j) \in \mathcal{E}_S, \\ \forall t \in \mathcal{T} \end{array} \tag{3.1.19}$$

At sink connectors, flow is constrained solely by the upstream cell's ability to send vehicles—specifically by its current occupancy and its sending capacity. Since sinks represent vehicles exiting the network, they are modeled as having effectively unlimited receiving capacity. Consequently, no receiving or backward propagation constraints are imposed on these connectors.

Merging & Diverging Cell Connectors:

$$y_{ij}^t - x_i^t \le 0, \quad \begin{array}{c} \forall (i,j) \in \mathcal{E}_M \\ \forall t \in \mathcal{T} \end{array} \tag{3.1.20}$$

$$y_{ij}^t \le Q_i^t, \quad \begin{array}{c} \forall (i,j) \in \mathcal{E}_M \\ \forall t \in \mathcal{T} \end{array} \tag{3.1.21}$$

$$y_{ij}^t \leq Q_j^t, \quad \begin{array}{c}\forall (i,j) \in \mathcal{E}_D \\ \forall t \in \mathcal{T}\end{array} \tag{3.1.22}$$

$$y_{ij}^t + \delta_j^t x_j^{t-1} \leq \delta_j^t N_j^t, \quad \begin{array}{c}\forall (i,j) \in \mathcal{E}_D \\ \forall t \in \mathcal{T}\end{array} \tag{3.1.23}$$

Merging and diverging cell connectors represent the interfaces between adjacent cells, where individual cell connector flows are governed by local flow and capacity limits. Unlike the cell-level constraints for merging and diverging cells, which include summations to capture the interaction among multiple flows, the connector constraints are defined at the cell connector level and are applied to each pair (i, j) independently. Constraints (3.1.20)–(3.1.23) specify that each individual flow y_{ij}^t is restricted by the occupancy, sending capacity, and receiving capacity of the connected cells. These inequalities ensure that flow along each connection remains physically feasible but, by themselves, do not describe how multiple upstream or downstream flows interact. That collective interaction is instead captured by the corresponding cell-level merging and diverging constraints described previously.

Taken together, the merging and diverging connector constraints ensure that individual cell connector flows remain physically feasible by adhering to local occupancy and capacity limits. While they do not directly capture the interaction or competition among multiple flows, they complement the cell-level constraints—which govern those aggregate behaviors—by expressing the same physical principles as approximated linear inequalities suitable for inclusion in the optimization model.

Initial Conditions & Non-Negativity:

$$x_i^0 = \xi_i, \forall i \in \mathcal{C} \tag{3.1.24}$$

$$y_{ij}^0 = 0, \forall (i,j) \in \mathcal{E} \tag{3.1.25}$$

$$x_i^t \geq 0, \quad \begin{matrix} \forall i \in \mathcal{C}, \\ \forall t \in \mathcal{T} \end{matrix} \tag{3.1.26}$$

$$y_{ij}^t \geq 0, \quad \begin{matrix} \forall (i,j) \in \mathcal{E}, \\ \forall t \in \mathcal{T} \end{matrix} \tag{3.1.27}$$

The initial conditions establish the initial state of the network, serving as the foundation for its dynamic evolution throughout the time horizon. The first condition sets the initial occupancy of each cell 3.1.24, ensuring that the system begins from a defined state, where ξ_i denotes the initial occupancy parameter as described by Ziliaskopoulos [41]. The second specifies that there are no flows at the initial time step, preventing artificial vehicle movements at the beginning of the time interval 3.1.25. The final two constraints enforce non-negativity on both occupancies and flows, ensuring that no physically unrealistic values (e.g., negative vehicles or flow rates) can occur 3.1.26 and 3.1.27. Together, these conditions provide the baseline from which the linear program evolves the network dynamics over time.

3.2 Goal Programming as a Framework

3.2.1 Definition & Motivation

Goal Programming (GP) is an extension of the linear programming framework designed to handle decision problems with multiple, and often conflicting, objectives. Instead of optimizing a single criterion, GP introduces goals and minimizes deviations from pre-specified targets. The concept was first introduced by Charnes and Cooper in 1961 [47], who framed GP as a systematic approach to incorporating multiple objectives into optimization models.

Later, Romero in 2001 [48] broadened the definition by emphasizing GP as a multi-criteria decision-making tool that provides compromise solutions. This approach allows several goals to be addressed simultaneously within a unified structure, yielding solutions that are realistic and practical.

Initially, linear goal programming was applied to personnel planning problems that involved managing a large number of defined goals. Over time, its use has expanded beyond multi-criteria decision analysis into fields such as transportation, finance, and resource management. In traffic demand management, goal programming is particularly well suited because of the inherent conflicts between objectives. For instance, maximizing flow on a given link often conflicts with the need to minimize sudden demand surges across the network. Traditional single-objective models may produce mathematically optimal solutions, for one or the other objectives; however, these are often impractical and unlikely to be implemented. For example, a linear program might minimize demand surges but fail to account for maximizing flow on critical links. Goal programming, by contrast, provides solutions that are both feasible and realistic, as it considers multiple objectives simultaneously as well as distinguishing the trade offs. For this reason, it is often described as a 'satisficing' methodology: When strict optimality is unattainable, the focus shifts to satisfying the key goals set within the model.

3.2.2 Variants of Goal Programming

Several formulations of goal programming exist, the standard model being the weighted (Archimedean), lexicographic, and Chebyshev methods [50]. The weighted sum method assigns specific weights to each goal to reflect their relative importance; however, its main limitation lies in the difficulty of setting appropriate weights and targets. The lexicographic method ranks goals from most to least important, ensuring that higher-priority goals are satisfied before lower-priority ones are considered. This avoids conflicts between goals, but the strict ranking may overlook potentially beneficial trade-offs. The Chebyshev method, in contrast, minimizes the maximum deviation among goals, producing balanced or "middle ground" solutions. Its drawback is that such evenness may come at the cost of missing a better near-optimal solution. Because both the weighted and Chebyshev approaches are sensitive to weight and target selection, careful controls must be applied when implementing them.

This research adopts the weighted sum method (Archimedean), as it allows goals to be prioritized through explicitly assigned weights. The weights will be determined according to the relative importance of each goal, while target levels will be carefully defined to ensure that the model produces meaningful and robust results.

3.2.3 Goal Programming in Standard Form

The Weighted Sum Method (Archimedean) can be expressed in the following general form:

$$
\begin{aligned}
\text{Minimize} \quad Z \quad &= \sum_{i=1}^{m} \left(w_i^- d_i^- + w_i^+ d_i^+ \right) \\
\text{s.t.} \quad & Ax \leq b, \\
& \sum_{j=1}^{n} c_{ij} x_j + d_i^- - d_i^+ = g_i, \quad i = 1, \ldots, m, \\
& x_j \geq 0 \quad (j = 1, \ldots, n), \quad d_i^-, d_i^+ \geq 0 \quad (i = 1, \ldots, m).
\end{aligned}
$$

Here, x_j are the decision variables, g_i are the target levels for each goal i, and d_i^-, d_i^+ are the negative and positive deviations from these targets. The weights w_i^-, w_i^+ represent the relative importance of under and over-achieving each goal. The constraint set $Ax \leq b$ represents the system's resource limitations or, in the case of this research, the physical restrictions of the network.

Goal and Target Setting

Since goals and their corresponding targets are established by the decision maker, both are inherently subject to bias [50]. Consequently, the outcome of a GP model can be influenced by subjective preferences introduced during the target-setting stage. To mitigate this, targets should be determined through a transparent and systematic procedure—for example, by deriving them from optimal single-objective solutions or established policy benchmarks. This approach reduces the potential for bias and ensures that model outputs reflect the physical realities of the system rather than arbitrary judgments, consistent with the recommendations of [51].

3.2.4 Extension & Contribution

This research considers three conflicting objectives, one derived from the linear program of the cell transmission model, along with two additional objectives introduced as extensions for this research:

- Maximize the demand released from source cells i in each time step t,
- Minimize occupancy in cells i in each time step t, adopted from [41]
- Maximize sink throughput from sink cells i in each time step t

The selection of these objectives is to achieve the overall goal of flattening the demand surge curve by regulating the timing of demand release, minimizing cell occupancies, and maximizing flow through the sink cells. The principal contribution of this research lies in the application of the goal programming methodology to these objectives. While linear programming identifies a single optimal solution, goal programming seeks to accommodate multiple, often conflicting goals by satisfying a hierarchy of targets. This methodological extension provides a more robust and realistic framework for decision-making, particularly in contexts where trade-offs are unavoidable. In the case of demand management, for example, goal programming enables the simultaneous consideration of throughput maximization and congestion minimization, yielding solutions that are both feasible and practically implementable as well as provide insights into the trade offs that occur between the objectives.

3.3 The Network: From Geographical to Cellular

Figure 3.4: Transformation from a geographic map to a node–arc network and then to a discretized cellular network.

In this study, the transformation of the road network into its cellular representation is performed using a proposed systematic method developed specifically for this research. The process begins with a detailed geographical map of the study area, where major decision intersections—those that significantly influence route choice and congestion—are represented as nodes, and the connecting road segments as arcs. This abstraction intentionally omits minor access points and local intersections to focus on the primary junctions governing network-wide flow, forming the foundation of the proposed cellular structure. This step produces the node–arc representation of the network, which serves as the base framework from which each roadway segment is subdivided into discrete cells according to its physical and operational characteristics. The intersections on the map correspond directly to nodes in the network, and the collection of these intersections forms the set of nodes used to define the spatial boundaries for the cell segmentation process.

The next step in the proposed transformation method is to define the length of each cell and determine the number of cells within each arc. In the proposed framework, the cell length (see equation 3.1.1) is calculated as the product of each link's free-flow speed (or posted speed limit) and the model's time step duration, ensuring that vehicle propagation across cells aligns with the network's operational conditions. Once the cell length is established, the number of cells along each link is obtained by dividing the physical length of the roadway segment by the computed cell length (see equation 3.1.2), allowing the proposed procedure to preserve the physical scale of the real-world network. Through this procedure, the node–arc network is systematically transformed into a cellular network using the proposed segmentation method, which serves as the structural basis for the cell network applied in this research.

3.3.1 Network Transformation Procedure

To standardize the conversion of road networks for replication in other scenarios, this research introduces a five–step framework specifically developed to transform any geographical map into its cellular representation for use within the modeling framework. This procedure formalizes the systematic approach proposed in this study, allowing consistent application across different urban contexts. **Five–Step Framework:**

1. **Select the area of study:** Identify the study region on a geographical map based on the modeling objectives.

2. **Identify points of interest:** Mark the source locations on the map, determine the major decision intersections and network boundaries.[9]

3. **Construct the node–arc network:** Connect nodes using links that represent roadway segments characterized by specific lengths and associated free–flow speeds (speed limits).[10]

4. **Discretize the node–arc network:** Using the formulas for cell length (3.1.1) and number of cells (3.1.2), subdivide each arc into discrete cells to construct the corre-

[9] A major decision intersection is defined as a location where a critical routing decision influences the flow of traffic along the network segment.

[10] In this research, a distance–measurement tool on Google Maps was used to determine the arc lengths between nodes.

sponding cell–based network.

5. **Identify cell types:** Using Figure 3.2, classify each cell according to its function (e.g., source, sink, ordinary, merging, or diverging).

3.4 Goal Programming - Cell Transmission Model Formulation

3.4.1 Model Introduction

This section introduces the proposed CTM–GP model, which extends Ziliaskopoulos' linear programming formulation of the cell transmission model. While the LP formulation demonstrated that the CTM could be expressed as an optimization problem, it was limited to a single objective—minimizing cell occupancy at all time periods. This research advances that framework by applying a goal programming methodology, enabling the simultaneous treatment of multiple, and often conflicting, objectives.

The GP formulation in this study incorporates three primary goals: (1) minimizing cell occupancy across time periods, (2) maximizing flow across links (i, j), and (3) maximizing the demand released at each time step t. Together, these objectives provide a more realistic and implementable framework for traffic management. In particular, the GP model allows the system to regulate both the amount and timing of demand release, thereby reducing demand surges while maintaining sufficient throughput and avoiding excessive congestion within the network.

3.4.2 Notation

Sets

C Set of cell types: $\{C_O$ (Ordinary), C_D (Diverging), C_M (Merging), C_R (Source),

C_S (Sink)}

$\mathcal{E}$ Set of cell connector types: $\{\mathcal{E}_O$ (Ordinary), $\mathcal{E}_D$ (Diverging), $\mathcal{E}_M$ (Merging), $\mathcal{E}_R$ (Source), $\mathcal{E}_S$ (Sink)$\}$

$\Gamma(i)$ Set of downstream (successor) cells connected to cell i (e.g., $i \to j$)

$\Gamma^{-1}(i)$ Set of upstream (predecessor) cells connected to cell i (e.g., $j \to i$)

$\mathcal{T}$ Set of discrete time steps $t \in \{0, 1, \ldots, T\}$, representing the model's time horizon

Parameters

N_i^t Maximum number of vehicles in cell i at time t

Q_i^t Maximum number of vehicles that can flow out of cell i at time t. When indexed by i, this represents sending capacity; when indexed by j, it represents downstream receiving capacity

δ_i^t Congestion propagation factor, defined as the ratio v/w for each cell at time t, where v is the free-flow speed and w is the backward wave speed

W_k Weight assigned to the deviation variable associated with goal k

D_i Amount of demand at source i, for all source cells $i \in C_R$

$\psi_i^{\min}$ Minimum flow requirement for all sink cells $i \in C_S$

T_1, T_2, T_3 Target values for Goals 1–3

Decision Variables

x_i^t Number of vehicles in cell i at time t. Cells are indexed by i and j, and time steps by t.

y_{ij}^t Flow from cell i to j at time step t, representing vehicles that depart from i at t and arrive at j at $t+1$.

d_i^t Demand (inflow to the network) from cell i at time t.

S_1, S_3 Slack variables corresponding to Goals 1 and 3, each representing the underachievement (shortfall) from their target values.

E_2 Excess variable corresponding to Goal 2, representing the overachievement (surplus) beyond its target value.

T_1, T_2, and T_3 represent the target values corresponding to the three goals that the model aims to achieve. Each target is obtained by solving the linear program for its respective goal independently under ideal conditions. W_1, W_2, and W_3 are the weights assigned to the deviational variables associated with each goal, determining their relative importance in the overall optimization. Three deviational variables are defined: S_1 (slack) for Goal 1, E_2 (excess) for Goal 2, and S_3 (slack) for Goal 3. The letter S denotes a slack variable, representing a negative deviation (underachievement) from the target in Goals 1 and 3. The letter E denotes an excess variable, representing a positive deviation (overachievement) from the target in Goal 2.

3.4.3 Model Formulation

Objective Function

$$\text{Minimize} \quad \boldsymbol{Z} = (W_1 \cdot S_1) + (W_2 \cdot E_2) + (W_3 \cdot S_2) \tag{3.4.1}$$

Subject to:

$$\text{Goal 1:} \quad \sum_i \sum_t d_i^t + S_1 = T_1, \ \forall i \in C_R \tag{3.4.2}$$

$$\text{Goal 2:} \quad \sum_i \sum_t x_i^t - E_2 = T_2, \ \forall i \in C \setminus C_S \tag{3.4.3}$$

$$\text{Goal 3:} \quad \sum_i \sum_j \sum_t y_{ij}^t + S_3 = T_3, \ \forall (i,j) \in E_S \tag{3.4.4}$$

$$x_i^t - x_i^{t-1} - \sum_j y_{ji}^{t-1} + \sum_j y_{ij}^{t-1} = 0 \qquad \forall i \in \mathcal{C} \setminus \{\mathcal{C}_{\mathrm{R}}, \mathcal{C}_{\mathrm{S}}\}, \ \forall t \in \mathcal{T} \tag{3.4.5}$$

$$x_i^t - x_i^{t-1} + \sum_j y_{ij}^t = d_i^{t-1} \qquad \forall i \in \mathcal{C}_{\mathrm{R}}, \ \forall t \in \mathcal{T} \tag{3.4.6}$$

$$x_i^t \leq N_i^t \qquad \forall i \in \mathcal{C}, \ \forall t \in \mathcal{T} \tag{3.4.7}$$

$$\sum_t d_i^t = D_i \qquad \forall i \in \mathcal{C}_{\mathrm{R}} \tag{3.4.8}$$

$$\sum_t \sum_i y_{ij}^t \geq \psi_j^{\min} \qquad \forall j \in \mathcal{C}_{\mathrm{S}} \tag{3.4.9}$$

$$\sum_j y_{ij}^t - x_i^t \leq 0 \qquad \forall i \in \mathcal{C}_{\mathrm{D}},\ \forall t \in \mathcal{T} \tag{3.4.10}$$

$$\sum_j y_{ij}^t \leq Q_i^t \qquad \forall i \in \mathcal{C}_{\mathrm{D}},\ \forall t \in \mathcal{T} \tag{3.4.11}$$

$$\sum_i y_{ij}^t \leq Q_j^t \qquad \forall j \in \mathcal{C}_{\mathrm{M}},\ \forall t \in \mathcal{T} \tag{3.4.12}$$

$$\sum_i y_{ij}^t + \delta_j^t x_j^t \leq \delta_j^t N_j^t \qquad \forall j \in \mathcal{C}_{\mathrm{M}},\ \forall t \in \mathcal{T} \tag{3.4.13}$$

$$d_i^t \leq Q_j^t \qquad \forall (i,j) \in \mathcal{E}_{\mathrm{R}},\ \forall t \in \mathcal{T} \tag{3.4.14}$$

$$y_{ij}^t - x_i^t \leq 0 \qquad \forall (i,j) \in \mathcal{E}_{\mathrm{O}} \cup \mathcal{E}_{\mathrm{R}},\ \forall t \in \mathcal{T} \tag{3.4.15}$$

$$y_{ij}^t \leq Q_j^t \qquad \forall (i,j) \in \mathcal{E}_{\mathrm{O}} \cup \mathcal{E}_{\mathrm{R}},\ \forall t \in \mathcal{T} \tag{3.4.16}$$

$$y_{ij}^t \leq Q_i^t \qquad \forall (i,j) \in \mathcal{E}_{\mathrm{O}} \cup \mathcal{E}_{\mathrm{R}},\ \forall t \in \mathcal{T} \tag{3.4.17}$$

$$y_{ij}^t + \delta_j^t x_j^t \leq \delta_j^t N_j^t \qquad \forall (i,j) \in \mathcal{E}_{\mathrm{O}} \cup \mathcal{E}_{\mathrm{R}},\ \forall t \in \mathcal{T} \tag{3.4.18}$$

$$y_{ij}^t - x_i^t \leq 0 \qquad \forall (i,j) \in \mathcal{E}_{\mathrm{S}},\ \forall t \in \mathcal{T} \tag{3.4.19}$$

$$y_{ij}^t \leq Q_i^t \qquad \forall (i,j) \in \mathcal{E}_{\mathrm{S}},\ \forall t \in \mathcal{T} \tag{3.4.20}$$

$$y_{ij}^t \leq Q_j^t \qquad \forall (i,j) \in \mathcal{E}_{\mathrm{D}},\ \forall t \in \mathcal{T} \tag{3.4.21}$$

$$y_{ij}^t + \delta_j^t x_j^t \leq \delta_j^t N_j^t \qquad \forall (i,j) \in \mathcal{E}_{\mathrm{D}},\ \forall t \in \mathcal{T} \tag{3.4.22}$$

$$y_{ij}^t - x_i^t \leq 0 \qquad \forall (i,j) \in \mathcal{E}_{\mathrm{M}},\ \forall t \in \mathcal{T} \tag{3.4.23}$$

$$y_{ij}^t \leq Q_i^t \qquad \forall (i,j) \in \mathcal{E}_{\mathrm{M}},\ \forall t \in \mathcal{T} \tag{3.4.24}$$

$$d_i^t = 0 \qquad \forall i \in \mathcal{C} \setminus \mathcal{C}_{\mathrm{R}} \tag{3.4.25}$$

$$x_i^0 = \xi_i \qquad \forall i \in \mathcal{C} \tag{3.4.26}$$

$$y_{ij}^0 = 0 \qquad \forall (i,j) \in \mathcal{E} \tag{3.4.27}$$

$$d_i^t \geq 0 \qquad \forall i \in \mathcal{C},\ \forall t \in \mathcal{T} \tag{3.4.28}$$

$$x_i^t \geq 0 \qquad \forall i \in \mathcal{C},\ \forall t \in \mathcal{T} \tag{3.4.29}$$

$$y_{ij}^t \geq 0 \qquad \forall (i,j) \in \mathcal{E},\ \forall t \in \mathcal{T} \tag{3.4.30}$$

3.4.4 Model Description

Objective Function

The objective function, shown in Equation 3.4.1, defines the model's primary objective — minimizing the overall deviation from the specified performance goals. Z represents the total weighted deviation from the target values associated with each goal. Each goal is assigned a weight (W_1, W_2, W_3) reflecting its relative importance or priority within the model. The deviational variables (S_1, E_2, S_3) measure the extent to which each goal is under- or over-achieved:

- S_1 represents the *slack*, or negative deviation from the first goal—indicating how much the solution falls short of the target value.
- E_2 represents the *excess*, or positive deviation from the second goal—indicating how

much the solution surpasses the target.

- S_3 represents the *slack*, or negative deviation from the third goal.

The objective function therefore minimizes Z, the weighted sum of all deviational variables, thereby balancing trade-offs among the goals based on their assigned weights.

Goal Constraints

Equations (3.4.2 – 3.4.4) define the goal constraints of the model. Goal 1 specifies that the total admitted demand should meet the target value T_1. This goal applies to all source cells, as they represent the network entry points where demand is released. Goal 2 requires that the total cell occupancy matches the target value T_2. This goal applies to all cells except the sink cells, since sink cells do not retain vehicles and therefore have no occupancy. And goal 3 specifies the total flows on all cell connectors leading to a sink cell aspire to reach the target value T_3. This goal applies exclusively to sink cells and represents the model's measure of evacuation efficiency—that is, the rate at which demand exits the network. These goals reflect three competing objectives of the system: regulating demand entry into the network, managing overall congestion, and maximizing flow on cell connectors to the sink cells. Deviational variables linked to each goal measure any shortfall or excess relative to these targets, ensuring that the model can remain feasible even when both goals cannot be satisfied simultaneously.

Flow Constraints

Equations (3.4.5 – 3.4.30) define the flow constraints of the formulation. Adapted from Ziliaskopoulos's formulation, these constraints ensure that the model accurately represents the traffic dynamics of the network. The constraints can be grouped into two primary categories: occupancy constraints for cells and flow constraints for cell connectors. The initial conditions and non-negativity constraints are specified at the end of the formulation, in equations (3.4.25 – 3.4.30). Within this framework, both cells and cell connectors are subject to constraints that vary depending on the type of cell or cell connector. The key distinction among these constraints lies in the relationship between upstream and downstream cells. For example, a diverging cell differs from an ordinary cell in its flow-capacity structure: a diverging cell connects to two downstream cells and one upstream cell, whereas an ordinary cell connects to a single upstream and a single downstream cell.

Cell and Connector Constraints

Ordinary Cells & Connectors:

Equation (3.4.5) defines the mass conservation constraint for all cells except source and sink cells. In minimum cost network flow formulations, this constraint is often referred to as a flow-balance constraint. It ensures that the number of vehicles in cell i at time t equals the number of vehicles in the previous time step, adjusted by the inflows and outflows occurring during that interval. Equations (3.4.15 – 3.4.18) define the constraints applied to the connectors associated with ordinary and source cells. Equation (3.4.15) constrains the outgoing flow by the occupancy level of the upstream cell i, ensuring that flow cannot exceed the number of vehicles available to move downstream. Equations (3.4.16) and (3.4.17) impose the receiving and sending capacity limits, respectively, restricting flow to the maximum feasible level along each connector (i, j). Finally, Equation (3.4.18) defines the queue spill-back constraint, which limits flow based on both the propagation factor δ_j^t [11] and the maximum occupancy N_j^t of the downstream cell.

In the standard cell transmission model, the parameter δ_i^t represents the propagation factor, defined as the ratio between the free-flow speed v and the backward wave speed w, that is, $\delta = \frac{v}{w}$. This parameter governs how congestion propagates upstream through the network: when $w < v$, a reduction in downstream capacity causes backward-moving shockwaves that limit upstream flow, representing queue spillback behavior. In this study, δ is fixed to 1, implying that $v = w$. This simplification assumes that the forward and backward wave speeds

[11]Note. When a variable is indexed by j this refers to it being downstream or a receiving variable

are equal, effectively removing backward propagation effects. The decision to set $\delta = 1$ allows the model to isolate and evaluate the performance of the demand-release mechanism without introducing additional variability due to congestion-wave dynamics. While this assumption simplifies network behavior, it remains a valid approximation for analyzing the effectiveness of demand management policies in controlled scenarios.

Source Cells & Connections:

Equation (3.4.6) defines the mass-conservation constraint for source cells, governing how new demand is injected into the network. It ensures that the total flow released from each source cell at time t equals the available demand from the previous time step, maintaining consistency between externally generated demand and the flow admitted into the network. The flow from each source is summed across all downstream connections j to account for demand entering the system in multiple directions. This modeling approach is particularly relevant to urban networks, where a single demand source—such as a school or residential area—may release vehicles onto several adjoining road segments leading to different destinations. This constraint links the external demand boundary to the internal cell dynamics, bridging the transition from demand generation to physical vehicle movement within the modeled network. Operationally, source cells act as controlled entry points—they cannot discharge more vehicles than their available demand, preserving realistic release limits in congestion-management strategies.

Equation (3.4.7) introduces a cell-level capacity constraint that limits occupancy to each cell's maximum allowable density N_i^t. This ensures that no cell can exceed its jam-density condition, reflecting the physical upper bound of road segment capacity. By enforcing this limitation, the model preserves the realism of congestion effects and prevents infeasible accumulation of vehicles in highly saturated regions. Together, Equations (3.4.6) and (3.4.7) establish the dynamic relationship between demand injection and physical storage limits across the network.

Equation (3.4.8) ensures that the total demand released from each source cell over all time steps equals the demand parameter D_i that is predetermined for that source. This constraint guarantees that every demand source fully discharges its assigned number of vehicles by the end of the time horizon. Similarly, Equation (3.4.14) restricts the instantaneous demand release rate by bounding d_i^t with respect to the capacity of its downstream cell Q_j^t. Together, these constraints establish both temporal and spatial control over demand release: the former ensures that total demand is met, while the latter prevents over-saturation by linking source inflow rates to the physical receiving capacity of adjacent cells. These constraints also reflect the structure of urban networks, where demand originates from within the system rather than entering from its boundaries. In such settings, sources represent localized generators of traffic—such as schools or residential clusters—embedded directly within the network, rather than peripheral entry points along the network border.

Sink Cells & Connections:

Sink cells represent the network boundaries where vehicles exit the system. This study models multiple exit points, yielding a multiple-destination network. To avoid degenerate solutions that leave some exits unused, Equation (3.4.9) imposes a per-sink minimum total discharge over the horizon. This requirement ensures strictly positive usage of every sink (via $\psi_j^{\min} > 0$), promoting balanced exit utilization consistent with a System Optimum (SO)–type traffic assignment, where total network performance is prioritized over individual routes. Equations (3.4.19) and (3.4.20) specify the connector constraints into sink cells. The first constraint limits flow by the upstream occupancy. The second caps flow by the upstream sending capacity, preventing discharge beyond the cell connectors's physical limit.

Diverging Cells & Connectors:

Diverging cells are characterized by a single upstream cell that distributes flow to multiple downstream cells (See Figure 3.2). Physically, this cell type corresponds to a road segment that splits into two or more separate paths, such as a fork or junction. The equations in this section describe the flow dynamics and capacity constraints associated with diverging movements. These equations sum over all downstream cells j connected to a common upstream cell i, capturing the total discharge distributed across multiple directions. Equation (3.4.10) limits the total outflow to the current occupancy of the diverging cell, ensuring that discharge does not exceed the number of vehicles available for release. Equation (3.4.11) further constrains total outflow by the cell's sending capacity Q_i^t, imposing a physical upper bound on the discharge rate. Equations (3.4.21) and (3.4.22) apply to the diverging connectors that link an upstream cell to its downstream neighbors, ensuring that flow constraints are consistently enforced across all outgoing branches. The first of these limits flow entering each downstream cell by its receiving capacity Q_j^t, ensuring that inflow does not exceed the available receiving space. The second introduces a queue-spillback condition that couples flow with the downstream cell's propagation factor δ_j^t and its maximum occupancy N_j^t, thereby reducing inflow as downstream congestion builds.

Merging Cells & Connectors:

In contrast to diverging cells, merging cells represent locations where multiple upstream flows converge into a single downstream cell. These constraints are distinguished by where the summation is applied: here, summations are taken over the upstream cells i to capture the total inflow entering the common downstream cell j. Physically, merging junctions correspond to locations such as highway on-ramps or intersections where two or more road segments combine into one. Equations (3.4.12) and (3.4.13) apply directly to merging cells. These equations aggregate inflows from all upstream cells into a single downstream cell, representing the total volume entering that location. Equation (3.4.12) ensures that the total inflow does not exceed the downstream cell's receiving capacity Q_j^t, while Equation (3.4.13) introduces a queue-spillback condition that limits inflow when the downstream cell approaches its maximum occupancy N_j^t. Equations (3.4.23) and (3.4.24) apply to merging connectors, which represent the individual links feeding into the downstream cell. Equation (3.4.23) enforces the relationship between flow and occupancy, ensuring that discharge from each upstream cell does not exceed the number of vehicles available for release. Equation (3.4.24) defines the sending capacity, restricting flow to the physical maximum Q_i^t for each upstream cell connector.

Initial Conditions & Non-Negativity:

Equations (3.4.25 – 3.4.30) define the initial and non-negativity conditions of the model. Equation (3.4.25) ensures that demand is injected only from designated source cells, preventing unintended inflows elsewhere in the network. Equation (3.4.26) establishes the initial occupancy levels for all cells, while equation (3.4.27) initializes cell connector flows to zero at the beginning of the time horizon. Finally, Equations (3.4.28 – 3.4.30) enforce non-negativity for all decision variables—occupancy, demand, and flow—ensuring that all quantities remain physically meaningful and that the model remains feasible throughout the optimization.

3.4.5 Additions to the Ziliaskopoulos Linear Program

Ziliaskopoulos's linear program establishes the foundation for optimizing the cell transmission model to identify optimal traffic flow conditions [41]. This research extends that framework by reformulating the CTM into a goal programming model. The GP formulation addresses multiple, often conflicting objectives: maximizing the release of demand units from all source cells i throughout the time horizon, minimizing network-wide cell occupancy, and maximizing the flow on cell connectors leading to sink cells to ensure evacuation of all the in-network demand units. By employing a multi-objective optimization approach, this method feasibly balances competing goals and offers a more realistic framework for managing network demand and congestion.

While optimization is valuable, it often lacks practical applicability because strict optimality assumes and requires ideal conditions. Goal programming offers a more realistic alternative by balancing optimal conditions in a way that better reflects how objectives interact in real networks. It also provides explicit insight into the trade-offs that emerge when one objective is prioritized over another. The originality of this research lies in reformulating the LP-CTM by Ziliaskopoulos into a goal programming model specifically tailored to urban networks, thereby extending the framework from single- to multi-objective optimization. Furthermore, the proposed model is applied to a real-world case study representing a multiple-source, multiple-destination network, demonstrating its capacity to capture complex urban traffic interactions and evaluate system-level performance.

In addition to introducing a multi-objective optimization structure, this research modifies several constraints of the original LP-CTM to more accurately represent real-world traffic conditions and demand-management objectives. Equation (3.4.6) extends the source cell flow balance by summing flows across all downstream cell connectors, enabling each source to distribute demand in multiple directions simultaneously, an essential adaptation for urban networks with multiple directional exits. Equation (3.4.7) formalizes a generalized capacity limit for all cell types, ensuring that occupancy does not exceed each cell's dynamic maximum capacity N_i^t. Equation (3.4.9) introduces a minimum sink flow requirement, ensuring strictly positive utilization of all sink cells to promote balanced network outflows in multi-destination systems.

Equation (3.4.8) enforces complete satisfaction of demand for each source over the time horizon, maintaining conservation between external demand inputs and admitted flows. This assumption—that demand originates externally—forms the basis of the model's structure. Understanding the magnitude of this external demand provides valuable insight into how it can be managed to mitigate congestion within the network. Finally, equation (3.4.14) constrains the maximum discharge rate per time step, capturing operational restrictions such as release schedules or intersection throughput limits.

Together, these additions extend the LP-CTM framework into a more comprehensive and policy-relevant goal programming-cell transmission model (GP-CTM) model, capable of modeling controlled release strategies and evaluating system-wide evacuation efficiency in urban environments. The model demonstrates that effective demand management can enhance overall network occupancy and performance. The next chapter presents a case study applying this formulation to a real traffic network, demonstrating its ability to capture trade-offs and support decision-making under realistic conditions.

Methodological Limitations

The GP–CTM developed in this research is based on the linear programming LP formulation proposed by Ziliaskopoulos [41], which reformulated the nonlinear Cell Transmission Model CTM to obtain a system-optimal SO solution. However, the LP formulation is an approximation of Daganzo's ([36], [37]) CTM, as it replaces the nonlinear minimum operators governing sending and receiving flows with a set of linearly relaxed inequalities. This linearization enhances computational efficiency but abstracts from the full complexity of traffic dynamics and provides an aggregate approximation of flow propagation rather than an exact physical representation, a simplification also noted by Aziz [42]. A known consequence of this linear relaxation is the so-called *holding-back phenomenon*, in which upstream cells may retain flow even when downstream capacity is available. Two potential approaches for addressing this issue can be gleaned from Aziz [42] and Ukkusuri [39].

The first, as noted by Aziz, suggests introducing additional constraints and modifying the objective function to maximize network flow and thereby reduce holding-back occurrences. The second, proposed by Ukkusuri, introduces a penalty term in the objective function to discourage vehicle retention and incentivize forward propagation, thereby mitigating the holding-back phenomenon. The proposed GP–CTM does not explicitly address this issue but acknowledges the limitation in its formulation and recommends incorporating one of these variations to the formulation in future work.

Chapter 4

Case Study: Sabah Al Salem

4.1 Context & Background

A lack of effective demand management strategies in traffic networks often leads to sudden increases in traffic density. Such spikes inevitably produce congestion and, in severe cases, gridlock that can last for hours. This is particularly true in Kuwait, where reliance on private vehicles is high due to the structure and organization of the country's towns and cities as well as cultural factors. In 2020, Kuwait had approximately one private vehicle for every two residents. With a population of about 4.4 million, this translates to roughly 2.4 million registered vehicles [52] [6]. Notably, Kuwait's total number of vehicles is higher than that of the United Kingdom, despite its much smaller geographic area. The United Kingdom, with a population of approximately 67 million, has 41 million registered vehicles, roughly one car for every 1.6 people [53]. According to data from the World Bank, Kuwait is approximately fourteen times smaller than the United Kingdom [54] (See Figure 4.1). The consequences of this imbalance are significant: in 2020, congestion was estimated to have caused a loss of approximately 633 million Kuwaiti dinars in lost productivity and travel delays [52]. As noted in chapter 1, commuters in Kuwait spend an average of 67 minutes per day in traffic [5], underscoring the severity of congestion across the country's urban areas.

Figure 4.1: An illustration of the relative land area of Kuwait compared to the United Kingdom.

In response to these challenges, Kuwait has primarily relied on supply-side interventions—such as signal timing optimization [14] and physically increasing the capacity of the roadway, which according to braes paradox [12] is not an effective congestion mitigation strategy. While these measures provide short-term relief at the local level, they fail to address the root issue, unmanaged spikes in travel demand. In contrast, demand-side strategies, particularly those that regulate traffic inflow at its source, remain significantly underutilized. This study aims to bridge this gap by demonstrating how a demand-release model can mitigate congestion in real-world urban contexts affected by recurrent traffic demand surges.

To demonstrate the potential of a demand-management approach, this chapter applies the model developed in chapter three to a real-world case study. The original LP-CTM formulation was evaluated on a hypothetical network to illustrate its theoretical potential. In contrast, this study applies the extended model to a real-world urban network to assess its practical performance. The model is designed to regulate the inflow of demand entering the system from external sources. Its primary purpose is to smooth demand surges so that network capacities are not exceeded, thereby preventing congestion and reducing the risk of gridlock, preemptively.

The selected case study focuses on a block of approximately 2 km^2 in the Sabah Al Salem area of Kuwait [1] (See figure 4.2). This block features a distinctive mix of land uses, including international hospitals, schools, gyms, salons, and other commercial facilities, that generate varying levels of traffic activity across different hours. Given its limited geographical size, even moderate spikes in demand can strain the local network and lead to recurrent congestion. While such challenges may partly stem from shortcomings in urban planning, this study does not aim to evaluate local planning policies. Instead, it examines how the proposed model can provide practical solutions to the pressing issue of traffic demand management within the existing network conditions.

The area was selected primarily due to its notably high concentration of schools within a compact geographic area. There are six K–12 schools in the area. The synchronized and predictable dismissal times of these schools produce concentrated, recurring surges in traffic demand. These characteristics make Sabah Al Salem a suitable environment for testing the demand-release model. Additionally, the area has experienced chronic congestion since its development, highlighting the need for innovative traffic control strategies that address the limitations of earlier planning decisions.

Accordingly, the model application in this case study focuses on the critical period of 2:00 p.m., when all six schools dismiss their students. The stakeholders most directly affected include students, parents, and local residents. At the institutional level, the Ministry of Education and the Ministry of Interior are responsible for school scheduling and traffic regulation, respectively. Local businesses are also indirectly affected, as recurring congestion

[1] In Kuwait, each area is composed of multiple blocks. This definition of a block differs from that used in the United States, as Kuwaiti blocks are considerably larger.

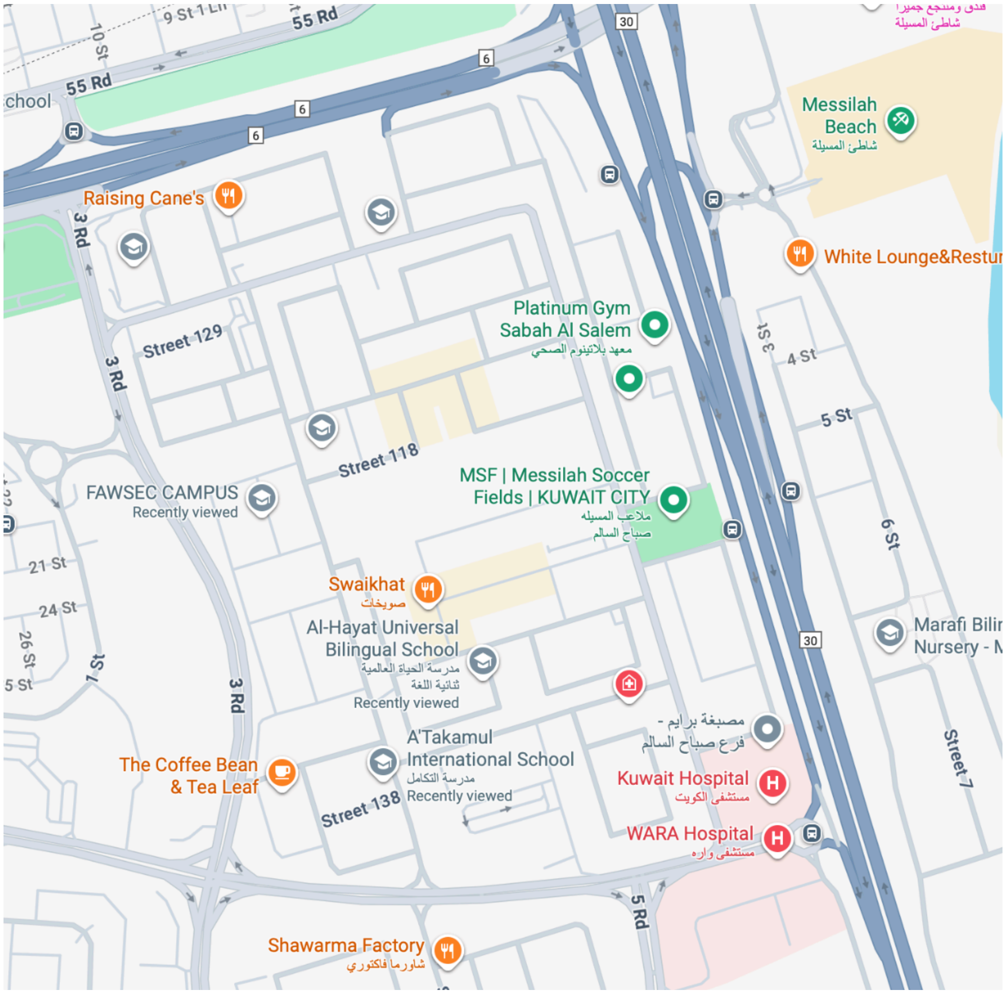

Figure 4.2: Map of the case study area, Sabah Al Salem, Kuwait (Map data ©2025 Google).

limits accessibility to the area. By employing the GP-CTM framework to develop a demand-release schedule for managing stored demand at its sources—most notably schools—this study seeks to demonstrate how managing demand can increase traffic flow. In doing so, it provides an opportunity to evaluate the model's capacity to improve mobility conditions in an area where existing infrastructure is consistently stressed by demand surges. Sabah Al Salem also serves as a representative example of several urban areas in Kuwait facing similar conditions. Its compact size allows the study to generate meaningful insights that can be scaled up to inform larger applications.

The remainder of this chapter is organized as follows. Section 4.2 describes the network transformation that converts the Sabah Al Salem road system into a cell-based structure suitable for the GP–CTM framework. Section 4.3 defines the model parameters and target settings used in the formulation. Section 4.4 verifies and validates the implementation by applying the formulation to the Ziliaskopoulos test network. Section 4.5 reports results comparing the baseline 'All-at-Once' policy with the optimized GP–CTM demand-release schedules. Interpretation and broader implications are reserved for Chapter 5. By embedding the GP–CTM framework in a real-world context, this study highlights its technical feasibility and broader potential for managing traffic congestion in Kuwait.

4.2 Network Transformation

In this section, theoretical principles are applied in practice to develop a node–arc representation of the study area, which is then transformed into a cellular structure consistent with the CTM framework. The transformation process—from physical map to network to cell-based representation—follows the five-step procedure outlined in Chapter three. By adhering to this framework, the resulting model maintains the essential dynamics of traffic flow while ensuring computational tractability. Figure 4.3 summarizes the proposed five-step transformation procedure, illustrating how the physical layout of Sabah Al Salem is systematically converted into a cell-based network suitable for GP–CTM implementation.

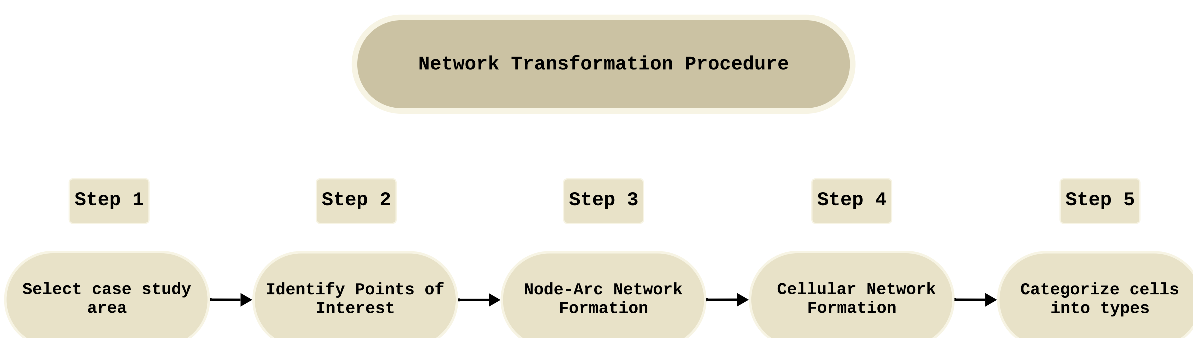

Figure 4.3: Five-step network transformation procedure used to develop the GP–CTM model. Step 1 selects the case study area, Step 2 identifies key network elements, Step 3 forms the node–arc network, Step 4 generates the cellular network, and Step 5 categorizes cells by type.

4.2.1 Network Transformation Procedure

Step 1: Case Study Area Selection

The first step in the transformation procedure is to select the case study area, shown in Figure 4.2. Defining the spatial scope establishes the foundation for subsequent network modeling. As discussed in Section 4.1, Sabah Al Salem provides a suitable environment for applying the GP–CTM demand-release model because of its high concentration of demand sources within a compact area. Within approximately 2 km^2, there are six K–12 schools. Based on an interview with the principal of an international private school in Kuwait, each of these schools has an estimated enrollment of (1,000–1,500) students [2]. The network layout surrounding these schools provides important spatial context for understanding local traffic behavior. The network comprises three types of roads: secondary, minor, and residential. Secondary roads consist of two-lane, one-way corridors, with a physical median separating opposite directions of travel. Minor and residential roads are narrower, typically comprising one lane in each direction separated only by a painted line.

This area provides three key advantages for demonstrating the effectiveness of the model. First, the high concentration of demand sources aligns with the model's primary goal—to regulate inflows and release rates in order to maintain optimal traffic flow within the network. Second, using schools as demand sources provides a predictable and consistent daily demand pattern, making the scenario both repeatable and representative of recurrent traffic congestion. Third, Sabah Al Salem is not heavily affected by other types of congestion; rather, the main issue stems from the imbalance between business activity and road capacity.

Step 2: Identifying Points of Interest

The second step of the Network Transformation Procedure identifies key points of interest: demand sources, major decision intersections, and network boundaries—that serve as

[2] Personal communication with the principal of an international private school in Kuwait, 2025 [55].

the nodes of the network. Following the node-definition guidelines outlined by Chiu [56], demand sources, primarily schools, major decision intersections, and network boundaries were designated as nodes to capture the essential flow-control points within the study area. The node–arc network was constructed using OpenStreetMap (OSM) data as the foundational spatial layer, ensuring accurate road geometry and connectivity [57].

To represent the flow of the traffic network, only major decision intersections were designated as nodes. This approach maintains the analytical focus of the model while capturing the essential structure of traffic flow within the network. Although it is possible to model all intersections as nodes, this approach substantially increases computational requirements due to the resulting high number of cells. To ensure model efficiency, only major decision intersections, those most relevant to traffic flow, were retained as nodes. This simplification allows the analysis to concentrate on critical junctions that influence demand release and traffic flow, while a more detailed, intersection-level model could be explored in future research. The goal of this research is not to model traffic dynamics and movement in detail; rather, it aims to analyze aggregate-level flow and network occupancy. A more granular perspective would require alternative modeling techniques that fall outside the scope of this study. Figure 4.2 shows the selected decision nodes overlaid on the road network.

Step 3: Constructing the Node-Arc Network

The third step connects the identified nodes to form the node–arc network, which represents the road system as a directed graph. This step is essential for establishing network connectivity before discretizing it into cells. The node–arc network enables arc lengths to be defined, which is pivotal for determining cell lengths and the number of cells per arc in the next step. Arc lengths were measured using the distance measurement tool in Google Maps [58], which provides accurate travel distances along road segments. Because node identification was simplified to include only major decision points, some arcs incorporate curved or turning segments, meaning the recorded arc length reflects the total travel distance along the path rather than straight-line geometry. Each arc represents a road segment between

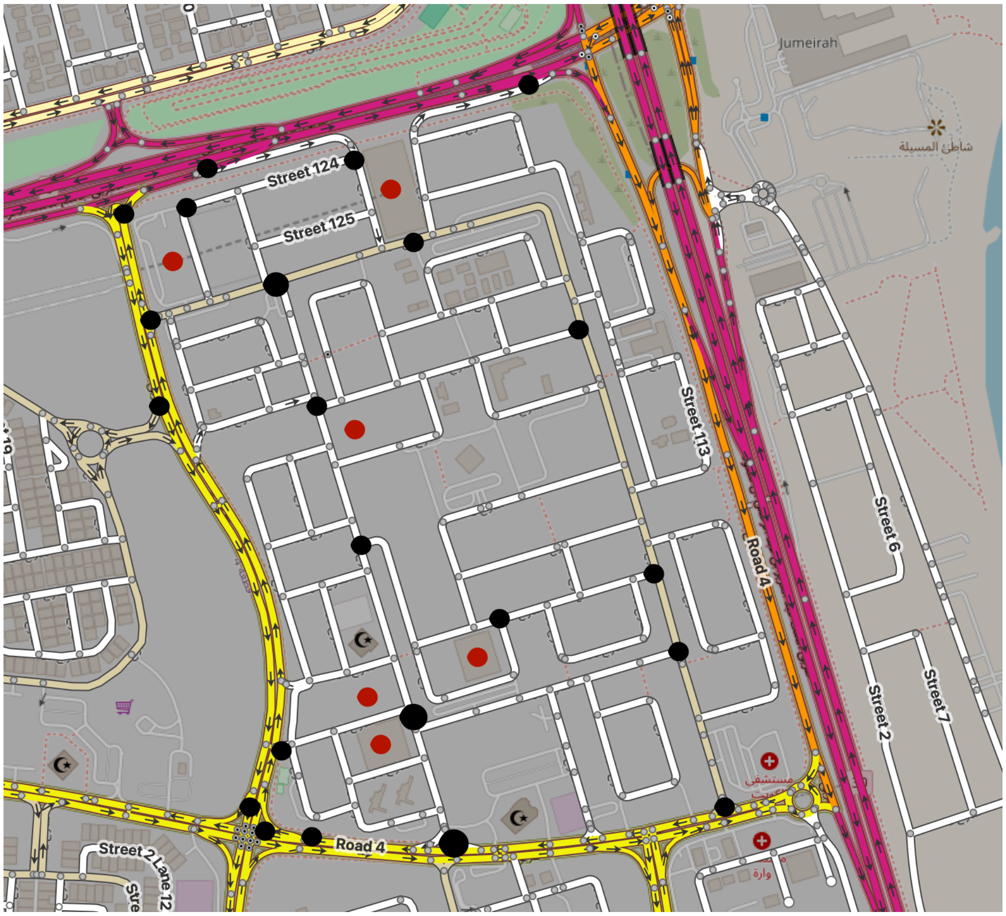

Figure 4.4: Node identification in the case study area, Sabah Al Salem. Red nodes denote demand sources, while black nodes indicate major decision intersections and network entry points. This configuration defines the nodal structure used for subsequent network transformation. (Map data © OpenStreetMap contributors).

intersections, with directionality assigned according to observed traffic flow patterns.

Two criteria were applied to exclude non-essential road segments:

Criterion 1: Roads forming closed loops without connecting to demand sources or points of interest.

Criterion 2: Roads not classified as secondary, minor, or residential in the OpenStreetMap dataset.

Figure 4.5 shows the resulting node–arc network. It includes both unidirectional and bidirectional flows, reflecting the actual roadway layout of the study area. The figure also identifies demand sources (1–6), entry points (7–11) connecting those sources to the network, and the boundary nodes (25–29) that define the network's spatial limits. The next step discretizes each arc into cells to prepare for the formation of the cellular network.

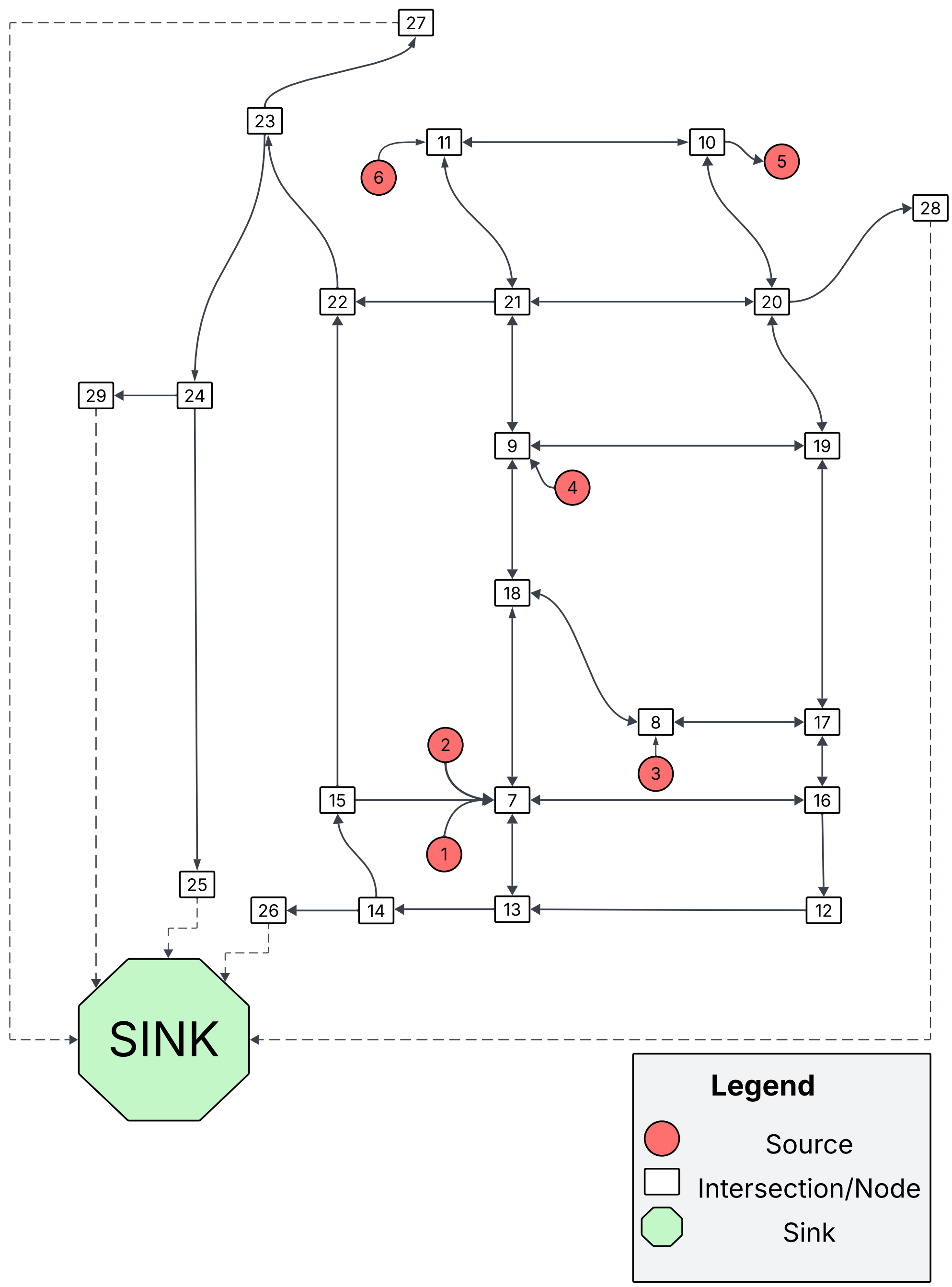

Figure 4.5: Completed node–arc network for the case study area, Sabah Al Salem. The network includes both unidirectional and bidirectional traffic flows.

Step 4: Discretizing the Node–Arc Network

In this step, each arc in the network is discretized into a series of cells following the method introduced by Daganzo [36] and summarized in Section 3.1. In this formulation, cell length and the number of cells are determined by two primary equations, which together define the spatial discretization required by the cell transmission model . The first equation (3.1.1), which determines the cell length (L), requires two key parameters: the free-flow speed v (ft/s) and the model time-step duration Δt. This equation ensures that the model adheres to the *"time-scan"* strategy outlined by Daganzo [36, 37], in which a vehicle must be able to traverse an entire cell within a single time step. The second equation (3.1.2) determines the number of cells along each arc, thereby defining the cellular structure of the network.

Speed Adjustments: Free-flow speeds were assigned to each road segment based on road classification and adjusted for local geometric or operational conditions such as curvature and intersection density. Speeds ranged from 25–60 ft/s, converted from posted limits (45–80 km/h for secondary roads and 30–45 km/h for minor and residential roads).

Time Step: The model uses a 10-second time interval ($\Delta t = 10$ s), consistent with Daganzo's CTM guidelines [36].

Length Adjustments: Arc lengths represent effective travel distances between decision nodes and were measured using the Google Maps distance tool [58]. These distances account for curves and lane shifts rather than straight-line geometry.

Network Calibration: The discretization process ensures that cell lengths, free-flow speeds, and arc distances satisfy CTM modeling constraints. While certain simplifications were introduced, they do not compromise the study's objective of evaluating the aggregate effects of demand-release strategies on traffic conditions. Figure 4.6 illustrates the resulting cell-based network, and the characteristics of each arc are summarized in Appendix A, Table A.1.

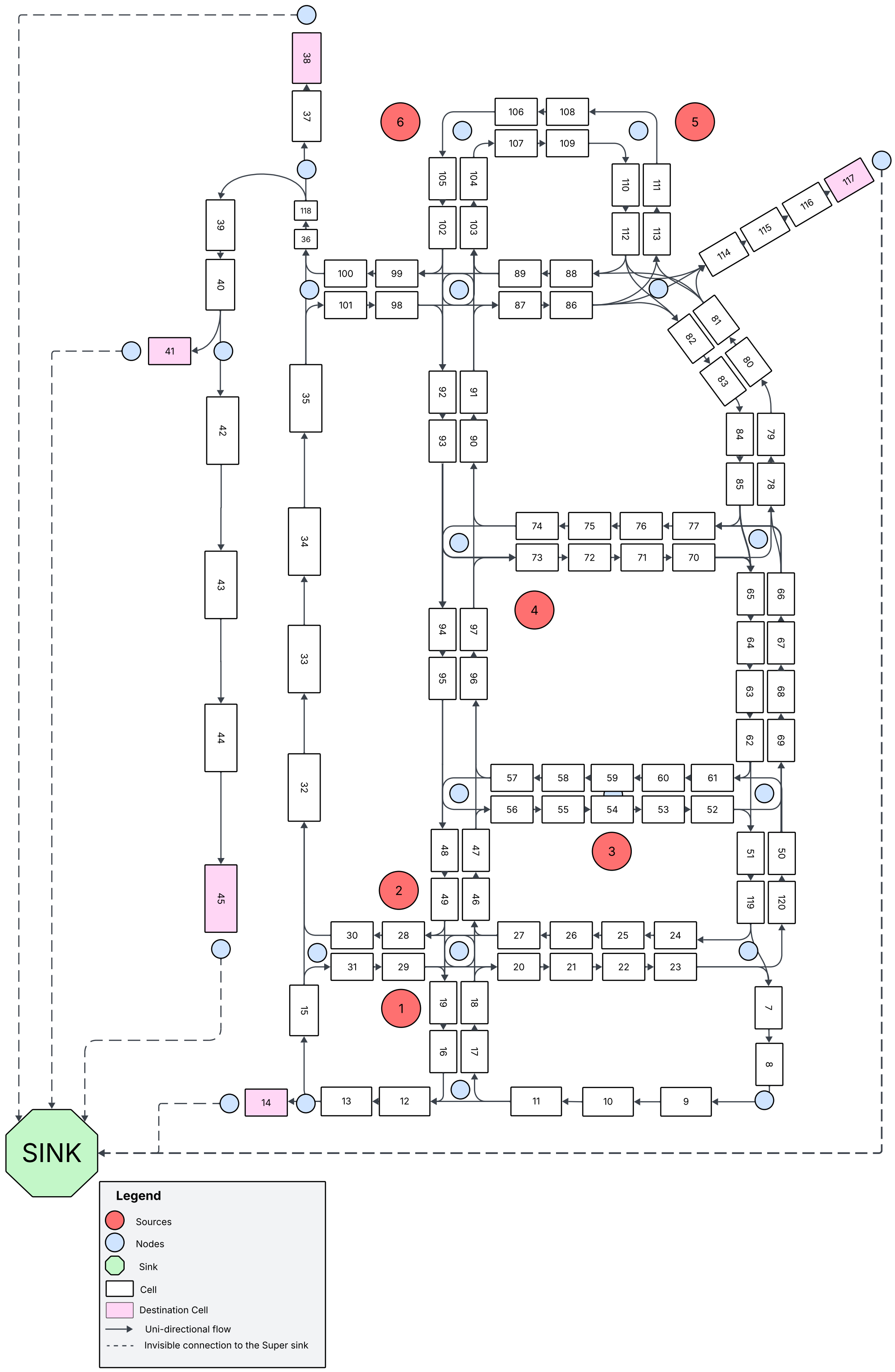

Figure 4.6: Cell-based representation of the Sabah Al Salem traffic network. Red circles denote demand sources, blue circles mark major decision nodes, and the green octagon represents the system sink. Purple cells correspond to destination cells connecting to the super sink. Dashed lines indicate invisible connections to the super sink used to balance network outflows.

Step 5: Cell Type Identification

There are five cell types described by Daganzo [37] (see Figure 3.2). These include: (1) ordinary cells, which have one upstream and one downstream cell; (2) diverging cells, which have one upstream cell and multiple downstream cells where vehicles split into different paths; (3) merging cells, which combine flows from multiple upstream cells into a single downstream cell; (4) source cells, which have no upstream cells and represent entry points into the network; and (5) sink cells, which represent exit points or the end of the physical network. Based on this criterion, the cells in the network shown in Figure 4.6 are categorized accordingly.

Table 4.1: Cell classification by type

Cell Type	**Cell Numbers**
Source Cells	(1–6)
Ordinary Cells	(8, 9, 10, 16, 17, 21, 22, 24, 25, 26, 30, 31, 33, 34, 37, 39, 42, 43, 44, 53, 54, 55, 58, 59, 60, 63, 64, 67, 68, 71, 72, 75, 76, 80, 83, 84, 100, 101, 104, 105, 106, 107, 108, 109, 110, 111, 115, 116, 120)
Merging Cells	(7, 12, 19, 20, 28, 32, 36, 46, 48, 51, 56, 61, 65, 69, 73, 77, 82, 87, 88, 90, 92, 94, 96, 99, 103, 113, 114)
Diverging Cells	(11, 13, 15, 18, 23, 27, 29, 35, 40, 47, 49, 50, 52, 57, 62, 66, 70, 74, 78, 81, 85, 86, 89, 91, 93, 95, 97, 98, 102, 112, 118, 119)
Sink Cells	(14, 38, 41, 45, 117)

4.3 Model Integration and Parameter Definition

The GP-CTM model relies on a set of parameters that characterize the physical and operational properties of the network. These parameters include: cell storage capacity (N_i), cell flow capacity (Q_i), and external demand (D_i) at source cells. Unlike traditional implementations of the cell transmission model, such as that proposed by Ziliaskopoulos [41], the GP-CTM formulation developed in this study does not incorporate time-dependent demand profiles. Instead, the model assumes that demand is held at its sources and released in controlled quantities determined through system-wide optimization. This approach effectively transforms external demand from a time-varying input into a decision variable. As a result, the model relies entirely on time-invariant parameters to characterize system constraints, while the time evolution of the system emerges from internal dynamics and the chosen demand release schedule.

A key conceptual contribution of this study is a reconceptualization of how traffic demand is represented within the modeling framework. Traditional traffic models typically represent demand as a volume-based, time-dependent input—essentially a forecasted number of vehicles attempting to enter the system at each time step [41]. In contrast, this study conceptualizes demand as a form of potential energy, a latent quantity that resides outside the network but can be actively regulated. Under this view, demand transitions from a constraint to be accommodated to a controllable variable, one that can be stored, timed, and released to enhance overall system performance. This shift moves from a reactive approach, which responds to congestion after it occurs, to a proactive one that actively manages inflow rates to maintain stable network conditions. This model assumes that demand is a fully controllable variable. While this represents a limitation of the approach, in practice demand can be influenced and regulated indirectly through incentive structures and policy interventions.

4.3.1 Cell Storage Capacity (N_i)

The storage capacity of each cell depends on the jam density (k_j), the cell length (L), and the number of lanes (m). Following [59], jam density is approximately 142 vehicles per kilometer per lane, based on typical passenger vehicle lengths and standstill gaps.

Converting to feet (where 1 km = 3280.84 ft):

$$k_j = \frac{142}{3280.84}\ \text{veh/km/lane} \ = \ 0.0433\ \text{veh/ft/lane} \tag{4.3.1}$$

Thus, the maximum number of vehicles in a cell is calculated as:

$$N_i = \lfloor k_j \cdot L \cdot m \rfloor \tag{4.3.2}$$

4.3.2 Flow Capacity (Q_i)

The flow capacity (Q_i) represents the maximum number of vehicles that can exit a cell within a single time step. When indexed by i, Q_i denotes the *sending capacity* of cell i, while when indexed by j, it represents the *receiving capacity* of cell j. Consistent with HCM recommendations for ideal, uninterrupted flow conditions, a base capacity of 2,000 passenger cars per hour per lane (pcphpl) is adopted as an upper-bound estimate [28]. Although the study area comprises local and minor roads, this assumption provides a standardized benchmark for evaluating demand-release performance. With a model time step of 10 seconds $\left(\Delta t = \frac{10}{3600}\,\text{h}\right)$, the per-lane, per-step capacity is computed as:

$$Q_i = \lfloor q_{\text{cap}} \cdot \Delta t \cdot m \rfloor \tag{4.3.3}$$

where q_{cap} is the hourly per-lane flow capacity (veh/h/lane), Δt is the time step (hours), and m is the number of lanes in cell i.

4.3.3 Demand per Source (D_i)

Source-level demand estimates were informed by an interview with a principal of a private school in Kuwait [55]. The principal indicated that the schools corresponding to sources 5 and 6 are larger institutions, each serving a higher student population than the other four schools. Based on her estimates, school enrollment across the study area ranges from approximately 1,000 to 1,500 students per institution. Accordingly, sources 1–4 were assigned an estimated demand of 1,000 students each, while sources 5 and 6 were assigned 1,500 students each.

Table 4.2: Estimated demand at each source cell (based on interview data).

Source Cell	Associated School	Estimated Demand (students)
1	A'Takamul International School	1,000
2	AlAwael School	1,000
3	Hayat Universal Bilingual School	1,000
4	American Summit Academy	1,000
5	American International School	1,500
6	Al Reyadah Model School	1,500

Table 4.3 summarizes key model parameters and derived values of Q_i and N_i based on typical cell lengths and lane configurations.

Table 4.3: Time-invariant cell parameters

Cell Length (ft)	Lanes	$\mathbf{Q_i}$	$\mathbf{N_i}$
300	2	11	26
400	1	6	17
400	2	11	35
500	2	11	43
600	2	11	52

Note. The jam density is constant across all cells and defined as $k_j = 0.0433$ vehicles/ft/lane. The simulation time step is $\Delta t = 0.00278$ h, and the flow capacity is 2,000 vehicles per lane per hour (veh/lane/hr).

4.3.4 Target setting

The targets of the goal programming model are determined by solving each objective independently as a single-objective linear program to obtain its individual optimal value. This approach is consistent with standard practices in goal programming formulations [51]. This method ensures that the resulting target set reflects the Pareto-efficient frontier, allowing the model to explore trade-offs within an optimal solution space. This procedure addresses a key shortcoming of traditional goal programming, specifically the Archimedean weighting approach, which can obscure non-dominant Pareto solutions when objectives have different scales or magnitudes.

4.3.5 Scenarios

To evaluate the effectiveness of the demand-release schedule, the model is tested under a single representative time horizon. The selected scenario examines how a controlled demand-release strategy influences overall system performance, particularly with respect to congestion mitigation and network clearance time. The model is evaluated over a time horizon of 360 time steps, each time step represents 10 seconds, consistent with CTM guidelines (360 time steps = one hour). This duration captures the critical school-dismissal period during which network demand peaks sharply. This one-hour horizon represents a practical and policy-relevant duration for assessing short-term demand management interventions. Thus, the goal is to identify an optimal balance between total throughput and delay.

The controlled demand-release scenario is evaluated against a baseline case in which all demand is released simultaneously at the start of the simulation—an uncontrolled surge referred to as the 'All-at-Once' release policy. Comparing the baseline and controlled-release cases illustrates the potential benefits of implementing a time-regulated demand-release mechanism in a high-demand context such as Sabah Al Salem.

This model examines a single configuration of weight assignments, referred to as *Sce-*

nario A. Alternative configurations will be explored in future research.

- **Scenario A:** $W_1 = W_2 = W_3$ — *Equal-weight configuration* (non-dominating case).

4.4 Example & test Network

To validate and verify the proposed GP-CTM model, it was first applied to the benchmark network described in [41]. This simplified network provides a controlled environment for evaluating the model's logic, numerical stability, and feasibility prior to its application to the full Sabah Al Salem case study. Specifically, it enables verification that the demand-release mechanism behaves as expected and produces results consistent with theoretical traffic flow principles. This controlled test case also supports calibration of key components such as cell parameters, demand profiles, target outflows, and objective function weights, where network behavior is predictable and easily interpreted.

4.4.1 Network Description

In Ziliaskopoulos's model, the cell transmission model is applied to a simplified six-node, seven-link network, illustrated in Figure 4.7. This example network is discretized and solved as a linear program to identify optimal traffic conditions. The physical and operational characteristics used for discretization are provided in Table 4.4. This test network serves as a verification benchmark to ensure the GP-CTM produces valid and stable results.

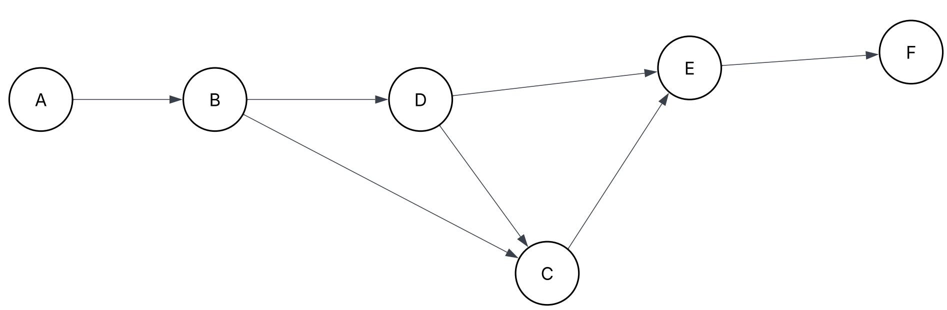

Figure 4.7: Simple six node, seven link example (adapted from Ziliaskopoulos).

Table 4.4: Characteristics of the example network

Arc	AB	BC	BD	DC	DE	CE	EF
Length (ft)	500	1000	500	500	500	1000	500
No. of Lanes	2	1	1	1	1	1	2
Speed Limit (ft/sec)	50	50	50	50	50	50	50
Max Flow (vphpl)	4320	2160	2160	2160	2160	2160	4320

The key characteristics of the network were determined by assuming values for saturation flow, which defines the maximum traffic flow rate (vehicles per hour per lane). The time discretization was set to $\mathcal{T} = 10$ seconds, following the recommendations of Daganzo [36,37]. The total time horizon was defined as 360 seconds, 36 time steps t. The simplified network shown in Figure 4.7 was then discretized, and a corresponding cell-based representation was created following the method described by Daganzo. Arc segments of 1,000 ft, such as BC and CE, were represented by two cells in the cell network 4.8.

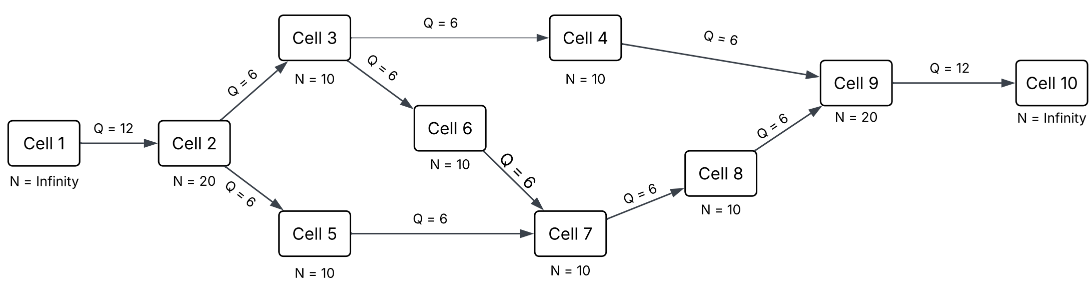

Figure 4.8: Simple six node, seven link example in cell form (Adapted from Ziliaskopoulos).

4.4.2 Model Parameters and Target Calibration

Table 4.5: Time-invariant cell properties

Cell	2	3	4	5	6	7	8	9
N_i	20	10	10	10	10	10	10	20
Q_i	12	6	6	6	6	6	6	12
x_i^0	0	0	0	0	0	0	0	0
δ_I	1	1	1	1	1	1	1	1

Objectives and Goals: The objectives in this section are the same as those defined in Chapter three. The purpose of this section is to apply the GP-CTM model to the example network presented by Ziliaskopoulos [41] to validate and verify the model's performance with respect to both network dynamics and optimization logic.

Targets: Targets for Goals 2 and 3 were obtained by independently solving the deterministic linear program associated with each objective—cell occupancy and sink flow. The demand goal (T_1) was set to represent the total external demand waiting to enter the system. The resulting values of x_i^t, y_{ij}^t, and d_i^t constitute the benchmark trajectory that the GP-CTM solution seeks to reproduce. The target for the demand goal (T_1) was set to 250 units of demand to be served through the network. The occupancy goal (T_2) was set to a cumulative total of 960 vehicles across all cells and time steps. Finally, the sink-flow goal (T_3) was set to 200 vehicles exiting through the sink, slightly above the optimal LP value of 192 vehicles. This adjustment was introduced intentionally to test the responsiveness of the deviational variables.

Weights: All goal weights were assigned equal importance in this validation test, such that $W_1 = W_2 = W_3$.

4.4.3 Results and Validation Criteria

Solution Summary

The goal programming model was formulated as an integer goal program to preserve the discrete nature of vehicle counts within the CTM framework, where each decision variable represents an integer number of vehicles. This ensures that all modeled flows and occupancies reflect realistic, count-based traffic dynamics.

The results of the GP-CTM on this network are $S_1 = 43$, $E_2 = 1$, and $S_3 = 12$. Objective function value = 56. To assess the model's validity, the deviational variables associated with each goal were examined. The objective function results confirm that the goal programming framework performs as intended, correctly representing both under and overachievement across the defined goals. In addition, the model's ability to propagate flow through the network was evaluated. Table 4.6 presents the optimal arc-level flow values (y_{ij}^t) across all time steps. This table illustrates how traffic propagates through the network under the optimal demand-release configuration.

Examining the flow results for the test network in Table 4.6, several key patterns emerge. First, the connecting arc $(3, 6)$ between the upper and lower routes shows no recorded flow during the entire time horizon, indicating that the model excludes this path from the optimal solution. Second, the model shows that it takes approximately five time steps for vehicles to travel from the source to the sink, with the first instance of flow entering cell 9 occurring at that point. Afterward, cell 9 consistently receives flow, reflecting stable traffic propagation once the network reaches steady state. There are two distinct paths that are used by the model, the upper route (2, 3, 4, 9), and the lower route (2, 5, 7, 8, 9). The observed flow dynamics confirm that the model's network logic and temporal evolution are consistent with the theoretical behavior of the cell transmission model .

Figure 4.9 summarizes the system-level performance of the GP–CTM model applied to the Ziliaskopoulos network over the 6-minute simulation horizon. The total network

Arc	0	1	2	3	4	5	6	7	8	9	10	11	12	13	14	15	16	17	18	19	20	21	22	23	24	25	26	27	28	29	30	31	32	33	34	35	36
(1,2)	0	2	6	6	6	6	6	6	6	6	6	6	6	6	6	6	6	6	6	6	6	6	6	6	6	6	6	6	6	6	6	6	6	0	0	3	0
(2,3)	0	0	0	0	6	4	6	4	6	2	0	4	6	4	0	2	0	6	0	6	4	6	4	6	0	6	0	6	4	6	0	6	4	0	0	0	0
(2,5)	0	0	2	6	0	2	0	2	0	4	6	2	0	2	6	4	6	0	6	0	2	0	2	0	6	0	6	0	2	0	6	0	2	6	0	0	0
(3,4)	0	0	0	0	0	6	4	6	4	6	2	0	4	6	4	0	2	0	6	0	6	4	6	4	6	0	6	0	6	4	6	0	6	4	0	0	0
(3,6)	0	0	0	0	0	0	0	0	0	0	0	0	0	0	0	0	0	0	0	0	0	0	0	0	0	0	0	0	0	0	0	0	0	0	0	0	0
(4,9)	0	0	0	0	0	0	6	4	6	4	6	2	0	4	6	4	0	2	0	6	0	6	4	6	4	6	0	6	0	6	4	6	0	6	4	0	0
(5,7)	0	0	0	2	6	0	2	0	2	0	4	6	2	0	2	6	4	6	0	6	0	2	0	2	0	6	0	6	0	2	0	6	0	2	6	0	0
(6,7)	0	0	0	0	0	0	0	0	0	0	0	0	0	0	0	0	0	0	0	0	0	0	0	0	0	0	0	0	0	0	0	0	0	0	0	0	0
(7,8)	0	0	0	2	6	0	2	0	2	0	4	6	2	0	2	6	4	6	0	6	0	2	0	2	0	6	0	6	0	2	0	6	0	2	6	0	0
(8,9)	0	0	0	0	2	6	0	2	0	2	0	4	6	2	0	2	6	4	6	0	6	0	2	0	2	0	6	0	6	0	2	0	6	0	2	6	0
(9,10)	0	0	0	0	0	2	6	6	6	6	6	6	6	6	6	6	6	6	6	6	6	6	6	6	6	6	6	6	6	6	6	6	6	6	6	6	6

Optimal Arc Flows Over Time ($t = 0$–36)

Table 4.6: Optimal arc flows over time ($t = 0$–36)

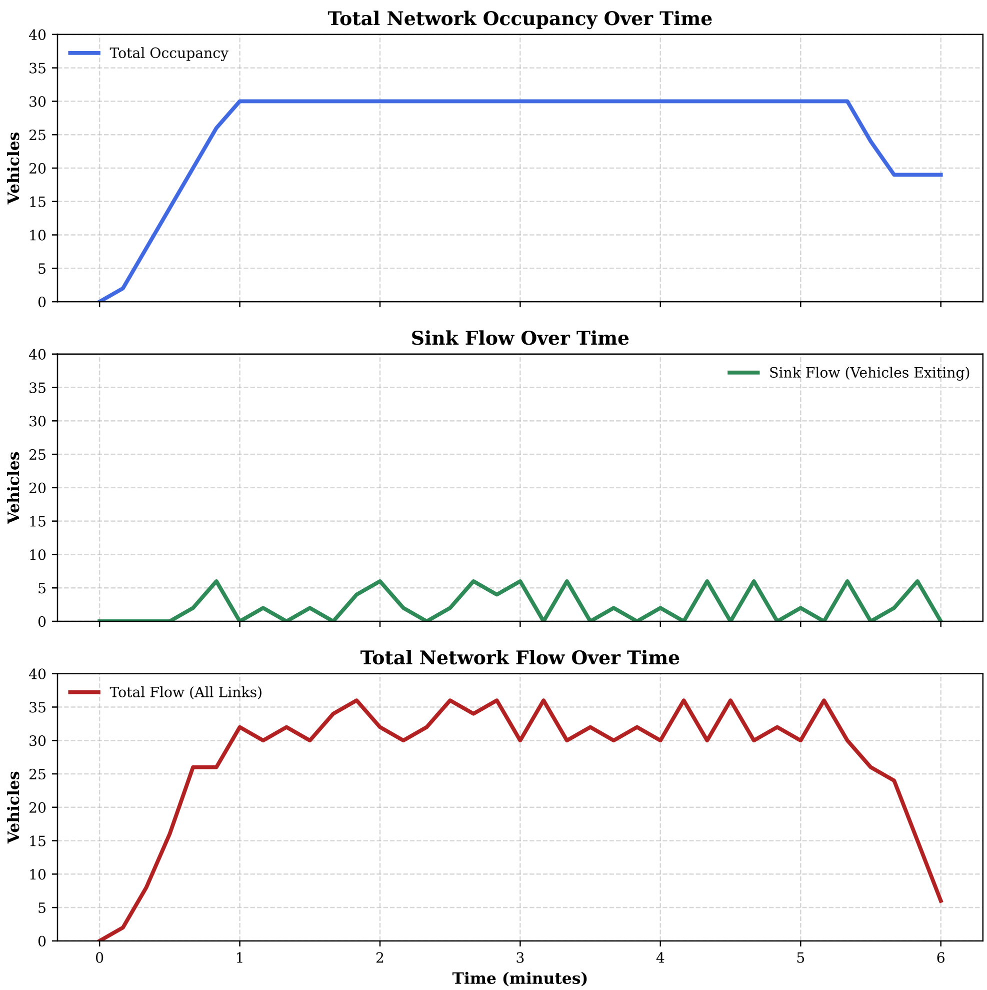

Figure 4.9: Network-level traffic performance over time: total occupancy (Blue), total flow (Green), and sink throughput(Red).

occupancy represents the number of vehicles present in the network at each time step, while the total flow and sink throughput curves indicate the overall movement and discharge of vehicles, respectively. These metrics were derived by aggregating the optimal cell occupancy and flow variables from the model solution, capturing the macroscopic evolution of traffic across both routes.

Model Validation

Post-optimization verification confirmed that all CTM constraints were satisfied. Capacity constraints: all cell occupancies remained within their jam density limits ($x_i^t \leq N_i^t$). Flow constraints: all arc flows respected their sending and receiving capacity limits ($y_{ij}^t \leq Q_i^t$). Mass balance: 207 vehicles were admitted, of which 188 exited and 19 remained in the network. The solution is both physically feasible and mathematically consistent, validating the network dynamics and the optimization model's functionality.

4.5 Results and Analysis

4.5.1 Overview

This section presents and analyzes the results of applying the GP-CTM model to the Sabah Al Salem network. It compares the performance of the baseline scenario—uncontrolled demand release— with the optimized GP-CTM demand release schedule. Both models operate under identical network constraints to maintain consistent traffic dynamics, which are derived from the CTM linear program developed by Ziliaskopoulos [41].

The baseline model mimics the current dismissal policy, which releases all the demand from a source at the beginning of the time horizon, and illustrates how this "All-at-Once" strategy affects the network's congestion levels and overall efficiency. In this model, the objective value maximizes the release of demand while also weighting early discharge highly to encourage the model to release the demand in the first-time step. This mechanism represents the dismissal policy currently adopted by the schools in this area. This research demonstrates that the unmanaged scenario places significant demand pressure on the network, leading to rapid and prolonged traffic congestion. The optimized model generates a novel discharge policy to flatten the demand surge curve by way of a preemptive release mechanism which lowers the risk of the system becoming congested. The goal of the GP-CTM model is to organize the demand being released in a way that satisfies the three goal programming objectives of (1) maximizing the demand released by source cells in each time step, (2) minimizing cell occupancy, and (3) maximizing sink throughput.

Metrics such as flow, occupancy, and total demand discharged are analyzed to assess the model's performance at three levels: global, temporal, and spatial. The GP-CTM aims to schedule demand releases that maintain network efficiency while satisfying school demand in the shortest amount of time. Global metrics show the aggregate effects of the release schedule on the system. Temporal metrics assess the model's performance over the time horizon, since spikes in occupancy indicate congestion build-up. Spatial metrics provide insight into cell-level utilization, serving as a proxy for congestion and bottleneck formation.

Targets

Goal targets were established by independently solving the linear program for each of the three decision variables. Table 4.7 presents the target values obtained from these optimizations. These target values refine the solution space of the goal programming model by using the optimal results of each LP to indicate the approximate location of the Pareto front. This, in turn, establishes upper and lower bounds that guide the model toward truly optimal solutions. A common shortfall of goal programming is that it does not inherently reveal whether the resulting solution lies on the Pareto front. This target-setting approach mitigates that limitation by anchoring the model to known Pareto-optimal reference points.

Table 4.7: Target setting results for individual linear programs (LP1–LP3)

LP Run	Objective	Occupancy	Demand Admitted	Sink Throughput
LP1 – Minimize Occupancy	Minimize $\sum x_i^t$	34,300	7,000	7,000
LP2 – Maximize Sink Flow	Maximize $\sum y_{ij}^t$ (sinks)	45,831	7,000	7,000
LP3 – Maximize Demand Release	Maximize $\sum d_i^t$ (sources)	67,522	7,000	7,000

Normalizing weights

The goal weights were determined by examining the relative magnitudes of the target values associated with the three objectives: demand admitted, total occupancy, and sink throughput. Since the target values for the occupancy goal were approximately four times larger than those of the flow and demand goals, a smaller relative weight was assigned to occupancy to maintain numerical balance in the goal programming objective function. The resulting ratio of weights, $W_1 : W_2 : W_3 = 4 : 1 : 4$, provides a balanced representation of the competing objectives and ensures that deviations from the targets contribute equally to the overall objective function value Z . This 4:1:4 weighting scheme was retained for all subsequent analyses.

4.5.2 Baseline Model Results

Global Network Performance

Examining the baseline model results reveals that, although all demand was successfully released into the network, the "All-at-Once" release policy resulted in severe congestion. Over the time horizon, total network occupancy reached 81,062 vehicles, and only 82% of the released demand exited through the sink cells. The simultaneous surge of vehicles injected into the network created bottlenecks that prevented efficient downstream propagation. This led to high occupancy and inefficient network utilization.

At the end of the time horizon, 1,148 units of demand remained at the source cells, demonstrating the effects of unmanaged demand release. In the model, source cells function as control gates between the external demand pools and the internal network. When downstream cells approach capacity, the sources hold excess demand, effectively buffering inflow and maintaining proper flow balance at the sources. In this scenario, holding vehicles at the sources was the only mechanism that prevented total system failure during the demand surge.

Table 4.8: Baseline model performance results

Metric	**Value**
Total Demand Released	7,000
Total Evacuated (Sink Throughput)	5,756
Evacuation Rate (%)	82.2
Average Waiting at Sources	3,398
Total Network Occupancy (Global)	81,062
Vehicles Remaining at Sources ($t = 360$)	1,148

Cell occupancy is a key indicator of congestion; higher occupancy values correspond to more severe traffic congestion. Table 4.9 summarizes the global network occupancy results of the baseline model. These values represent current network conditions under the existing "All-at-Once" policy. In the first 10 minutes, network occupancy peaks at 288 vehicles. The overall peak occurs approximately 28 minutes into the time horizon, reaching 315 vehicles. Average occupancy over the full time horizon is 244 vehicles. This serves as the baseline for comparison with the optimized model.

Table 4.9: Global network occupancy values.

Metric	**Value**
Average Occupancy (First 10 Minutes)	228.9
Peak Occupancy (First 10 Minutes)	288.0
Average Occupancy (All Time)	224.5
Peak Occupancy (Overall)	315.0
Time of Peak Occupancy (Minutes)	27.7
Time Step of Peak Occupancy	166

Figure 4.10 illustrates these global occupancy trends over time. The blue curve shows the total network occupancy for the baseline scenario. During the first 30 minutes, occupancy increase slightly and then begins to decrease. Comparatively, the green and red curves indicate sink throughput and internal network flow, respectively. As occupancy increases, both sink throughput and network flow decline, indicating backward-propagating congestion and system-wide traffic buildup. Around the 40-minute mark, flow rises while occupancy decrease as a result, indicating flow is picking up in the system.

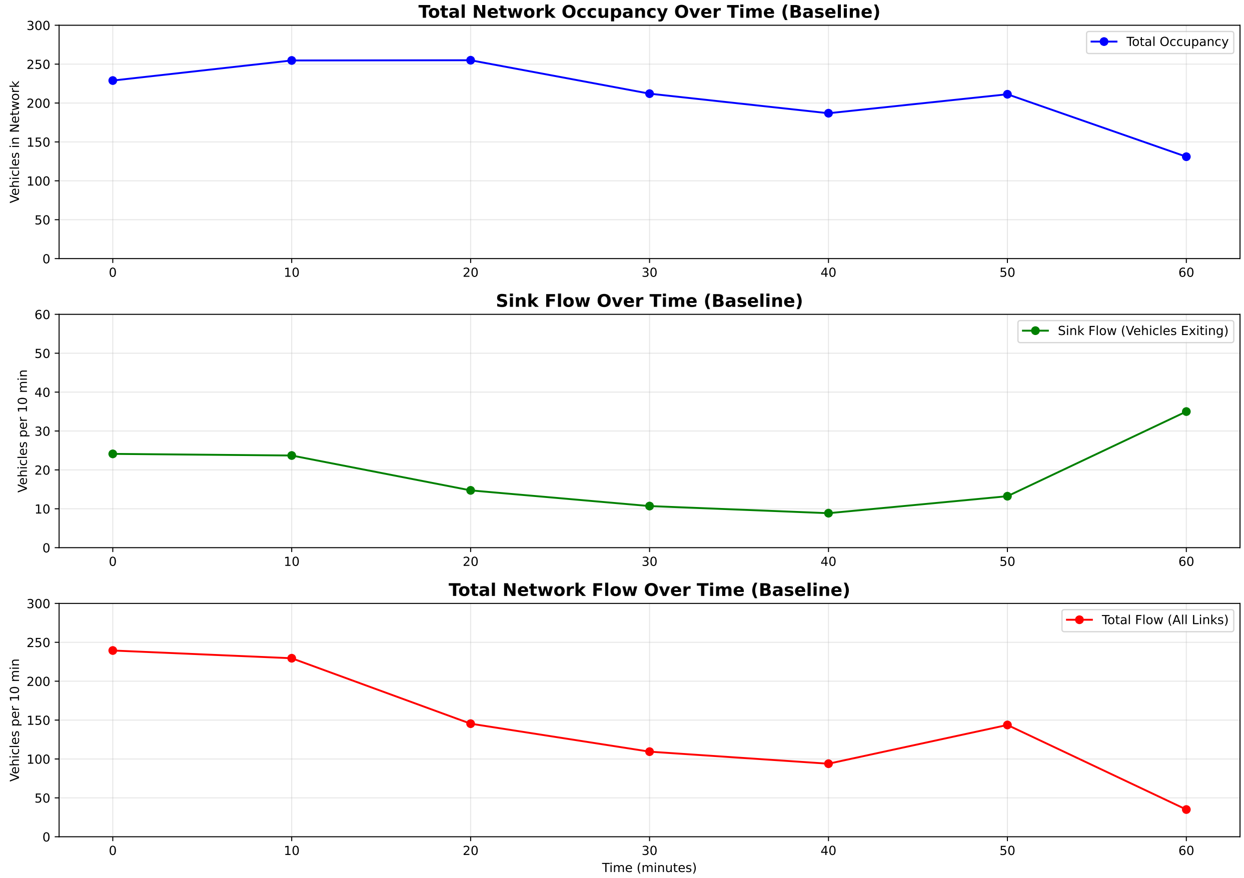

Figure 4.10: Global network performance (Baseline).

Figure 4.11 further illustrates the decrease in sink flow, which drops off earlier than the network average shown previously. Although sink flow spikes between minutes 40 and 60, it remains insufficient to serve all demand within the time horizon.

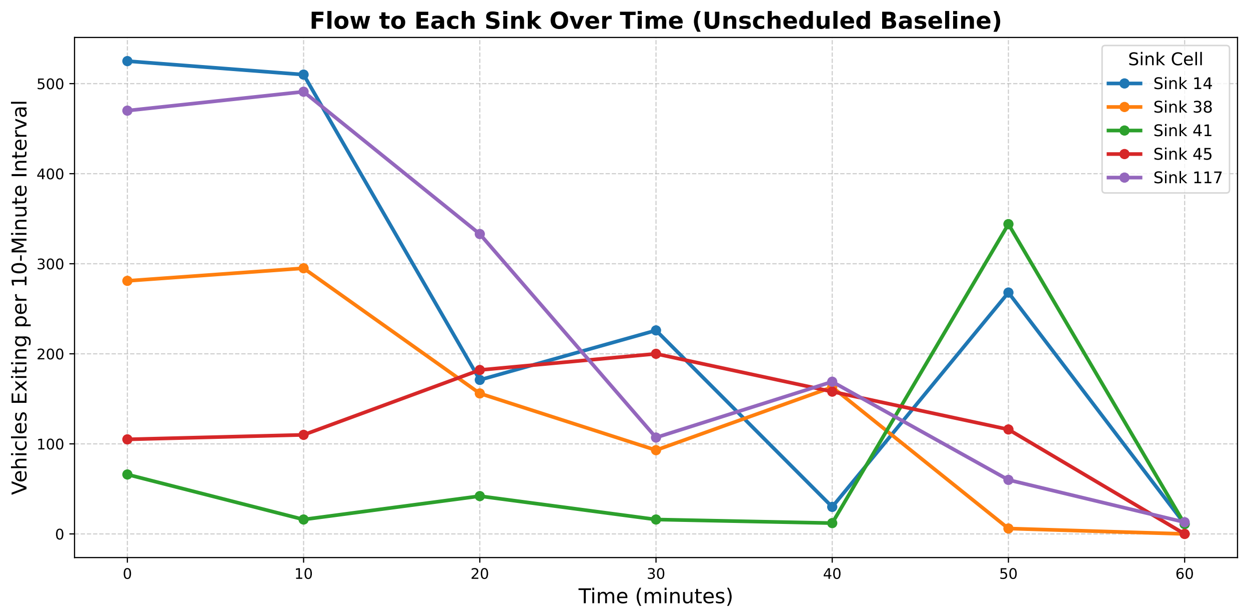

Figure 4.11: Flow to each sink cell over time (Baseline).

These figures and tables establish system-wide performance baselines for occupancy, sink throughput, and internal network flow. The next set of metrics examines temporal performance for the source cells and the internal network. The temporal metrics serve to provide insight into how congestion builds over time at the cellular level relative to the release of demand into the system.

Temporal Performance Metrics

Figure 4.12 presents three time-series: orange represents demand released to source cells, blue shows actual cell occupancy, and green depicts actual sink outflow per time step.

At the start of the time horizon, the demand surge causes occupancy to spikes. Although, this is not a direct demand curve, it serves as a proxy indicator for the demand surge. It also illustrates the relationship between traffic demand and network performance. In the baseline case, the model pushes vehicles into the system to clear source cells rapidly; however, the network capacity is the limiting factor. This demonstrates how unmanaged demand destabilizes a capacitated traffic network. One objective of this research is to develop a model that flattens the demand surge curve, which is the primary cause of congestion and gridlock

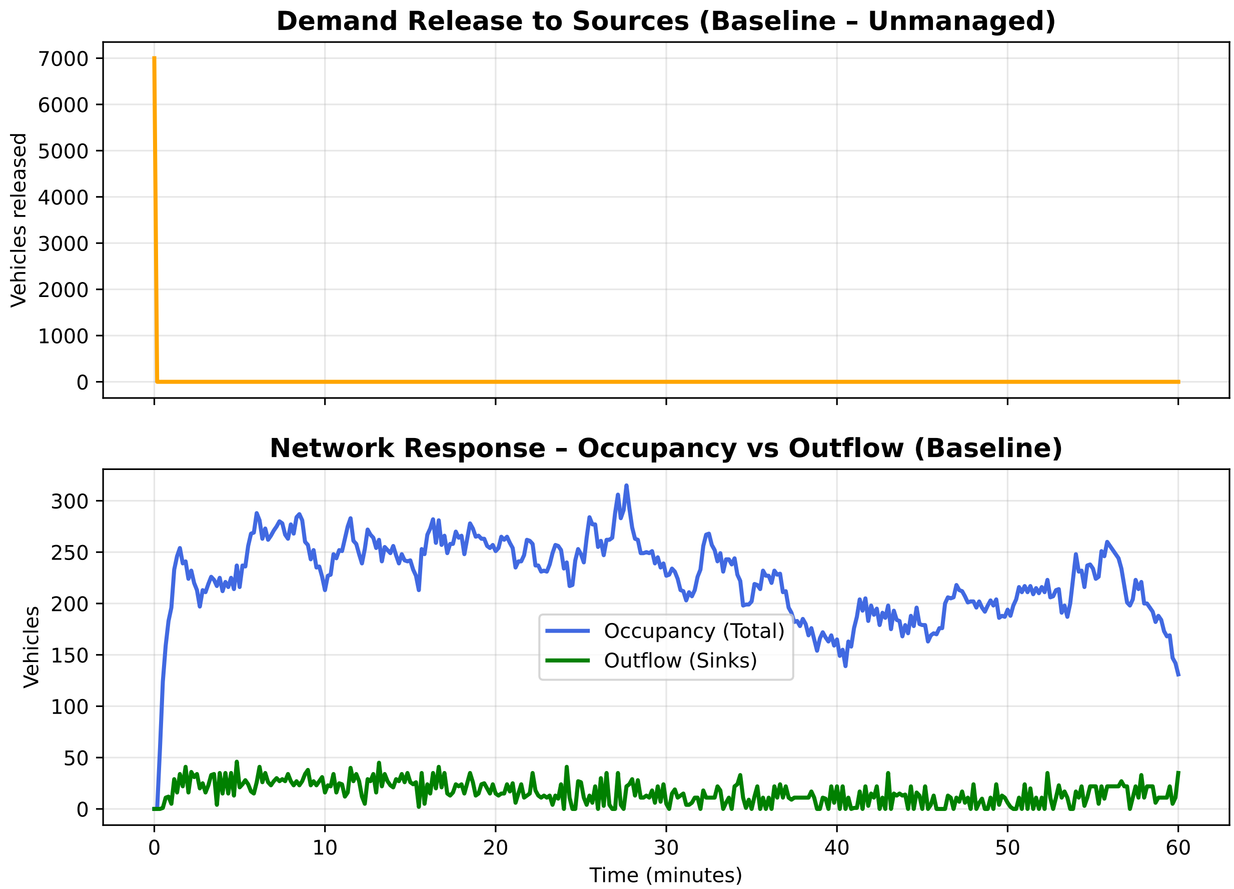

Figure 4.12: Temporal network performance (Baseline).

Spatial Analysis

The spatial analysis examines congestion at the cell level. Having established aggregate congestion and occupancy surges, cell-level spatial metrics provide insights into how demand surges affect the Sabah Al Salem Network. Figures 4.13 and 4.14 show the ten most congested cells in the Sabah Al Salem cell network. The figures show that cells 15 and 40 reach jam density at times during the time horizon. Cells 13, 15, 40, and 54 also exceed the 80% threshold-near jam density- indicating a substantial congestion risk. Cells 74 and 115 briefly exceed the threshold, but most of the cells hover above 40% utilization throughout the time horizon. These patterns indicate that the network is operating near its jam density and in a congested state, which is consistent with reduced sink throughput and diminished internal flow. Together, these baseline results establish a clear benchmark: unmanaged “All-at-Once” release induces severe and persistent congestion, limiting throughput and leaving residual demand at the sources.

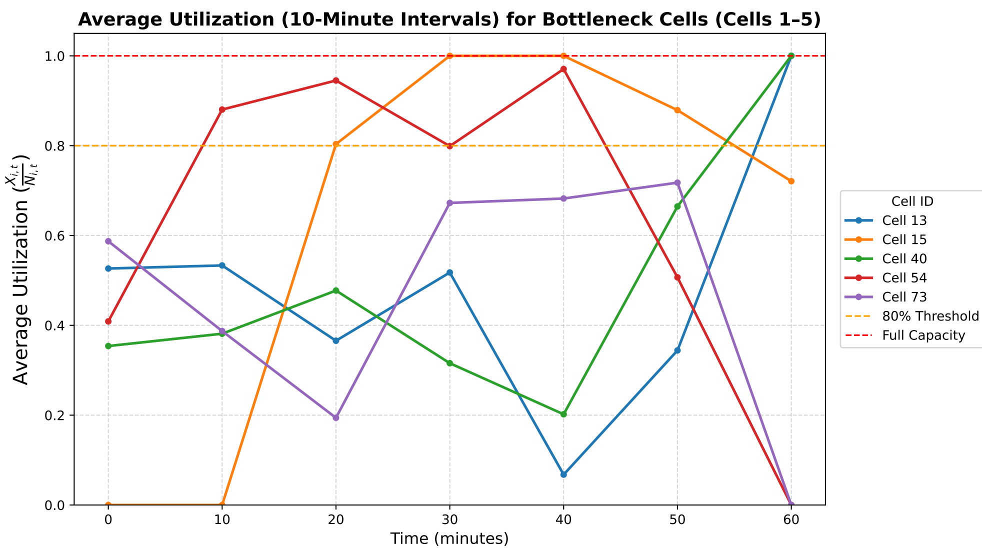

Figure 4.13: Cell utilization 1-5(Baseline).

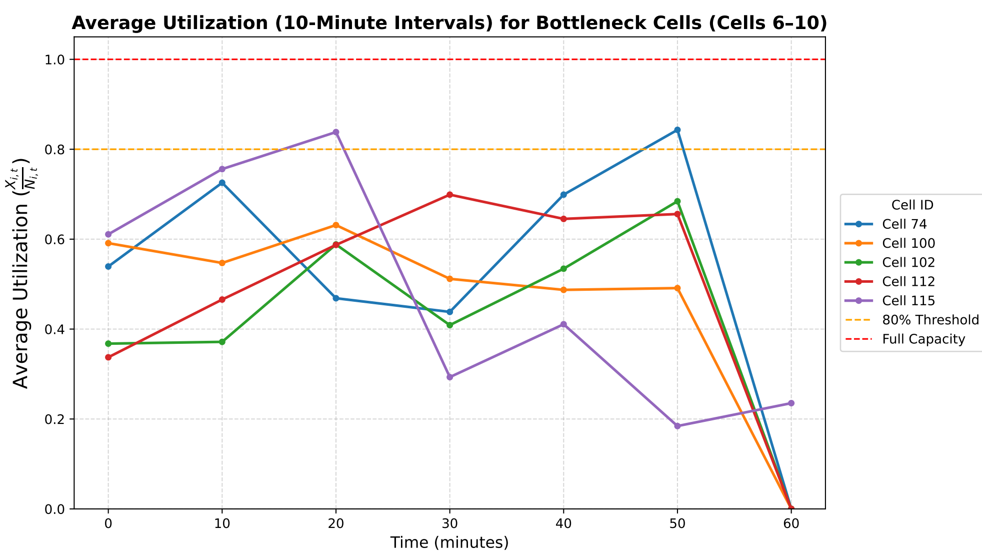

Figure 4.14: Cell utilization 6-10 (Baseline).

4.5.3 GP-CTM Results

Optimized Demand Release Schedule

The GP-CTM shifts the focus of the modeling process to three main objectives: maximizing demand release, minimizing cell occupancy, and maximizing sink throughput. Unlike the time-dependent demand release approach, this model decides when and how much demand should be released. One possible formulation would follow Ziliaskopoulos [41] in minimizing cell occupancy, but instead define the decision variable to maximize demand release. However, as shown in table 4.7 such an approach would lead to higher levels of total occupancy. This highlights the advantage of goal programming: the ability to formulate a model that simultaneously considers multiple, and often conflicting, objectives. The GP-CTM developed in this research achieves exactly that.

The model converged efficiently, producing the demand release schedule shown in Table 4.10. The release quantities are sufficiently high to serve all demand within the time horizon, demonstrating the model's effectiveness. This serves to be the optimal policy of the schools in the area and would provide more effective network performance to ensure everyone got home in a timely fashion. Compared with the baseline's "All-at-Once" policy, this optimized schedule releases demand in a manageable way over time to preemptively avoid congestion.

Table 4.10: Demand released per source (Baseline Model, 10-Minute Intervals).

Time (minutes)	**1**	**2**	**3**	**4**	**5**	**6**	**Total (All Sources)**
0.0	233	179	127	205	277	245	1,266
10.0	116	209	195	155	257	248	1,180
20.0	153	165	199	104	258	278	1,157
30.0	172	127	175	171	212	243	1,100
40.0	177	129	185	207	238	232	1,168
50.0	149	191	119	158	258	254	1,129
60.0	0	0	0	0	0	0	0
Total Released	**1,000**	**1,000**	**1,000**	**1,000**	**1,500**	**1,500**	**7,000**

As shown in Table 4.10, the optimized demand release schedule distributes vehicle inflows smoothly across the entire time horizon, with no major spikes in the quantity released.

The release volumes range from a minimum of 104 to a maximum of 278 units, resulting in a steady and balanced discharge pattern. This spread-out release strategy effectively titrates demand into the network—introducing vehicles gradually rather than in concentrated surges. By doing so, the GP-CTM flattens the demand surge curve and prevents the abrupt system overloads that characterized the baseline scenario. The outcome is a smoother utilization of network capacity, where each source contributes incrementally to total flow without triggering congestion propagation. The pattern described here is illustrated in Figure 2 in Appendix 5.5, where the demand releases from each source appear as a smooth curve with no major spikes, confirming the model's controlled discharge behavior.

Global Network Performance

Table 4.11 summarizes the model's global performance metrics. The optimized model released and served all the demand through the sink in the time horizon achieving a 100% evacuation rate while maintaining a total network occupancy of approximately 34,300 vehicles over the time horizon. This represents a 63% reduction in total network occupancy, illustrating the effectiveness of the GP-CTM in managing demand and mitigating congestion associated with unmanaged release policies.

Table 4.11: Global performance metrics for the GP-CTM optimized model.

Metric	**Value**
Total Demand Released	7,000
Total Evacuated (Sink Throughput)	7,000
Evacuation Rate (%)	100.0%
Average Waiting at Sources	14
Total Network Occupancy	34,300
Vehicles Remaining at Sources (t=360)	0

These results demonstrate that the GP-CTM enables the network to operate in a much more stable regime. The significant reduction in total occupancy—from over 81,000 vehicles in the baseline to roughly 34,300—indicates that queues are shorter and congestion pockets dissipate quickly. Moreover, the minimal waiting at sources-average of 14 vehicles- confirms that the system experiences little to no back-pressure, suggesting that inflow and outflow remain well balanced. Together, these outcomes reflect a network that continuously processes demand rather than storing it, translating directly to shorter travel times and higher throughput efficiency.

Table 4.12 summarizes the temporal metrics that assess the models performance. The key takeaway from this table is the average occupancy of 80.7 vehicles across the time horizon—an improvement of approximately 64% compared with the baseline model. Another difference in the two models is realized in the time of the occupancy peak, the baseline model spikes early within the beginning of the timeline. Whereas the optimized model spikes to its peak occupancy in the final 10 minutes of the time horizon. The relative difference between the two peaks is also notable: the baseline peaked at 315 vehicles, whereas the optimized model peaked at only 121.

Table 4.12: Temporal occupancy metrics for the GP-CTM optimized model.

Metric	**Value**
Average Occupancy (First 10 Minutes)	79.8
Peak Occupancy (First 10 Minutes)	107.0
Average Occupancy (All Time)	80.7
Peak Occupancy (Overall)	121.0
Time of Peak Occupancy (Minutes)	53.8
Time Step of Peak Occupancy	323

Global Network Occupancy Trends

From a global perspective, occupancy trends in the GP-CTM remain smooth, indicating that the system operates near equilibrium. As shown in Figure 4.15, the blue occupancy curve remains relatively flat throughout the time horizon, signifying that the system quickly stabilizes after the initial releases. Unlike the baseline case, there are no sharp spikes or oscillations, which indicates that inflow and outflow rates are well synchronized. In the final 10 minutes, occupancy decreases while sink flow rises, demonstrating that vehicles are exiting efficiently and that residual demand is minimal. This balance across occupancy, network flow, and sink throughput reflects the GP-CTM's ability to maintain dynamic equilibrium and continuous traffic circulation without congestion buildup.

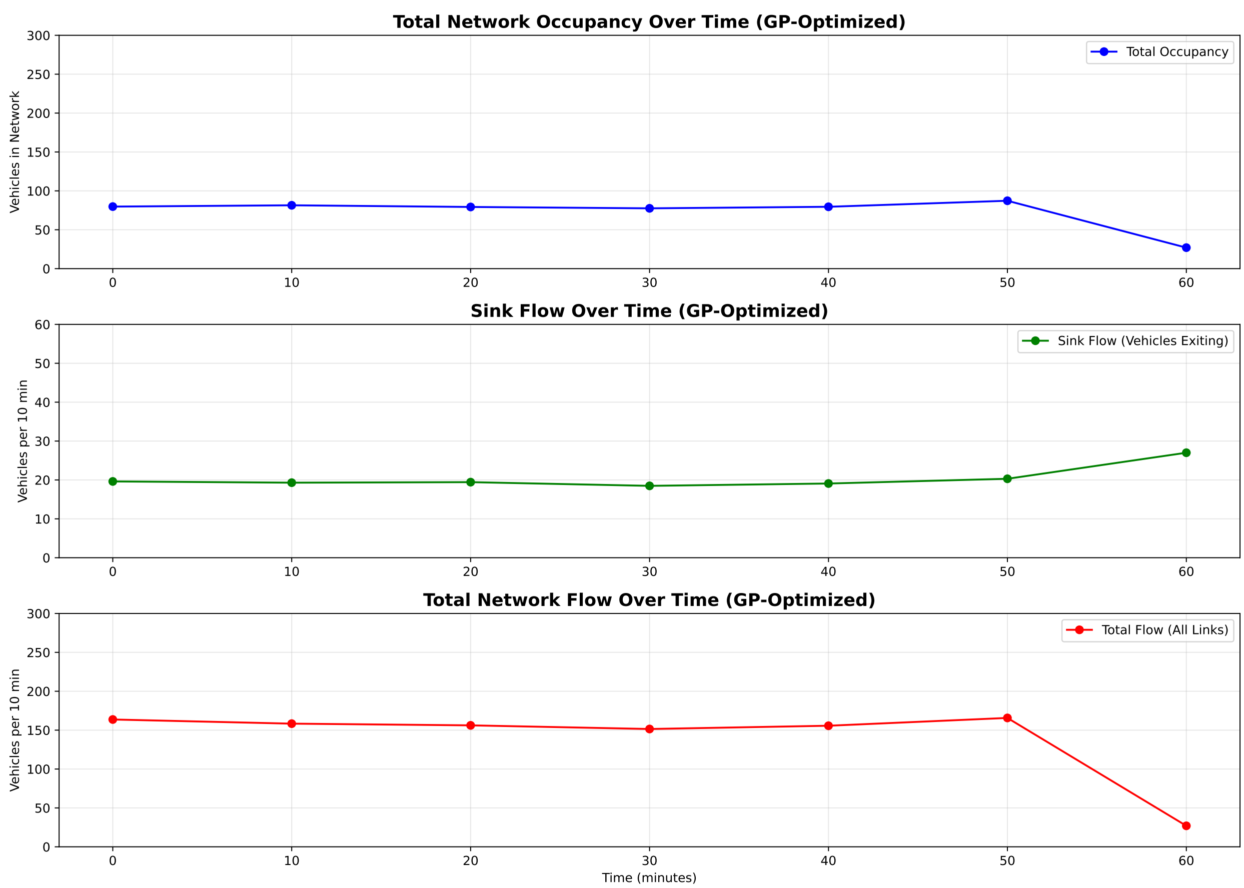

Figure 4.15: Sink flow over time for GP-CTM model.

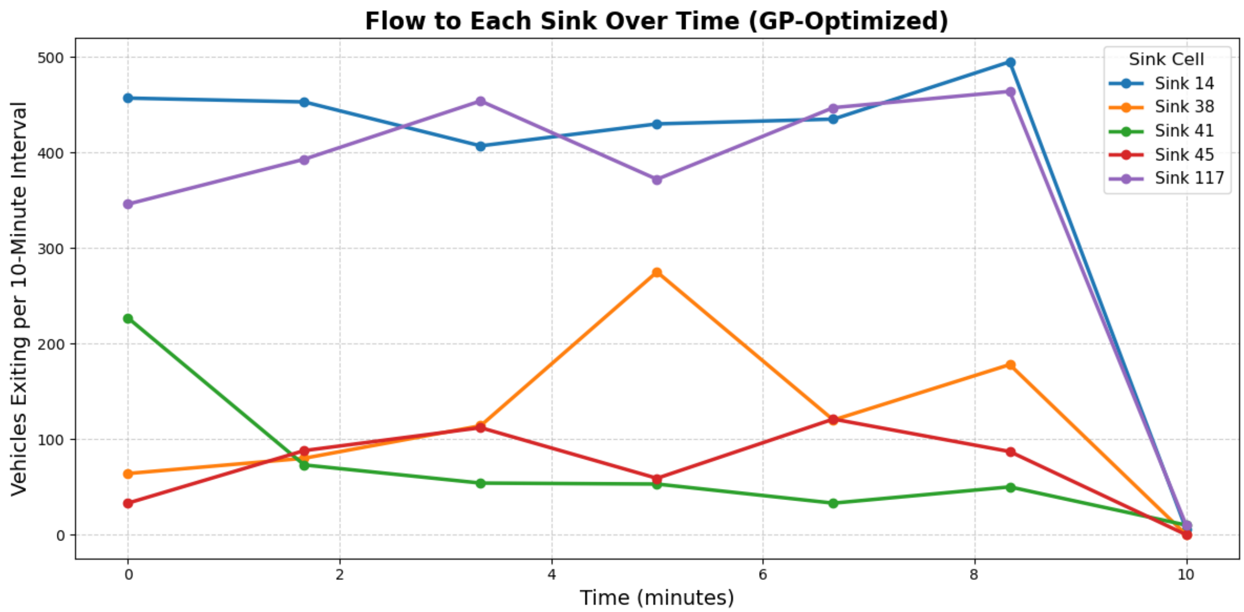

Figure 4.16: Sink flow over time for GP-CTM model.

Temporal Performance Metrics

The temporal metrics illustrate how the GP-CTM successfully flattens the demand surge curve by releasing demand at a controlled and steady rate throughout the time horizon. This regulation prevents the volatile surges observed in the baseline scenario and maintains low occupancy across the network. As shown in Figure 4.17, demand released to source cells remains nearly constant, while occupancy stabilizes early and stays below critical thresholds. The steady rise in sink outflow mirrors the controlled release pattern, indicating that the network continuously converts incoming demand into throughput rather than storing it as congestion. This temporal stability, achieved through proactive demand management, is the defining characteristic of the optimized system. Having confirmed the temporal stability of the network, the next step is to examine how this performance translates spatially across individual cells.

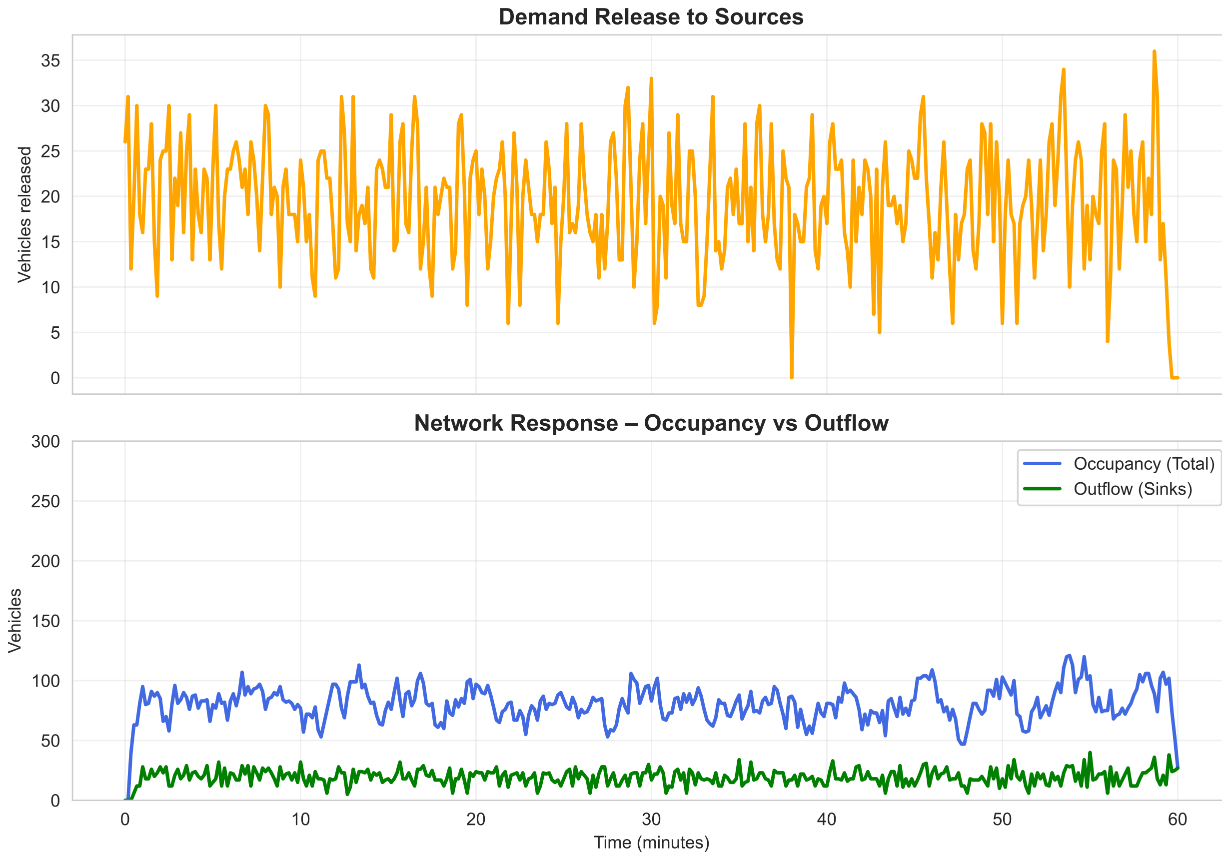

Figure 4.17: Temporal network performance (GP-CTM)
Note: The demand-release figure is plotted on a different scale than in the baseline scenario due to the significantly larger initial release in that case.

Spatial Analysis

At the cellular level, the optimized model achieves a maximum cell utilization of 40% for cell 13. Cells 16 and 100 remain just below that value, with noticeably lower utilization compared with the baseline results, where several cells operated above 50% for most of the time horizon.

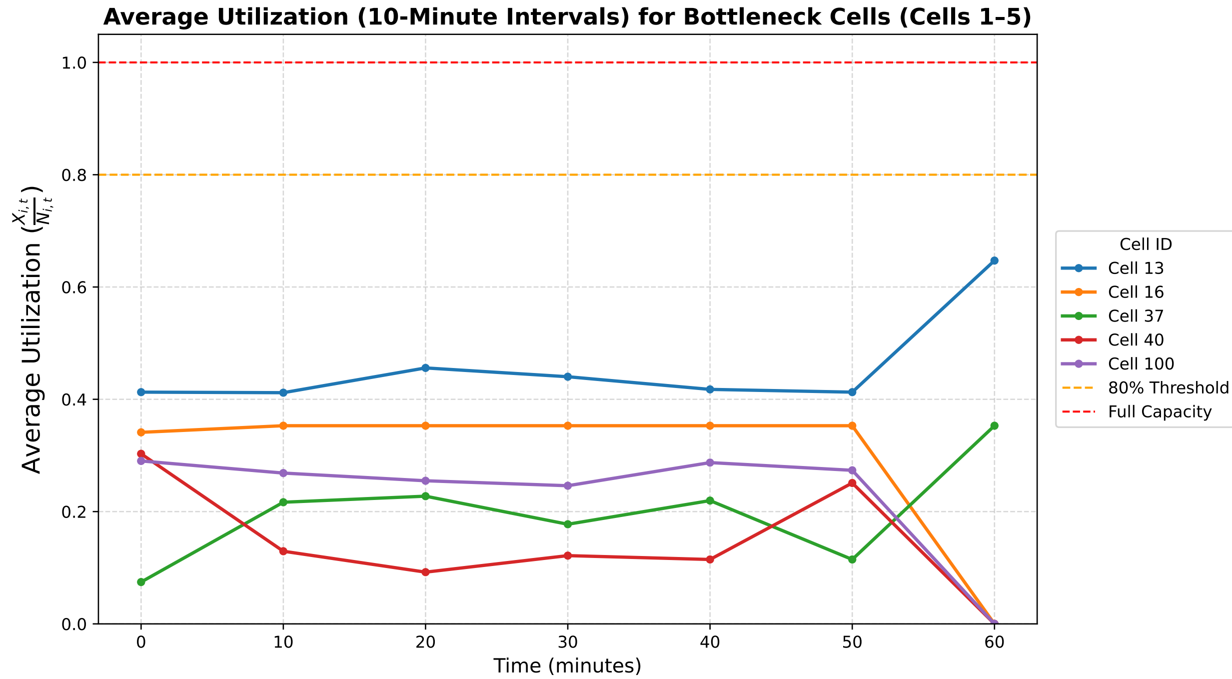

Figure 4.18: Ten most congested cells in the cell network (1-5).

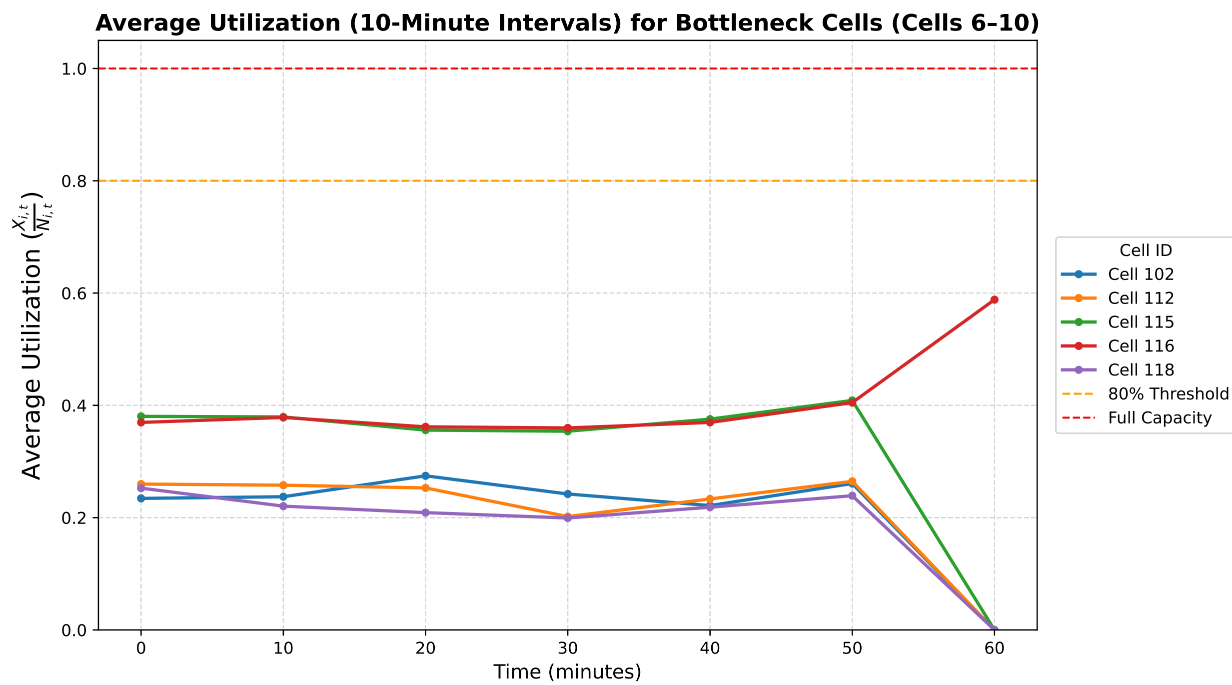

Figure 4.19: Ten most congested cells in the cell network (6-10).

Figures 4.18 and 4.19 reveal that no cells in the optimized network approach jam density. The highest utilization, observed in cell 13 at around 40%, remains well below critical thresholds, while the remaining cells operate comfortably between 25–35%. This spatial distribution contrasts sharply with the baseline scenario, where several cells consistently exceeded 80% utilization, particularly near key intersections. The even spread of occupancy suggests that the GP-CTM not only reduces congestion overall but also redistributes flow more evenly across the network, minimizing localized bottlenecks and improving reliability for all users.

4.5.4 Comparative summary

The GP-CTM releases all demand from the source cells and evacuates it through the sink while maintaining low total network occupancy and cell utilization. The model allows efficient operations of the traffic network and fulfills the objectives of serving all the demand through the traffic network. The GP-CTM provides the optimal demand release policy to the schools in the area. Compared with the baseline policy, the optimized schedule achieves 18% higher throughput—serving 100% of the total demand released from the sources—whereas the baseline scenario evacuates only 82% of the demand through the sink cells.

The improvement across all levels global, temporal, and spatial stems directly from the GP-CTM's controlled demand release mechanism. By dynamically regulating inflows, the model prevents over saturation and ensures that capacity is fully utilized but never exceeded. As a result, congestion never forms, throughput remains high, and every unit of demand is served within the time horizon. This contrasts sharply with the unmanaged baseline, where excessive early inflow triggered prolonged congestion and high residual demand. The optimized schedule thus represents a practical and implementable discharge policy for the Sabah Al Salem network, offering both operational efficiency and reduced travel times.

The defining difference between the two models lies in demand management: the optimized model's scheduled release policy allows the network to operate at full efficiency without breaching capacity limits. The novel GP-CTM model thus provides a practical and effective approach to preemptive congestion mitigation.

Chapter 5

Conclusion

5.1 Discussion

Traffic management is one of the primary approaches to addressing congestion. The effectiveness of any strategy depends on the type of traffic being targeted. Recurrent traffic is predictable and accounts for a large portion of total congestion, it represents a practical target for management interventions with significant potential benefits. One way to address congestion is through Dynamic Traffic Assignment (DTA) models, which estimate total system travel time. This can then be minimized using prescriptive optimization methods such as linear programming. However, the effectiveness of this approach depends on detailed origin–destination (O–D) data, which may be unavailable in practice. This limitation is particularly relevant in data-sparse countries such as Kuwait, where transportation engineering expertise remains limited.

Kuwait's economic prosperity, coupled with rapid population growth and limited transportation engineering expertise, has led to a disproportionate rise in congestion. This strain on the transport network affects not only economic productivity but also the social and psychological well-being of the population. While Maxwell argues that congestion is an inevitable outcome of a functioning transportation network, he also emphasizes that it remains a manageable one. This perspective highlights the need to rethink how congestion is addressed—particularly in an era where expanding physical infrastructure is no longer a sustainable or sufficient solution.

This research addresses that gap by providing a management-based tool for developing policy decisions using limited data. The approach is particularly relevant for countries like Kuwait—and many others outside Western Europe and North America—where detailed transportation data remains scarce. The proposed GP–CTM framework is novel, as goal programming has not been applied within the context of traffic management or dynamic traffic assignment in this manner. This integration underscores the originality and methodological contribution of the present research. The model provides aggregate-level insights into large traffic networks without requiring detailed (O–D) pair data. Instead, this model utilizes easily obtainable demand data—acquired through basic data collection efforts—to examine how pooled demand influences the network's capacity, providing actionable insights into congestion dynamics. The framework introduces a scheduled release mechanism that protects the network's capacity from being overwhelmed by excessive, simultaneous demand inflows. Rather than releasing all demand simultaneously, which forces delays and network inefficiency, the scheduled release approach enables the system to maintain near-equilibrium conditions throughout the time horizon.

5.2 Key findings

In Chapter four, the GP–CTM model was applied to the localized traffic network of Block 1 in Sabah Al Salem, Kuwait, which contains several major schools and experiences recurring congestion during peak periods. Due to its rapid development and proximity to residential neighborhoods, congestion in this area has increasingly affected residents' daily mobility and quality of life. Over a 360 time-step–one hour period– the demand release model achieved full release of all demand from the sources, with 100% of vehicles reaching the sink cells and exiting the study area. The baseline model, which released all demand simultaneously with the “All-at-once” policy, was only able to serve 82% of the total demand through the sink cells, highlighting its inefficiency under peak conditions. However, the model’s efficacy is not primarily reflected in the percentage of demand served or the proportion reaching their intended destinations; rather, it is demonstrated through key performance indicators such as occupancy levels and cell utilization. These temporal and spatial indicators reflect the network’s response to the implemented demand-release policy and serve as measures of congestion formation and intensity.

Under the optimized demand-release policy, the GP-CTM maintained cell utilization levels below 40% for the ten most congested cells in the system, indicating stable network performance. This result suggests that the most congested cells remained consistently utilized over the model’s time horizon, indicating sustained operational stability. However, the baseline scenario resulted in the five most congested cells operating at an average utilization of around 80%, with frequent spikes reaching full capacity 100%. These peaks indicate the onset of traffic jam formation and a heightened risk of gridlock within the network and the other 5 cells hovered around 50%+ for the 360 time steps. Under the optimized demand-release schedule, average network occupancy stabilized at approximately 80 vehicles per time step across the 360-step time horizon. In comparison, the baseline model exhibited an average of approximately 315 vehicles within the network per time step, representing a 64% increase in network occupancy relative to the optimized scenario. These findings demonstrate that a controlled release of demand can significantly improve network performance by reducing both congestion intensity and the likelihood of system-wide gridlock.

5.3 Limitations

These results demonstrate the effectiveness of the GP-CTM model in addressing demand management during the afternoon commuter period associated with school dismissal. While the GP-CTM model demonstrates strong potential for managing traffic demand, several simplifying assumptions were made to ensure computational efficiency and focus on the primary objectives of this research. These assumptions pertain to the estimation of free-flow speeds, the use of an idealized capacity value, the treatment of initial cell conditions, the one-way representation of network flow, and the assumption that each demand unit corresponds to a single vehicle. Although these simplifications were necessary for model tractability, they limit the model's ability to fully capture the complexity of real-world traffic dynamics.

First, the model assumes that free-flow speed is equivalent to the posted speed limit of each roadway segment. In reality, free-flow speed is influenced by several factors, including road geometry, surface conditions, driver behavior, and often deviates from the official speed limit. For instance, under adverse weather conditions or at curved sections, drivers naturally travel below the posted speed. This simplification may therefore reduce the precision of the model in representing real-world traffic flow. Second, the model uses an idealized free-flow capacity of 2,000 vehicles per hour per lane, based on the Highway Capacity Manual (HCM). While this assumption provides a reasonable benchmark, it may not accurately represent the true operational capacity of roads in the study area, where local driving habits, road design, and traffic composition can significantly influence flow capacity.

Third, The model assumes empty initial cell conditions at the start of the time horizon, meaning no vehicles are present in the network when demand release begins. In reality, roadways, particularly during peak hours, are rarely empty, and residual traffic from earlier periods can significantly influence system performance. Fourth, the model is structured as a one-way system, with traffic flowing outward from demand sources (schools) toward network exits. While this setup effectively captures the afternoon dismissal pattern that motivates the case study, it does not account for two-way interactions such as return trips or cross-flows between corridors. These assumptions were considered acceptable for the scope of this research, which emphasizes the effects of demand release strategies rather than fully replicating all operational dynamics of the network.

The fifth assumption concerns the control of demand release. The model assumes that demand can be released from any source cell at any time step within the simulation horizon. This represents an idealized level of control that enables the identification of an optimal, best-case release pattern. In practice, however, such flexibility rarely exists—school dismissal times, signal coordination, and driver behavior impose temporal and spatial constraints on when demand can realistically enter the network.

Finally, the model assumes a one-to-one relationship between demand units and vehicles, meaning that each unit of demand represents a single vehicle. In practice, this assumption oversimplifies real travel behavior, as multiple travelers may share a single vehicle—such as parents carpooling students or school buses transporting dozens of children. Ignoring this aggregation effect can overstate the number of vehicles entering the network and, consequently, the severity of congestion. Accounting for ride-sharing and public transport options would therefore enhance the realism and policy relevance of the model.

5.4 Future directions

The limitations identified in this study not only define the boundaries of the current work but also point to several valuable directions for future research. Each simplifying assumption presents an opportunity to extend the GP–CTM model toward greater realism and broader applicability. With the rise of sensor-based technologies capable of capturing real-time traffic conditions, parameters such as free-flow speed, free-flow capacity, and initial conditions can be determined dynamically. Incorporating such data would provide more accurate and context-specific inputs to the model, enhancing its realism and improving the quality of its results. While the use of estimations in this study provided an essential foundation for model development, integrating empirically derived values in future work would yield insights that more closely reflect actual network performance.

While the current model considers one-way traffic flow from demand sources to network boundaries, this limitation also presents an opportunity for application in evacuation modeling—where one-way flow is a desirable condition. This makes the GP–CTM a strong candidate for adaptation to evacuation scenarios, though further research is required to validate its applicability in that context. Although complete control of demand release is idealized, it establishes a foundation for future research in which this assumption can be relaxed to better represent real-world conditions. In addition, the proportions of demand units representing carpooling, school buses, and private vehicles could be examined in future studies. Incorporating these distinctions would enable the model to capture more realistic travel behaviors and yield more accurate and policy-relevant results. Ultimately, the limitations identified in this research provide a strong foundation for continued advancement, guiding the evolution of demand management and dynamic traffic assignment models toward more integrated and data-informed frameworks.

5.5 Concluding Remarks

Demand management in a world of rising populations and increasing travel is an area in which significant progress can still be made. Understanding that the perspective from which we view congestion and demand determines how we address it, by shifting our viewpoint, we open the door to more effective and sustainable solutions. Kuwait lacks comprehensive transportation data and expertise; thus, it requires a framework that provides policymakers with simple yet effective tools for decision-making. The GP–CTM does just that, enabling visualization of the effects of traffic demand on the network while offering insights into the trade-offs between demand release, congestion, and flow.

While the GP–CTM is limited in its assumptions, it provides DTA-like insights in data-scarce contexts, offering valuable information about the cause and effect of demand and congestion. More importantly, it represents a step toward accessible and scalable traffic management tools that can inform policy even in regions without advanced sensing infrastructure. By reframing demand as a controllable decision variable rather than a fixed condition, this research contributes to the growing shift from reactive to proactive traffic management.

As cities continue to expand and data accessibility improves, integrating approaches such as the GP–CTM into broader planning frameworks could support more resilient and efficient urban mobility systems. In this way, the work presented here not only addresses a local challenge but also contributes to a global conversation on how to manage congestion more intelligently in an increasingly connected world.

Bibliography

[1] D. J. Newsome, ""Traffic" and "congestion" in Rome's empire," *Journal of Roman Archaeology*, vol. 24, pp. 441–446, 2011.

[2] M. G. Lay, "An historical review of the assessment and management of congestion," *Road & Transport Research*, vol. 21, no. 2, pp. 32–45, 2012. [Online]. Available: https://www.researchgate.net/publication/259464046_A_history_of_congestion

[3] R. R. Thoker, R. Gupta, and N. Kumar, "Study on congestion of national highways due to traffic volume," *International Journal of Engineering Trends and Technology (IJETT)*, vol. 68, no. 2, pp. 36–41, February 2020. [Online]. Available: http://www.ijettjournal.org

[4] United Nations, Department of Economic and Social Affairs, Population Division. (2024) World population prospects 2024 – data for kuwait. Our World in Data. Data retrieved via Our World in Data. Based on UN World Population Prospects (2024). Accessed: October 18, 2025. [Online]. Available: https://ourworldindata.org/grapher/population-with-un-projections?time=earliest..2100&country=~KWT

[5] M. A. Al-Attar and N. Z. Al-Mutairi, "Quantification of time and fuel losses due to daily traffic congestion in kuwait," *International Journal of Crashworthiness*, 2019, published online: 18 Dec 2019. [Online]. Available: https://doi.org/10.1080/13588265.2019.1702411

[6] Central Statistical Bureau, "Transportation and communication statistical bulletin," https://www.csb.gov.kw/, 2023, accessed October 2025.

[7] D. P. Bertsekas and R. G. Gallager, *Data Networks*, 2nd ed. Englewood Cliffs, NJ: Prentice Hall, 1992.

[8] N. H. Gartner, C. J. Messer, and A. K. Rathi, "Traffic flow theory: A state-of-the-art report," Federal Highway Administration, U.S. Department of Transportation, Washington, D.C., Tech. Rep., 2001. [Online]. Available: https://www.fhwa.dot.gov/publications/research/operations/tft/

[9] U.S. Department of Transportation, Intelligent Transportation Systems Joint Program Office, "Annual modal research plans fy 2022–2023: Intelligent transportation systems joint program office (its jpo)," U.S. Department of Transportation, Washington, DC, Tech. Rep., 2021. [Online]. Available: https://its.dot.gov/

[10] O. Avatefipour and F. Sadry, "Traffic management system using iot technology – a comparative review," in *Proc. 2018 IEEE 61st International Midwest Symposium on Circuits and Systems (MWSCAS)*, Windsor, ON, Canada, 2018, pp. 1041–1047.

[11] K. Mandal, A. Sen, A. Chakraborty, S. Roy, S. Batabyal, and S. Bandyopadhyay, "Road traffic congestion monitoring and measurement using active rfid and gsm technology," in *Proc. 14th International IEEE Conference on Intelligent Transportation Systems (ITSC)*, Washington, DC, USA, 2011, pp. 1375–1379.

[12] D. Braess, A. Nagurney, and T. Wakolbinger, "On a paradox of traffic planning," *Transportation Science*, vol. 39, no. 4, pp. 446–450, 2005. [Online]. Available: https://doi.org/10.1287/trsc.1050.0127

[13] Y. K. Chin, K. C. Yong, N. Bolong, S. S. Yang, and K. T. K. Teo, "Multiple intersections traffic signal timing optimization with genetic algorithm," in *2011 IEEE International Conference on Control System, Computing and Engineering*, 2011, pp. 454–459.

[14] W. A. Othman and A. N. H. Zaied, "Development of a fuzzy logic traffic system for isolated signalized intersections in the state of kuwait," *Expert Systems with Applications*, vol. 38, no. 8, pp. 9434–9441, 2011.

[15] S. Kolte, A. Ingle, K. Kshirsagar, P. G. Gawande, K. A. Kumbhar, and R. S. Kawchale, "Traffic flow optimization using CNN and GCN for adaptive signal control," in *2023 3rd Asian Conference on Innovation in Technology (ASIANCON)*, Pune, India, 2023, pp. 1–4.

[16] M. Elhenawy, A. A. Elbery, A. A. Hassan, and H. A. Rakha, "An intersection game-theory-based traffic control algorithm in a connected vehicle environment," in *2015 IEEE 18th International Conference on Intelligent Transportation Systems (ITSC)*, Las Palmas, Spain, 2015, pp. 343–347.

[17] K. Shaaban, M. A. Khan, and R. Hamila, "Literature review of advancements in adaptive ramp metering," *Procedia Computer Science*, vol. 83, pp. 203–211, 2016. [Online]. Available: https://doi.org/10.1016/j.procs.2016.04.117

[18] H. Guan, Q. Meng, and X. Chen, "Dynamic lane management for emerging mixed traffic with semi-autonomous vehicles," *Transportation Research Part C: Emerging Technologies*, vol. 170, p. 104914, 2025.

[19] T.-S. Dao, C. M. Clark, and J. P. Huissoon, "Distributed platoon assignment and lane selection for traffic flow optimization," in *Proceedings of the IEEE Intelligent Vehicles Symposium (IV'08)*. Eindhoven, The Netherlands: IEEE, 2008, pp. 739–744.

[20] G. V. Lioudakis, C. A. Papagianni, D. I. Kaklamani, I. S. Venieris, and A. H. Salden, "An intelligent traffic management system for the eco-optimization of urban traffic flows," in *Proceedings of the 2010 IEEE International Conference on Intelligent Transportation Systems (ITSC)*. Athens, Greece: IEEE, 2010, pp. 1–8. [Online]. Available: https://doi.org/10.1109/ITSC.2010.5625023

[21] Y. Zhao, K. Triantis, D. Teodorović, and P. Edara, "A travel demand management strategy: The downtown space reservation system," *European Journal of Operational Research*, vol. 205, no. 2, pp. 584–594, 2010. [Online]. Available: https://doi.org/10.1016/j.ejor.2010.01.026

[22] P. Edara and D. Teodorović, "Model of an advance-booking system for highway trips," *Transportation Research Part C: Emerging Technologies*, vol. 16, no. 1, pp. 36–53, 2008.

[23] P. Olszewski and L. Xie, "Modelling the effects of road pricing on traffic in singapore," *Transportation Research Part A: Policy and Practice*, vol. 39, no. 7–9, pp. 755–772, 2005.

[24] N. Zheng, R. A. Waraich, K. W. Axhausen, and N. Geroliminis, "A dynamic cordon pricing scheme combining the macroscopic fundamental diagram and an agent-based traffic model," *Transportation Research Part A: Policy and Practice*, vol. 46, no. 8, pp. 1291–1303, 2012.

[25] D. R. Bish and H. D. Sherali, "Aggregate-level demand management in evacuation planning," *European Journal of Operational Research*, vol. 224, no. 1, pp. 79–92, 2013.

[26] Y.-C. Chiu, H. Zheng, J. Villalobos, and B. Gautam, "Modeling no-notice mass evacuation using a dynamic traffic flow optimization model," *IIE Transactions*, vol. 39, no. 1, pp. 83–94, 2007.

[27] M. Yildirimoglu, M. Ramezani, and M. Amirgholy, "Staggered work schedules for congestion mitigation: A morning commute problem," *Transportation Research Part C: Emerging Technologies*, vol. 132, p. 103391, 2021. [Online]. Available: https://doi.org/10.1016/j.trc.2021.103391

[28] *Highway Capacity Manual: A Guide for Multimodal Mobility Analysis*, 6th ed. Washington, D.C.: Transportation Research Board, National Academies of Sciences,

Engineering, and Medicine, 2016, vol. 1: Concepts, volume 1: Concepts. [Online]. Available: https://www.trb.org/Main/Blurbs/173949.aspx

[29] L. A. Pipes, "An operational analysis of traffic dynamics," *Journal of Applied Physics*, vol. 24, no. 3, pp. 274–281, 1953.

[30] R. W. Rothery, "Car following models," in *Traffic Flow Theory: A State-of-the-Art Report*. Transportation Research Board, Federal Highway Administration, 1992, ch. 4, pp. 4–1–4–50, fHWA, U.S. Department of Transportation. [Online]. Available: https://www.fhwa.dot.gov/publications/research/operations/tft/

[31] S. Benalia and A. Khoukhi, "Road traffic modeling," in *Road Traffic Modeling and Management*. Elsevier, 2022, pp. 15–50.

[32] M. J. Lighthill and G. B. Whitham, "On kinematic waves. i. flood movement in long rivers," *Proceedings of the Royal Society A: Mathematical, Physical and Engineering Sciences*, vol. 229, no. 1178, pp. 281–316, 1955.

[33] H. J. Payne, "Models of freeway traffic and control," in *Mathematical Models of Public Systems*. Simulation Council, 1971, vol. 1, pp. 51–61.

[34] A. Aw and M. Rascle, "Resurrection of "second order" models of traffic flow," *SIAM Journal on Applied Mathematics*, vol. 60, no. 3, pp. 916–938, 2000.

[35] C. F. Daganzo and N. Geroliminis, "An analytical approximation for the macroscopic fundamental diagram of urban traffic," *Transportation Research Part B: Methodological*, vol. 42, no. 9, pp. 771–781, 2008.

[36] C. F. Daganzo, "The cell transmission model: A dynamic representation of highway traffic consistent with the hydrodynamic theory," *Transportation Research*, vol. 28, no. 4, pp. 269–287, 1994.

[37] ——, "The cell transmission model, part ii: Network traffic," *Transportation Research*, vol. 29, no. 2, pp. 79–93, 1995.

[38] S. V. Ukkusuri, L. Han, and K. Doan, "Dynamic user equilibrium with a path based cell transmission model for general traffic networks," *Transportation Research Part B: Methodological*, vol. 46, no. 10, pp. 1657–1684, 2012.

[39] F. Zhu and S. V. Ukkusuri, "A cell based dynamic system optimum model with non-holding back flows," *Transportation Research Part C: Emerging Technologies*, vol. 36, pp. 367–380, 2013.

[40] P. Wang, L. S. Jones, Q. Yang, and S. Gurupackiam, "Cell transmission model based traffic signal timing in oversaturated conditions," *Journal of Central South University*, vol. 20, no. 4, pp. 1129–1136, 2013.

[41] A. K. Ziliaskopoulos, "A linear programming model for the single destination system optimum dynamic traffic assignment problem," *Transportation Science*, vol. 34, no. 1, pp. 37–49, 2000.

[42] H. M. A. Aziz, "Energy and mobility impacts of system optimal dynamic traffic assignment for a mixed traffic of legacy and automated vehicles," *Transportation Research Record*, vol. 2673, no. 12, pp. 1–18, 2019. [Online]. Available: https://doi.org/10.1177/0361198119845658

[43] J. G. Wardrop, "Some theoretical aspects of road traffic research," *Proceedings of the Institution of Civil Engineers, Part II*, vol. 1, no. 3, pp. 325–378, 1952.

[44] Y. Sheffi, *Urban Transportation Networks: Equilibrium Analysis with Mathematical Programming.* Englewood Cliffs, NJ: Prentice-Hall, 1985.

[45] S. Peeta and A. K. Ziliaskopoulos, "Foundations of dynamic traffic assignment: The past, the present and the future," *Networks and Spatial Economics*, vol. 1, no. 3–4, pp. 233–265, 2001.

[46] D. J. Zawack and G. L. Thompson, "A dynamic space-time network flow model for city traffic congestion," *Transportation Science*, vol. 21, no. 3, pp. 153–162, 1987.

[47] A. Charnes and W. W. Cooper, "Management models and industrial applications of linear programming," *Management Science*, vol. 8, no. 1, pp. 38–91, 1961.

[48] C. Romero, *Handbook of Critical Issues in Goal Programming.* Oxford: Pergamon, 2001.

[49] C. N. Rosyidi, A. M. Khasanah, and P. W. Laksono, "A goal programming model for joint decision making of order allocation, supplier selection, and carrier selection considering corporate social responsibility," *Jurnal Teknik Industri*, vol. 24, no. 1, pp. 45–52, 2022. [Online]. Available: https://doi.org/10.9744/jti.24.1.45-52

[50] V. Belton and T. J. Stewart, *Multiple Criteria Decision Analysis: An Integrated Approach.* Boston, MA: Springer US, 2002, ch. 7, pp. 269–316, goal and Reference Point Methods.

[51] M. Tamiz, D. Jones, and C. Romero, "Goal programming for decision making: An overview of the current state-of-the-art," *European Journal of Operational Research*, vol. 111, no. 3, pp. 569–581, 1998.

[52] Urban Kuwait. (2020) The real cost of traffic congestion. Accessed: 2025-09-20. [Online]. Available: https://urbankuwait.com/the-real-cost-of-traffic-congestion/

[53] D. for Transport, "Vehicle licensing statistics, united kingdom: 2024," https://www.gov.uk/government/statistics/vehicle-licensing-statistics-2024/

vehicle-licensing-statistics-united-kingdom-2024, 2025, published 11 June 2025, Crown copyright © 2025.

[54] World Bank, “Land area (sq. km),” https://data.worldbank.org/indicator/AG.LND.TOTL.K2?locations=KW-GB, 2024, data retrieved October 2025 from the World Bank Open Data portal.

[55] L. Walters, “Interview with the principal of an international private school in kuwait,” Personal communication, 2025, conducted January 2025.

[56] Y.-C. Chiu, J. Bottom, M. Mahut, A. Paz, R. Balakrishna, T. Waller, and J. Hicks, *Dynamic Traffic Assignment: A Primer*, ser. Transportation Research Circular. Washington, DC: Transportation Research Board, June 2011, no. E-C153. [Online]. Available: https://www.trb.org/Publications/Blurbs/165637.aspx

[57] OpenStreetMap contributors, “Openstreetmap,” https://www.openstreetmap.org, 2025, accessed: October 25, 2025.

[58] Google Maps, “Sabah al salem, kuwait,” https://www.google.com/maps/place/Sabah+Al+Salem,+Kuwait, 2025, accessed: October 25, 2025.

[59] V. L. Knoop, *Traffic Flow Theory: An Introduction with Exercises*, 3rd ed. Delft, The Netherlands: TU Delft Open Publishing, 2021, licensed under CC BY-NC-SA 4.0. [Online]. Available: https://doi.org/10.5074/t.2021.002

[60] World Population Review. (2023) Cars by country 2023. Accessed: 2025-09-20. [Online]. Available: https://worldpopulationreview.com/country-rankings/cars-by-country#countries-with-the-most-cars-per-capita

[61] MyLifeElsewhere. (2025) Country size comparison: United kingdom vs. kuwait. Illustrative comparison of national land areas. Accessed October 2025. [Online]. Available: https://www.mylifeelsewhere.com/country-size-comparison/united-kingdom/kuwait

Appendix A: Network Transformation Procedure

This appendix provides detailed arc-level information for the discretized Sabah Al Salem network, including arc lengths, assigned free-flow speeds, computed cell lengths, and the number of cells per arc. These data were used to determine the number and length of cells in the cellular network representation.

Table A.1: Arc characteristics for the discretized cell network.

From	To	Arc Length (ft)	Arc Speed (ft/s)	Cell Length (ft)	No. of Cells
22	23	600	30	300	2
14	26	400	40	400	1
15	7	800	40	400	2
7	15	800	40	400	2
22	21	800	40	400	2
21	22	800	40	400	2
11	21	800	40	400	2
21	11	800	40	400	2
10	11	800	40	400	2
10	20	800	40	400	2
20	10	800	40	400	2
20	28	1600	40	400	4
21	9	800	40	400	2
9	21	800	40	400	2
21	20	800	40	400	2
20	21	800	40	400	2
20	19	1600	40	400	4
19	20	1600	40	400	4
9	19	1600	40	400	4
				Total cells in the network	**120**

Table A.1 – continued from previous page

From	To	Arc Length (ft)	Arc Speed (ft/s)	Cell Length (ft)	No. of Cells
19	9	1600	40	400	4
9	18	800	40	400	2
18	9	800	40	400	2
18	8	1200	40	400	3
8	18	1200	40	400	3
8	17	800	40	400	2
17	8	800	40	400	2
17	16	800	40	400	2
16	17	800	40	400	2
16	7	1600	40	400	4
7	16	1600	40	400	4
7	13	800	40	400	2
13	7	800	40	400	2
16	12	800	40	400	2
17	19	1600	40	400	4
19	17	1600	40	400	4
7	18	800	40	400	2
18	7	800	40	400	2
24	29	400	40	400	1
12	13	1500	50	500	3
13	14	1000	50	500	2
14	15	500	50	500	1
23	24	1000	50	500	2
23	27	1000	50	500	2
15	22	2400	60	600	4
24	25	2400	60	600	4
				Total cells in the network	**120**

Appendix B: Example Network -Results

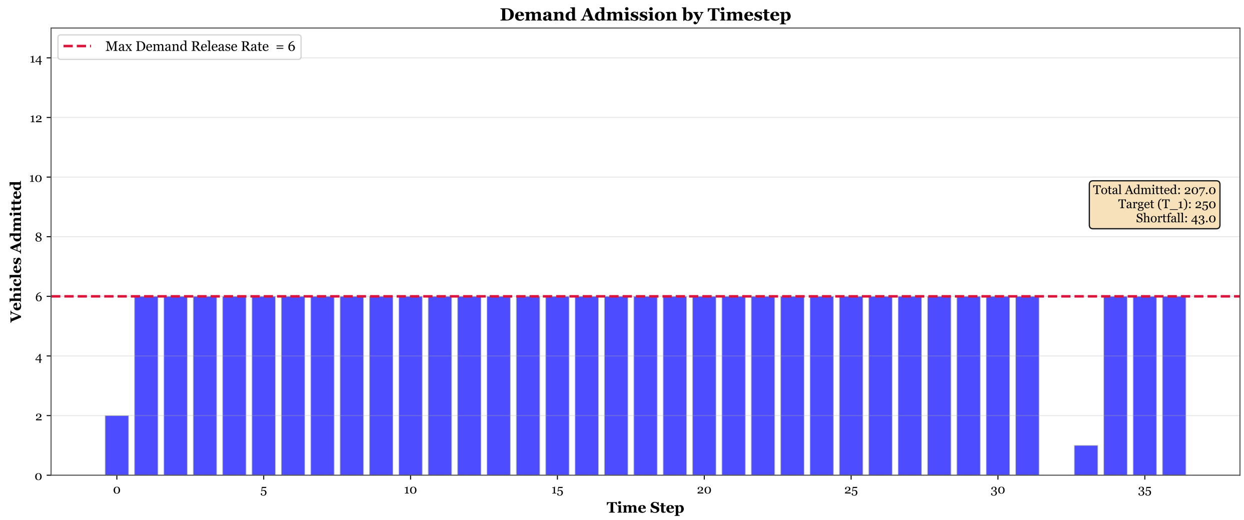

Figure 1: Amount of demand admitted per time step in the example network, illustrating the temporal distribution of demand release during the time horizon.

Appendix C: GP-CTM Results

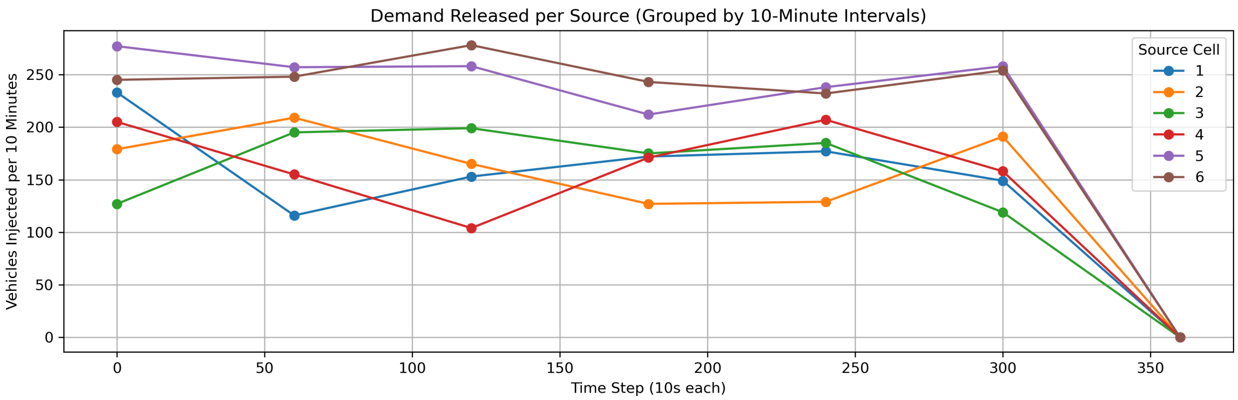

Figure 2: Demand released per source in the GP–CTM model, showing the optimized release pattern over the simulation horizon.